Design of Covalent Triazine Frameworks for Selective Carbon Capture and Storage

GUANGBO WANG

Department of Chemistry

Faculty of Science

Ghent University

Dissertation Submitted in Fulfillment of the Requirements for the Degree of Doctor of Science: Chemistry

October 2018

Promoter: Prof. Dr. Pascal Van Der Voort

Department of Chemistry, Ghent University

Members of the Examination Committee

Prof. Dr. Rik Van Deun	Ghent University (Chairman)
Prof. Dr. Christoph Janiak	University of Düsseldorf
Prof. Dr. Damien P. Debecker	University of Louvain
Prof. Dr. Kevin Van Geem	Ghent University
Prof. Dr. Karen Leus	Ghent University
Dr. Hannes Depauw	Vincotte nv.
Dr. Sven Rogge	Ghent University

Acknowledgements

This thesis would not be without the invaluable help and support of others. First and foremost, I would like to express my sincerest gratitude to my promoter, Prof. Pascal Van Der Voort, for providing me the opportunity to join the dynamic and prestigious COMOC group and I really enjoy this fascinating part of my life. Thank you so much, Prof. Van Der Voort for your support, understanding and inspiring supervision.

I want to thank Prof. Yingya Liu, who once worked as a postdoctoral fellow in the COMOC group, she gave me the confidence to come here and to start this fantastic journey. She is actually the "inventor" of COMOC series MOFs, she gave me lots of valuable suggestions and guidance at the beginning of my PhD, I do appreciate her and I wish her a bright future for her research and life.

I would like to specially thank Dr. Karen Leus. I still remember the scene that the first day I arrived at Gent-Sint-Pieters Station, I didn't have the Belgium SIM card to contact her, she waited for me at the station in the early morning and picked me up to my residence, I really appreciate her. Since then, we have worked together to discuss my research, help me to contact the collaborators to do some measurements, revise my manuscripts and my PhD thesis, thank you so much, Karen.

Special thanks also goes to Dr. Baoyi Yu, who once worked in the department for his master and PhD degree. At that time, he was the only Chinese person in our building, I didn't know anyone else, he helped me to adapt to the new environment and new culture, taught me how to improve my English, how to communicate and get along with the colleagues and how to start the research. I do appreciate him for his valuable help during my PhD.

I wish to express my gratitude to my (ex-) colleagues in COMOC group (Els, Yesid, Dolores, Asamanjoy, Thomas, Isabelle, Wannes, Kevin α and β, Hannes, Sander, Fu, Mei, Judith, Karen, Jeroen, Himanshu, Shuna, Xiao, Chidharth, Norini, Flora, Sara and Parviz) and the colleagues in the department. Many thanks for the nice atmosphere, the interesting discussion and group activities, the sharing of frustrations and success, I want to say that a thousand words

merged into one sentence: I wish you all a bright future.

I am grateful to Pierre, Kathleen, Tom, Funda, Katrien, Pat, Bart and Danny for helping me not only on documents and general stuff, but also on experimental and computer problems.

I would like to thank our collaborators, Prof. Veronique Van Speybroeck, Prof. Nathalie De Geyter and Prof. Rino Morent, Prof. Laszlo Vincze in Ghent University, Prof. Joeri F M Denayer in Vrije Universiteit Brussel and Prof. Yingya Liu in Dalian University of Technology, China. Many thanks for their invaluable support for data collection and analysis, constructive suggestions for manuscript preparation.

I would like to thank my Chinese friends in Ghent, especially Xiaolong, Xiaopeng, Cheng, Feilong, Zhiyue, Hui, Weiyang, Jing, Min, Pengshang and Jiaren for sharing delicious food and happiness, playing games and travelling. Without them, the life in Ghent will be boring and best wishes to all of them.

My parents, brother and sister are the persons who deserve all of my endless love and thanks. Without their continuous love, support and encouragement, this thesis would not exist, I want to say I love them all forever.

Here, I want to express my sincere gratitude to the examination committees for providing valuable and constructive suggestions and comments to improve my thesis. Many thanks.

Guangbo Wang

Ghent, Belgium

September, 2018

English Summary

A significant and ongoing challenge of the world is the continuous emission of carbon dioxide, which is mainly produced from the burning of fossil fuels and is widely accepted to be the primary contributor to global warming. A cleaner and sustainable future for the world with the transition of energy dependence from fossil fuels to more renewable and green energy sources is regarded as an ideal concept for a long time, however, there are too many obstacles and it really needs long time before the realization of this goal in practice. One can foresee that fossil fuels will still be the dominant source of energy for humans in the near future and it is absolutely and urgently required to explore more efficient and economical techniques for the reduction of the atmospheric CO_2 concentration. As a newly emerging class of advanced porous materials, metal organic frameworks (MOFs) and covalent organic frameworks (COFs) have exhibited promising potentials for the application of gas adsorption and separation due to their unique features and they are now being extensively studied and explored by both academic and industrial scientists.

In this thesis, we are especially interested in a subclass of covalent organic frameworks, namely covalent triazine frameworks (CTFs), which exhibit exceedingly high thermal and chemical stability, high permanent porosity, easy tunability and functionalities as well as rich CO_2-philic sites and they are supposed to be the excellent platforms for the application of carbon capture and separation. Thus, in this thesis, we designed and prepared different types of monomers with different types of functional groups as the building blocks for the construction of porous CTF materials and consequently explored and evaluated their gas adsorption and separation potentials.

In **chapter 1**, the background and state-of-art of the field of carbon capture and separation was given. More specifically, the post-combustion carbon capture process employing different types of materials was discussed

followed by the detailed description of the history, synthesis and applications of CTF materials.

In **chapter** 2, we firstly prepared a novel N-heteroaromatic tetranitrile as the building block to obtain a set of nitrogen-rich porous CTF materials. The effects of $ZnCl_2$/monomer ratio and temperatures on the structure and porosity of the materials was systematically examined. All the materials have been subjected to a comprehensive characterization and gas adsorption study, in which their performance in terms of adsorption capacity and selectivity is evaluated.

It has been proven that incorporation of some specific CO_2-philic sites, such as fluorine, oxygen and nitrogen, into the networks can significantly affect the materials' gas adsorption and separation properties. Therefore, in **chapter** 3, straightforward fluorination of the aforementioned N-heteroaromatic tetranitrile was adapted to synthesize a series of fluorine functionalized CTFs. Although the defluorination process and the loss of fluorine groups is inevitable during the synthesis, the resulting fluorinated materials still exhibit much higher gas adsorption and separation performance than their corresponding non-functionalized materials. These findings were attributed to the microporosity and fluorine groups of the materials as well as the structure defects created during defluorination processes.

In **chapter** 4, we reported on how the nitrogen functionalities affect the materials' properties. Specifically, we employed a novel and nitrogen-rich hexaazatrinaphthalene-based monomer as the building block to prepare a class of nitrogen-rich CTFs as the high-performance platforms for efficient carbon dioxide capture. The synergistic effects of the ultramicroporosity and abundant CO_2-philic nitrogen sites bestow upon the frameworks with superior CO_2 and H_2 adsorption capacity as well as high CO_2/N_2 and CO_2/CH_4 selectivity. More importantly, the studied materials can be reused for many times without significant loss of adsorption capacities.

As discussed in chapter 3, incorporation of fluorine groups into CTF structures is an efficient approach to improve the materials' gas adsorption performance, however, to further improve the carbon capture performance of this type of materials, introduction of more fluorine groups into the structures seems to be plausible. As a proof of concept, in **chapter 5**, we prepared a perfluorinated building block to obtain a set of fluorine-containing CTFs. The fluorine content was confirmed by transmission electron microscopy (TEM) and EDX mapping, X-ray photoelectron spectroscopy (XPS) and solid state nuclear magnetic resonance (ssNMR). All the materials were subjected to comprehensive adsorption study and the enhanced hydrophobicity of these materials after fluorination was confirmed by water vapor adsorption measurements.

In conclusion, this thesis has shown that rational design of novel building blocks with some task-specific functional groups is a promising approach for synthesis of porous materials with excellent gas adsorption and separation properties. In the following years, it may be expected that this research field will further expand and more task-specific functionalities will be explored and introduced into the frameworks for a variety of applications.

Nederlandstalige samenvatting

De excessieve emissies van CO_2 vormen een grote bedreiging voor onze maatschappij. Deze CO_2 emissies zijn grotendeels afkomstig van de verbranding van koolstofhoudende brandstoffen en worden aanzien als de primaire bron voor de opwarming van de aarde. Om deze CO_2 emissies te reduceren is een verschuiving naar het gebruik van hernieuwbare energiebronnen noodzakelijk. Dit is echter een proces dat gepaard gaat met de nodige obstakels en problemen. Er wordt verwacht dat koolstofhoudende brandstoffen de primaire energiebron zal blijven voor de mens in de nabije tokomst maar de noodzaak om de CO_2 concentratie in de atmosfeer te reduceren dringt zich op. Een nieuwe klasse van poreuze materialen, namelijk metaal organische roosters (MOFs) en covalent organische roosters (COFs) bezitten een groot potentieel voor hun gebruik als adorbenten en in de scheiding van gassen gezien hun unieke eigenschappen.

In deze thesis wordt een welbepaalde klasse van de covalent organische roosters besproken, namelijk de covalent triazine bevattende netwerken (CTFs). Deze materialen zijn uitermate interessant omwille van de volgende eigenschappen: (1) ze bezitten een hoge thermische en chemische stabiliteit, (2) ze bezitten een hoge porositeit, (3) het is eenvoudig om bepaalde functionele groepen te introduceren in deze materialen die een hoge affiniteit hebben voor CO_2 wat hun uitermate geschikt maakt voor de adsorptie van CO_2 en in scheidingen.

In deze thesis worden verschillende nieuwe monomeren gemaakt die diverse functionele groepen bezitten. Deze monomeren worden vervolgens als bouwstenen gehanteerd voor de synthese van de desbetreffende CTFs. In een finale stap worden de verkregen materialen geëvalueerd in de adsorptie van gassen o.a. CO_2 alsook wordt hun potentieel voor de scheiding van gassen onderzocht.

In **hoofstuk 1** wordt een overzicht gegeven omtrent de state of the art voor CO_2 adsorptie en de scheiding ervan. Hiernaast wordt een gedetailleerd overzicht gegeven omtrent de historiek, de verschilende synthesemethodes alsook de diverse toepassingen van CTFs.

In **hoofdstuk 2**, wordt de synthese van een nieuw tetranitrile gebaseerd monomeer besproken. Dit monomeer wordt vervolgens aangewend voor de synthese van een set stikstofbevattende CTF materialen. De invloed van de $ZnCl_2$/monomeer ratio alsook de invloed van de reactietemperatuur op de verkregen porositeit en structuur worden systematisch onderzocht en de verkregen CTFs worden onderworpen aan een grondige karakterisatie. Finaal wordt hun adsorptie capaciteit en selectiveit bepaald.

Hierbij stelde men vast dat de introductie van fluor, zuurstof en stikstof in het netwerk een positieve invloed had op de adsorptie van CO_2. **Hoofdstuk 3** vormt een verderzetting op de verkregen resultaten uit hoofdstuk 2, waarbij een *rechttoe rechtaan* synthese procedure wordt aangewend voor de synthese van fluor bevattende CTFs. Hoewel een groot deel van de fluor groepen verloren ging gedurende de synthese van de CTF materialen wordt een sterk verhoogde adsorptiecapaciteit vastgesteld alsook een beter scheidend vermogen in vergelijking met de niet-gefunctionaliseerde materialen. Dit is het gevolg van de verhoogde microporositeit en de aanwezige fluor groepen alsook door de aanwezigheid van structurele defecten die gevormd worden gedurende het defluorinatieproces.

In **hoofdstuk 4**, wordt de invloed van de stikstof functionaliteiten op de resulterende materiaal eigenschappen onderzocht. Meer bepaald wordt een nieuw stikstofrijk hexaazatrinaphthalene-gebaseerd monomeer gebruikt als bouwsteen voor de synthese van de CTFs. Er werd een duidelijke synergie vasgesteld tussen enerzijds de ultramicroporositeit van de verkregen CTF en de hoge CO_2 invloedrijke stikstofconcentratie anderzijds die aanleiding gaf tot een heel hoge CO_2 en H_2 adsorptie capaciteit alsook een hoge CO_2/N_2 en

CO_2/CH_4 selectiviteit. De onderzochte adsorbentia vertoonden bovendien ook een hoge regenereerbaarheid zonder een significante afname van de adsorptie capaciteit.

Na de vaststelling in hoofdstuk 3 dat de introductie van fluor groepen in de CTF structuur een ideale manier is om de gas adsorptie te verhogen wordt in hoofdstuk 5, een CTF gemaakt die een hoger fluor gehalte bevat in vergelijking met het materiaal gemaakt in hoofdstuk 3. In **hoofdstuk 5** wordt de synthese van een perfluorinated bouwsteen besproken alsook de synthese van de corresponderende CTF. Transmissie-elektronenmicroscopie (TEM) and EDX element mapping, X-straal –foto-elektronspectroscopie (XPS) and vaste stof NMR worden aangewend voor de karakterisatie van de CTF materialen. De toegenomen hydrofobiciteit van de gesynthetiseerde materialen wordt onderzocht door middel van de adsorptie van water.

Samenvattend, in deze thesis wordt aangetoond dat de synthese van nieuwe CTF bouwstenen die welbepaalde functionele groepen bezitten, het toelaat om veelbelovende materialen te maken voor de adsorptie van gassen alsook voor de scheiding ervan. In de komende jaren kan men dan ook een sterke toename verwachten in dit onderzoek waarbij er nog veel nieuwe bouwstenen met specifieke functionele groepen zullen worden geintroduceerd met het oog op hun gebruik ervan in diverse toepassingen.

List of Figures

List of Tables

List of Abbreviations

A

AMP   2-amino-2-methyl-1-propanol

B

BET   Brunauer-Emmett-Teller

C

CCS   Carbon Capture & Storage

CCU   Carbon Capture & Utilization

COFs   Covalent Organic Frameworks

CTFs   Covalent Triazine Frameworks

D

DCBP   4,4'-biphenyldicarbonitrile

DMSO   Dimethyl sulfoxide

DoE   US Department of Energy

E

EA   Elemental Analyses

EDX   Energy Dispersive X-ray Spectroscopy

F

F-DCBP   2,2',3,3',5,5',6,6'-octafluoro-4,4'-biphenyldicarbonitrile

FT-IR   Fourier Transform Infrared Spectroscopy

H

HATN   Haxaazatrinaphthalene

HATN-3CN   Diquinoxalino[2,3-a:2',3'-c]phenazine-2,8,15-tricarnonitrile

I

ILs   Ionic Liquids

M

MDEA   N-methyldiethanolamine

MEA   Monoethanolamine

MOFs   Metal Organic Frameworks

N

NMR   Nuclear Magnetic Resonance

NOAA   National Oceanic and Atmospheric Administration

P

PXRD   Powder X-ray Diffraction

PCPs   Porous Coordination Polymers

Piperazine   PZ

S

ssNMR   Solid state Nuclear Magnetic Resonance

SEM   Scanning Electron Microscopy

T

TEA   Triethanolamine

TEM   Transmission Electron Microscopy

TGA   Thermogravimetric Analysis

THF   Tetrahydrofuran

X

XPS   X-ray Photoelectron Spectroscopy

XRD   X-ray Diffraction

Table of Contents

CHAPTER 1

General Introduction and Aim of the Thesis
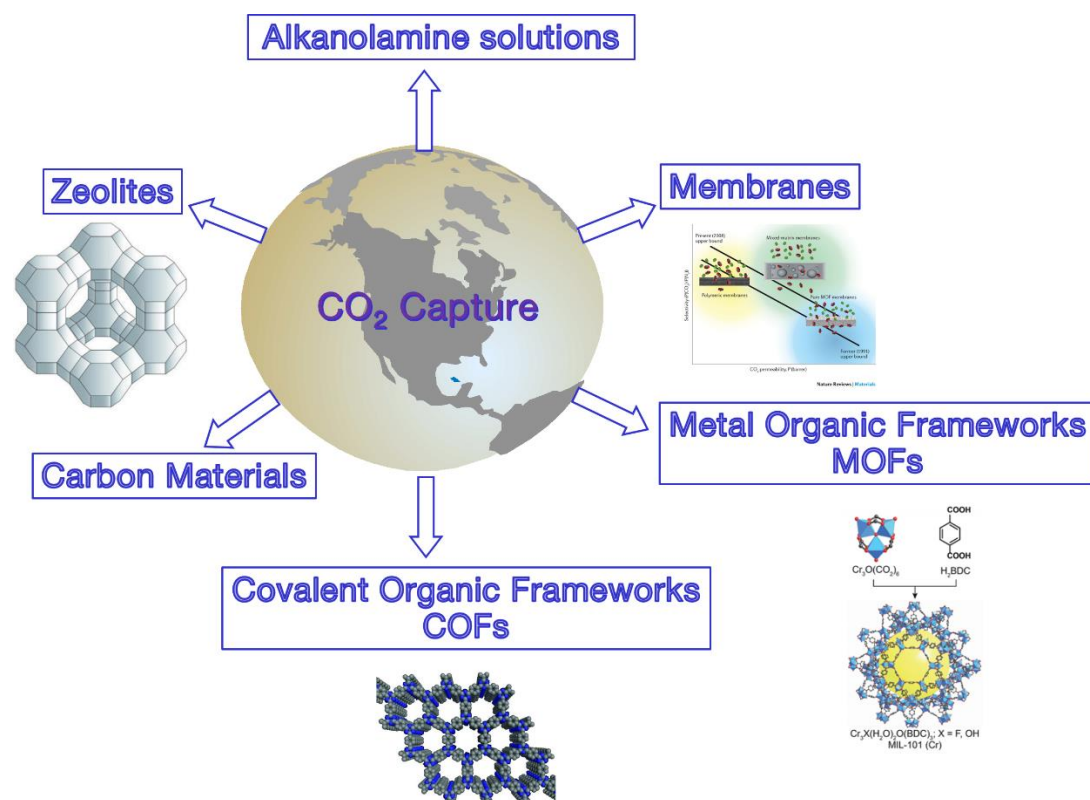
Introduction

With the ever increasing and development of the society and economy, the global warming of the earth's atmosphere and surface, also known as the greenhouse effect, has already become an intractable issue for humankind. Carbon dioxide (CO_2), regarded as the main anthropogenic greenhouse gas, is widely accepted to be the primary contributor to global warming.[1-2] According to the U.S. National Oceanic and Atmospheric Administration (NOAA), the CO_2 concentration in the earth's atmosphere has increased from approximately 315 to 410 ppm in September, 2018 and is expected to reach more than 550 ppm by 2050 even if the emission stabilizes (Figure 1.1).[3-5]
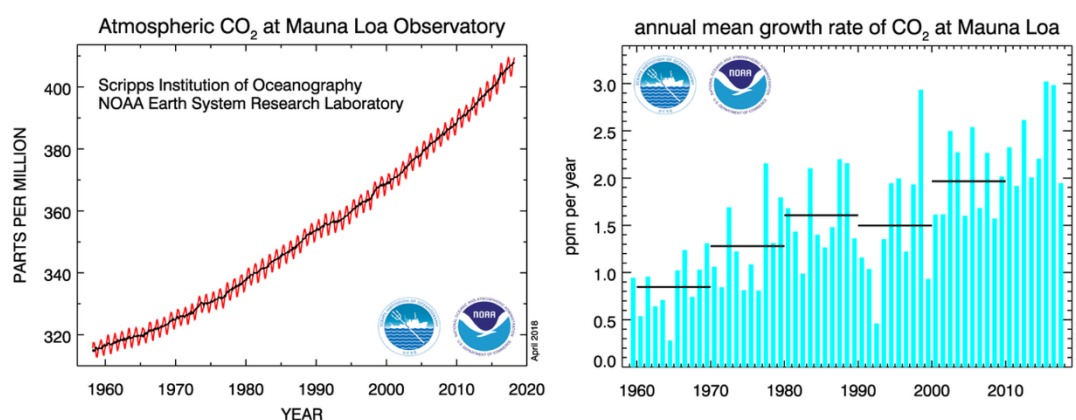
Figure 1.1. Atmospheric mean CO_2 concentration at Mauna Loa Observatory from 1960 to 2018 (left); Annual mean growth rate of the atmospheric CO_2 (right)[4].

This drastic CO_2 rise can be mainly attributed to human activities, including, but not limited to, the burning of fossil fuels (e.g. coal, petroleum and natural gas), which accounts for approximately 86 % of the anthropogenic greenhouse gas emissions and various chemical processes.[6] In recent decades, there is a growing awareness all over the world that anthropogenic CO_2 emissions must be reduced and now many countries and institutions are making attempts to decrease the greenhouse gas levels. The transition of the energy dependence from fossil fuels to much cleaner and more sustainable alternatives such as solar energy or hydrogen fuels would be ideal, however,

it is really a long-term goal and many more years are needed before the realization of sufficiently developed techniques in practical industrial implementation. Thus, considering that fossil fuels will still be the dominant source of energy for humans in the foreseeable future, it is beyond all doubt that exploring cost-effective and scalable technologies to keep the atmospheric CO_2 concentration at a safe level is urgently required. To address this issue, carbon capture & storage (CCS) or carbon capture & utilization (CCU) (Figure 1.2) have been proposed and deployed as one of the most promising strategies for reducing CO_2 emissions, particularly in the stationary point sources, such as coal-fired power plants and chemical industries.[7-8] However, within both strategies, CO_2 capture and separation is considered as the most crucial step, and approximately 70% of the cost of CCS or CCU is associated with the selective CO_2 capture from the post-combustion flue gas, which typically contains CO_2 (15-16%), a large quantity of N_2 (73-77%) and other minor components (e.g. SO_X, NO_X, H_2O, CO). Therefore, the breakthrough of new materials or techniques with high performance that can capture CO_2 in a low-cost, efficient and durable manner is the core for CCS or CCU success.
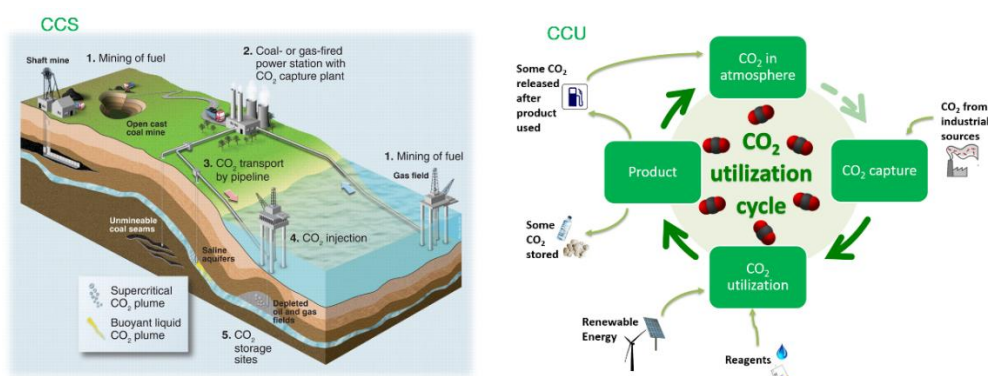
Figure 1.2. Diagrammatic representation of the CCS (left) and CCU (right) process (Adapted from [8-9]).

Several technologies have already been extensively explored and studied for efficient CO_2 capture so far, in the following of this chapter, a detailed overview of the status and technologies in the field of carbon capture will be presented

followed by a detailed introduction on covalent triazine frameworks (CTFs) as well as their potential applications, which is the core of this thesis and this chapter will end up with the aim of this thesis.

1.1. Introduction to Carbon Capture Strategies

In the global transition to a sustainable low-carbon economy, CO_2 capture and storage technologies play a crucial role for deep emission reduction, in particular, for the stationary sources from the burning of fossil fuels and industry. In general, three basic CO_2 capture scenarios can be adopted based on the fundamental chemical processes involved in the combustion of fossil fuels, i.e. 1) post-combustion capture; 2) pre-combustion capture and 3) oxyfuel-combustion (Figure 1.3).[10]
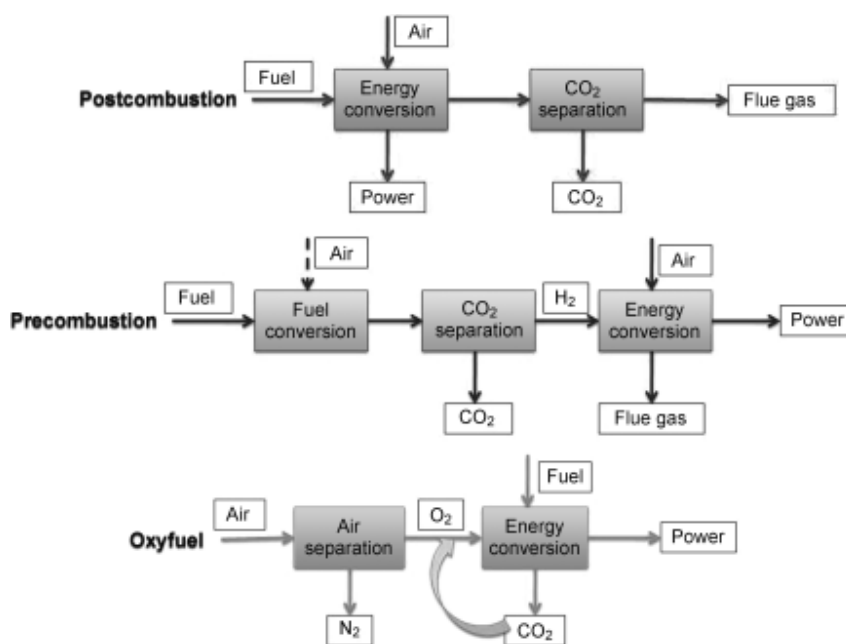
Figure 1.3. Schematic illustration of post-, pre- and oxyfuel-combustion processes (Adapted from[10]).

Post-combustion capture

As shown in Figure 1.3, the post-combustion capture process is to separate CO_2 from flue gas after the combustion of fuels before it was released to the atmosphere. Normally, the flue gas generated in current power plants is mainly

comprised of N_2 (73-77%) and CO_2 (15-16%) with a CO_2 partial pressure equivalent to 0.15 bar and a total pressure of approximately 1 bar. This process is the most feasible on a short time scale as most of the existing fossil fuel consuming power plants can be easily retrofitted and the post-combustion flue gas selective carbon capture will be the main focus of this thesis.

Pre-combustion capture

In the pre-combustion capture, the primary fuel firstly reacts at high pressure and temperature with O_2 or air to form the syngas containing CO, CO_2 and H_2. The second stage involves the conversion of CO using a water-gas shift reactor to produce CO_2 (25-35 %) and additional H_2 (30-50 %), in which the CO_2 and H_2 are separated prior to combustion. However, the temperature and efficiency associated with H_2-rich turbine fuel are problematic.

Oxyfuel-combustion

In contrast to post- and pre-combustion capture, oxyfuel-combustion takes place in a pressurized CO_2-rich stream in which N_2 is excluded through a preliminary air separation step (Figure 1.3). During oxyfuel-combustion, a combination of nearly pure oxygen (95%) and recycled flue gas (mainly CO_2) is used for combustion of the fuel. The recycled flue gas is used to control the flame temperature and make up the volume of the missing N_2 to ensure there is enough gas to carry the heat through the boiler. This process forms the basis for almost zero emission, which seems more promising than the other two methods. However, this process requires to redesign the turbines, such that the retrofitting of existing plants is not considered economical and the stringent requirements for nearly pure O_2 make the implementation of this method more challenging.

1.2. Current Carbon Capture Technologies and Materials.

The need for techniques that can be used within CO_2 capture systems

especially for coal- and gas-fired power plants has prompted the study of several classes of materials or methods to date. Generally, a diverse range of routes and materials exists for carbon capture, including aqueous alkanolamine absorbents, membranes and porous solid materials (e.g. zeolites, carbon-based materials, metal organic frameworks (MOFs) and covalent organic frameworks (COFs)). In the following, a detailed description of each technique will be presented.

1.2.1. Aqueous Alkanolamine Absorbents

From a current point of view, the absorption of CO_2 into aqueous alkanolamine solutions is among the most effective technologies and has been widely used for CO_2 capture from coal- or natural gas fired power plants for more than 50 years. Figure 1.4 illustrates the CO_2 capture process using amine scrubbing. Generally, the flue gas flows countercurrently to the aqueous alkanolamine solvent in the absorber, where CO_2 is removed via chemical reaction into the liquid stream at ~40 °C. This liquid stream then goes to a stripper using water vapor and operating at 100-120 °C, where the solvent is regenerated and CO_2 is released into the gas stream. Then, pure CO_2 can be produced when water is condensed out of the gas stream, followed by CO_2 compression and storage.[11-12]
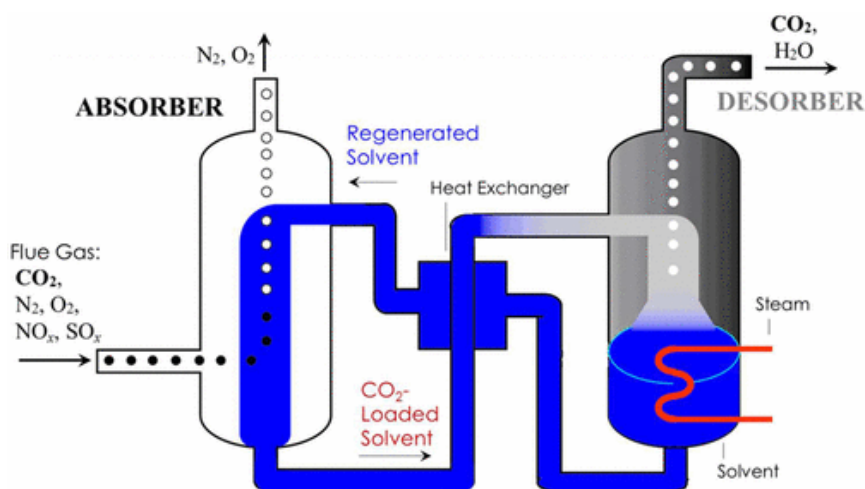
Figure 1.4. CO_2 capture from flue gas by aqueous amine in the absorber and solvent regeneration in the desorber (stripper) (Adapted from ref. 12).

In particular, monoethanolamine (MEA) is considered as the benchmark solvent and has been extensively employed and studied in industry since 1930s. It is regarded as a state-of-the-art process with the operating conditions of 20%–30% (by mass) aqueous MEA, 0.2-0.35 mol·mol^{-1} lean loading, and inlet temperature of approximately 40 °C. During the CO_2 absorption process, two amine molecules react with one CO_2 molecule to form a carbamate ion and a protonated amine (i.e., 2MEA + CO_2 $\rightarrow$ MEACOO$^-$ + MEAH$^+$), limiting the loading capacity to 0.5 mol CO_2 per mol amine. This has been proposed to occur via a single-step termolecular (direct) or two-step zwitterion mechanism (Figure 1.5).[13-14] However, it still faces numerous challenges, such as high energy consumption for solvent regeneration, low capacity to absorb CO_2, poor thermal stability and high corrosivity.

(a) Zwitterionic intermediate formation

(b) Deprotonation to form carbamate

2.
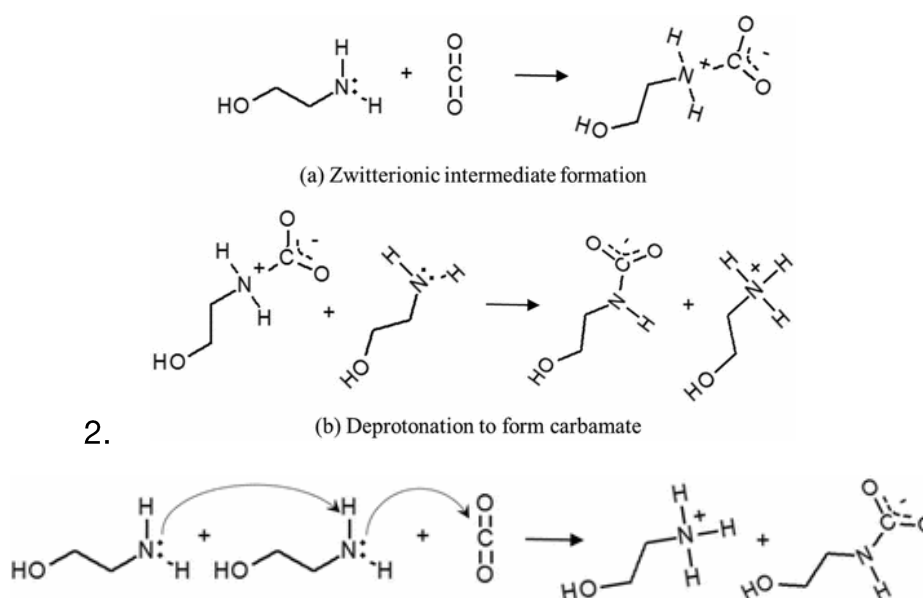
Figure 1.5. Proposed two-step zwitterion mechanism or one-step termolecular mechanism during CO_2 capture in aqueous amine solution (Adapted from ref. 12).

To overcome these disadvantages, in the recent years, blending of commercial solvents has been considered as potential applications in CO_2 absorption, such as MEA–MDEA (Methyldiethanolamine), DEA (Diethanolamine)–MDEA or AMP(2-amino-2-methyl-1-propanol)–PZ (piperazine). The system combines the advantages of primary/secondary amines (fast kinetics) and

tertiary/sterically hindered amines (high absorption capacity and low energy consumption to strip CO_2).[11, 15]

Ionic liquids (ILs), a new class of absorbents, have recently attracted much attention and been referred as green absorbents for gas adsorption and separation since they are non-volatile, thermally stable, non-flammable, and reusable and can be used in the process in a wide liquid range and virtually limitless tunabilities.[16] However, in addition to solubility and selectivity, multi-aspect performance of ILs, such as solvent cost, enthalpy of the reaction, density, biodegradability and toxicity, transport properties, volume expansion and micro-structures, inevitably needs consideration before large-scale applications of ILs.[17]

Although aqueous alkanolamine solution has been industrially employed for more than 50 years and will still be the dominant approach in industry for CO_2 capture, there are still many technical and fundamental constraints that need to be addressed and improved, including decomposition of the amine solvents, environmental concerns, high energy consumption and equipment corrosion.

Decomposition of the solvent

Solvent degradation is an undesirable operating problem caused by prolonged exposure of amine solvent to CO_2, O_2, SO_x and fly ash in the flue gas. It introduces unwanted by-products, such as heat stable salts, heavy hydrocarbons and particulates into the system. These by-products either reduce the ability of the solvent to absorb CO_2 or to strip CO_2 under typical regeneration conditions, which may be prevented by adding so-called inhibitors, lowering the solvent regeneration temperature or reducing residual SO_2 content of the flue gas.[11]

Experimental concerns

The current lack of information concerning the details of the chemistry associated with the degradation products that are associated with the amine

processes is a cause for some concerns, as preliminary results indicate that many of the degradation products will be harmful to both human health and the environment. Furthermore, it is known that some amine degradation products include amides and aldehydes as well as nitrosamines, which are potent carcinogens. Thus, of the thermophysical properties often considered in solvent selection for CO_2 capture, the volatility of the amines is very important, and should be given significant weight in any solvent design work in this area.[18]

High energy consumption

The energy input required for regenerating the solvent is decisive for the overall efficiency of the post-combustion technique. More specifically, CO_2 capture and separation requires a continuous supply of heat to the installation for the sorbent regeneration. The temperature of the heating medium supplied to the desorber should be heated to 393 K to regenerate the solvents. For examples, using MEA, the desorption process requires 2–5 MJ of heat per 1 kg of separated CO_2. Further potential savings can be obtained by selecting the amine solutions, optimal design and switching of the individual unit components as well as optimisation of the entire system in order to approach the thermodynamic limit.[12, 18]

Equipment corrosion

Equipment corrosion is another undesired operating problem in the CO_2 capture process using amines. It severely damages equipment, reduces operation efficiency and increases maintenance expenses. To minimize damage of plant units, inorganic or organic inhibitors are usually added to the amine solvent to prevent corrosion. Generally, the vanadium-containing compounds, especially sodium metavanadate ($NaVO_3$), are the most popular inorganic ones for CO_2 capture in MEA-treating plants, since they have less toxicity compared to other compounds,[11] while the most widely used organic

inhibitors for avoiding corrosion are the nitrogen-based surfactant inhibitors, such as imidazolines and their precursors.[19]

Overall, advanced solvent is of great importance for CO_2 capture processes, however, an appropriate selection of an attractive and possible commercializable solvent is very complex since it involves a series of steps from experiments in laboratory to pilot plant scales, as well as an accurate process simulation.

1.2.2. Membranes

The use of membranes for carbon capture and separation (e.g. CO_2/CH_4, CO_2/N_2) is a relatively novel technology and has gained significant attention as an alternative in comparison to traditional carbon capture technologies and is not being widely explored in detail.[20-21] It utilizes the differences in the diffusivity, solubility, absorption and adsorption abilities of different gases on different materials for specific gas capture and separation. Efforts to study membranes for CO_2 separation have mainly focused on a few different types of materials including polymers, zeolites and their derivatives, MOFs and COFs. Historically, polymeric-based membranes have been extensively studied owing to their low production costs, mechanical flexibility and ease of processability.[22] However, polymeric membranes suffer from short lifetimes and limited thermal and chemical stability.[20, 23] In recent years, MOFs and COFs have received increasing attention as viable materials for use in membrane-based gas adsorption and separation processes and considerable achievements have been made for increasing both the selectivity and permeability parameters in CO_2 capture and separation.[21, 24-26] In 2005, R. A. Fischer and C. Woll reported on the growth of the first pure MOF membrane, which serves as the basis for later developments in using MOF membranes for gas separation.[25] As this topic falls beyond the scope of this thesis, the readers are referred to some critical reviews on this type of materials.[21, 27-31]

1.2.3. Porous Solid Materials

Compared to the aforementioned approaches, CO_2 capture by physical adsorbents appears to be promising energy-efficient alternatives to the current state-of-art aqueous amine wet-scrubbing system. For this purpose, many physical adsorbents, such as zeolites and carbon-based materials, have been extensively evaluated and explored. Simultaneously, the emerging new classes of advanced porous materials, including MOFs and COFs, have been recognized as more promising candidates for carbon capture compared to the traditional porous adsorbents and have been comprehensively explored and studied in recent years. A brief description of the exploited porous materials will be given in the following paragraphs.

Zeolites

Zeolites are a class of crystalline porous aluminosilicates, whose frameworks are built of a periodic array of TO_4 tetrahedra (T = Si or Al) and they are amongst the most widely reported adsorbents for CO_2 capture in the patent and journal literature.[10] One of the most promising zeolites is 13X exhibiting a CO_2 uptake of 2-3 mmol/g at 0.1 bar (288-308 K), which is always regarded as the benchmark zeolite for CO_2 capture.[32] The gas adsorption and separation properties of zeolites are heavily dependent on the size, charge density as well as the chemical composition of cations in their porous structure.[2, 33] Thus, lots of research efforts have been directed towards obtaining zeolites with high surface area, large pore size or altering their composition of Si/Al ratio. Another research field of zeolites focuses on the exchange with alkali or alkali-earth cations (e.g. Na^+, K^+, Ca^{2+}, Mg^{2+}) in the structure of zeolites to enhance their CO_2 adsorption performance.[34] However, the low selectivity of CO_2 over other gases (e.g. N_2, CH_4, H_2, hydrocarbons) and rapid decline of their adsorption capacities with increasing temperature and presence of moisture and impurities needs to be addressed before they can be widely applied in practice.[35]

Carbon-based adsorbents

Carbon-based materials received great interest for CO_2 capture owing to their wide availability, low cost, high thermal stability and surface tunability.[36-37] However, the weak physical CO_2 adsorption of carbon materials leads to a high sensitivity to temperature and relatively low selectivity in operation. As a consequence, current research of this field mainly focuses on improving the CO_2 adsorption performance via two approaches: (1) increasing the surface area and tuning the pore structure of the carbon materials, either by using different precursors or forming different structures, such as carbon nanotubes, carbon molecular sieves; (2) increasing the alkalinity by impregnation of basic additives or incorporation of basic nitrogen-containing groups. A brief summary of the current research activities on carbon-based CO_2 adsorbents is summarized in Figure 1.6.
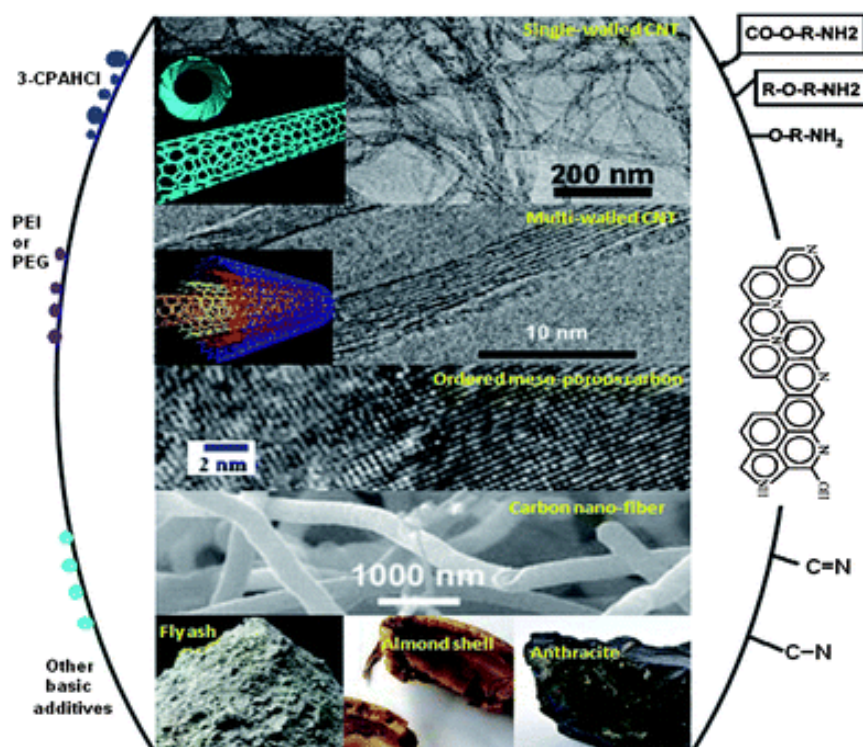
Figure 1.6. A summary of current research activities on carbon-based CO_2-adsorbents. The middle part shows the types of carbon adsorbents that have been studied, the left part shows the impregnation or grafting of basic additives, and the right part shows the incorporation of N-containing groups.[2]

Metal Organic Frameworks

Metal Organic Frameworks (MOFs), also known as Porous Coordination Polymers (PCPs), are a rapid growing class of crystalline porous materials that are built from inorganic units (metal ions or metal clusters) connected by organic ligands to form an ordered, porous network in one or more dimensions (Figure 1.7). The flexibility with which the constituents' geometry, size and functionality can be varied has led to more than 20,000 MOFs being reported and studied since the pioneer Yaghi reported the first metal organic framework in 1995.[38]
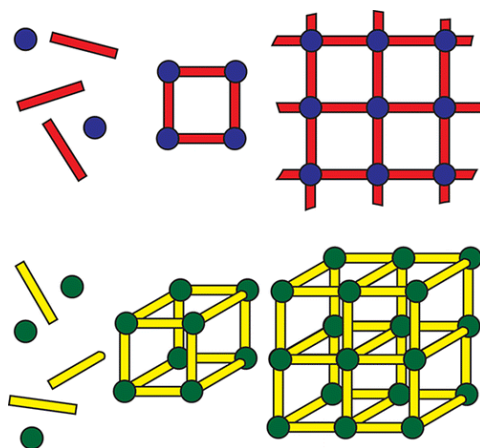
Figure 1.7. Schematic build-up of metal-organic frameworks with ligands (rods) connected through metal ions (circles) (Adapted from reference [39]).

A general timeline for the development of MOFs is provided in Figure 1.8, which is expected to give the readers a launching point to this vast and rapidly growing field of materials and corresponding properties. Importantly, the large surface areas, framework flexibility, tunable pore sizes as well as tailor-made framework functionalities of this type of materials over the traditional porous materials empower them as ideal platforms for the development of next generation selective CO_2 capture materials. In this regard, since the first reported MOF, denoted as MOF-2, was explored for CO_2 adsorption in 1998,[24] significant efforts and extensive achievements have been made in recent years for improving the gas adsorption and separation performance of metal organic frameworks. Generally, the gas adsorption and separation performance of

MOFs can be improved by precisely tuning the pore size or incorporation of task-specific functional groups, doping metals, introduction of weakly basic nitrogen groups or open metal sites. For example, as far as low pressure CO_2 adsorption, Mg-MOF-74 performs the best, exhibiting the CO_2 uptake of 8.6 mmol/g (37.8 %) at 298 K and 1 bar,[40] while both MOF-210 and MOF-200 currently hold the CO_2 storage record with the saturated CO_2 adsorption capacity of 2400 mg/g (54.5 mmol/g) at room temperature and 50 bar.[41] The benchmark MOFs for CO_2 capture at both low and high pressures are listed in Table 1.1.
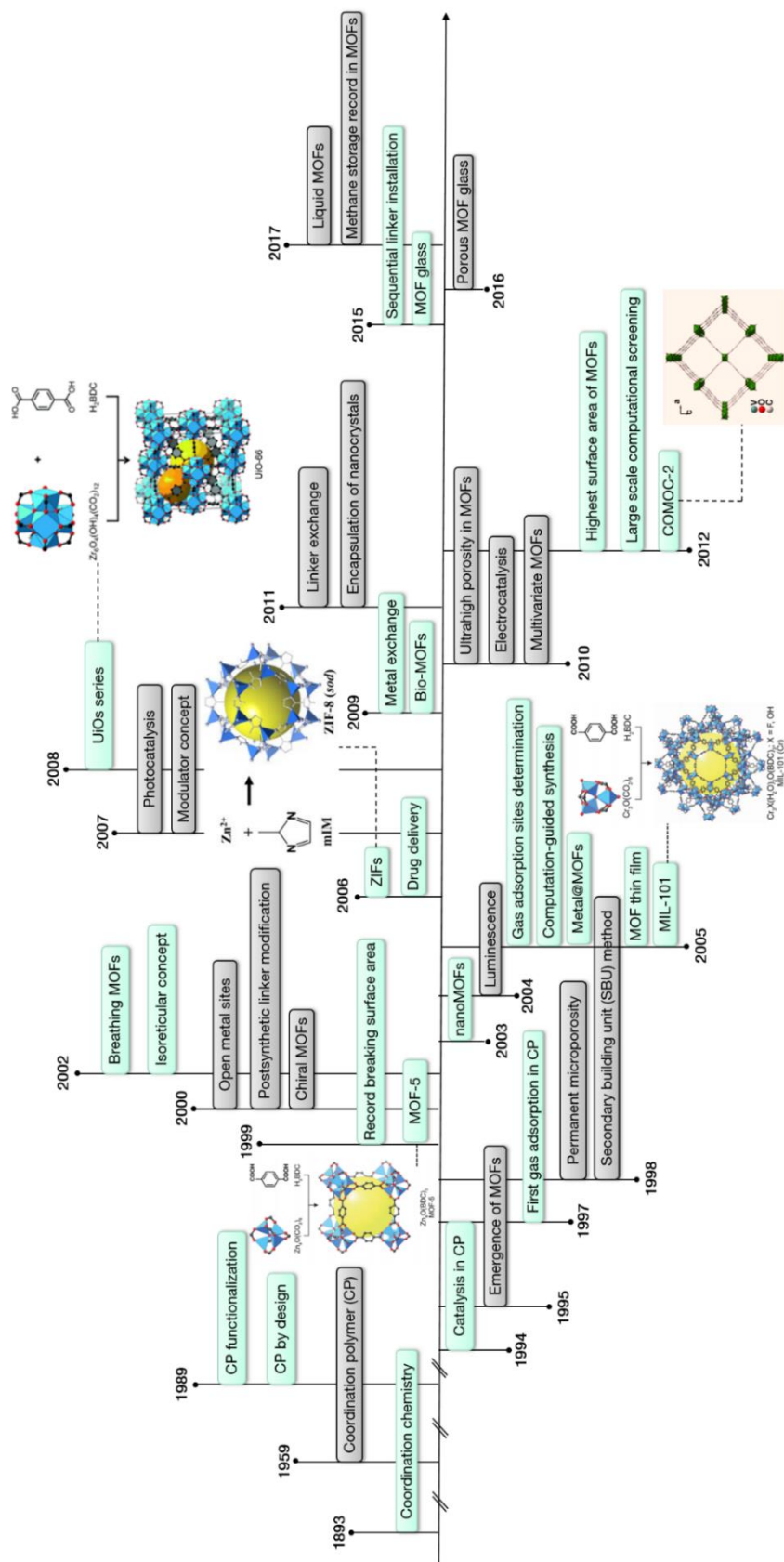
Figure 1.8. A timeline showing some of the breakthroughs in the discovery of MOF nanostructures.

Table 1.1. Current benchmark MOFs for CO_2 adsorption at both low and high pressures.

MOF	Temperature (K)	CO_2 uptake (mmol/g)	Pressure (bar)	MOF	Temperature (K)	CO_2 uptake (mmol/g)	Pressure (bar)
Mg-MOF-74	298	8.6	1	MOF-210	298	54.5	50
	296	8.0	1	MOF-200	298	54.5	50
$Cu_3(BTC)_2(H_2O)_{1.5}$ (hydrated 4 wt%)	298	8.4	1	NU-10	298	46.4	40
Co-MOF-74	298	7.5	1	MOF-205	298	38.1	50
MAF-X25ox	298	7.1	1	MIL-101	303	40	50
Ni-MOF-74	298	7.1	1	MOF-177	298	35	45

Methane, as the main component of natural gas, is considered to be an important candidate for clean transportation fuels. The storage of methane by using adsorbents has been pursued extensively as an alternative to compressed gas storage at high pressure. However, none of the conventional adsorbents have afforded sufficient CH_4 storage to meet the conditions required for commercial viability. In 2012, the US Department of Energy (DoE) set the ambitious volumetric storage target for adsorbed natural gas to 263 cm^3 (STP) cm^3 at room temperature and 65 bar.[3] To achieve higher adsorption capacity, it is necessary to ensure that micropores with sizes well suited to methane molecules are densely and uniformly distributed in the porous solid. MOFs are therefore good candidates as adsorbents for CH_4 storage because of their unique features. To our delight, in 2018, a sol-gel monolithic MOF (monoHKUST-1) was reported and the working capacity of this MOF material can reach up to 259 cm^3 (STP) cm^3,[42] reaching the target of DoE for CH_4 storage and holding the highest value reported to date for all kinds of porous adsorbents (Table 1.2).

Table 1.2. The benchmark MOFs with high CH_4 adsorption capacity up to 65 bar.

MOF	Temperature (K)	Total CH_4 uptake (cm^3/cm^3)	Working capacity (cm^3/cm^3)
DOE target	298	700 cm^3/g	263
monoHKUST-1	298	-	259
HKUST-1	298	267	183
UTSA-76a	298	257	187
MFM-115a	298	238	181
UTSA-110a	298	241	190
Al-soc-MOF-1	298	197	169

Working capacity is obtained between 5 bar and 65 bar.

Apart from CO_2 capture, the separation of CO_2/CH_4 and CO_2/N_2 is also of great importance in many industrial processes such as natural gas sweetening, biogas upgrading, oil recovery enhancement and landfill gas purification.[43] MOFs, as promising candidates, have been extensively studied for this application. However, due to the differences of the measurement conditions, it is difficult to conclude which material shows the best performance. The readers are referred to some critical reviews for clarification.[44-47]

As a potential renewable and clean energy source, the use of hydrogen as an alternative fuel would result in much lower CO_2 emission. To advance the move towards a hydrogen economy, the storage of H_2 seems to be the most important step. Among the different adsorbents, the use of MOF materials for H_2 storage systems is regarded as particularly promising and few MOFs have shown exciting results for H_2 storage.[48-52] Recently, the group of Farha and Hupp reported a benchmark study of hydrogen storage in a series of MOFs under temperature and pressure swing conditions. Remarkably, some of the tested fourteen MOFs exceeded the volumetric DoE 2025 target (40g/L) and a reasonable linear correlation between the pore volume and deliverable gravimetric capacity was observed (Figure 1.9).[53]
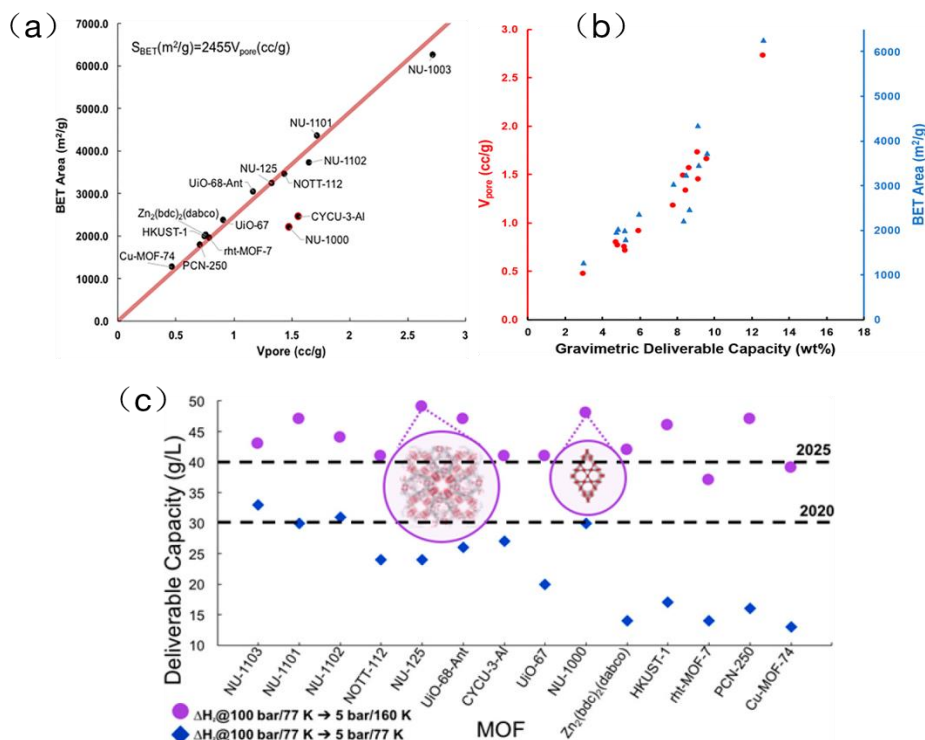
Figure 1.9. (a) Plot of BET area against pore volume. Roughly 1 cc/g pore volume gives about 2500 m^2/g BET area. (b) Plot of pore volume (red circles) and BET area (blue triangles) against gravimetric deliverable capacity. capacity with increasing pore volume (c) Volumetric H$_2$ deliverable capacity of the MOFs studied under different temperature and pressure conditions (Reproduced from[53]).

Covalent Organic Frameworks (COFs)

COFs, firstly discovered by Yaghi and co-workers in 2005,[54] are newly emerged crystalline porous materials that are constructed with organic building blocks via strong covalent bonds, whose structures can be precisely predetermined by molecular building blocks using reticular chemistry.[55] A brief timeline concerning the developments in the field of COFs is provided in Figure 1.10 to give the readers a better understanding on the history of this type of materials.
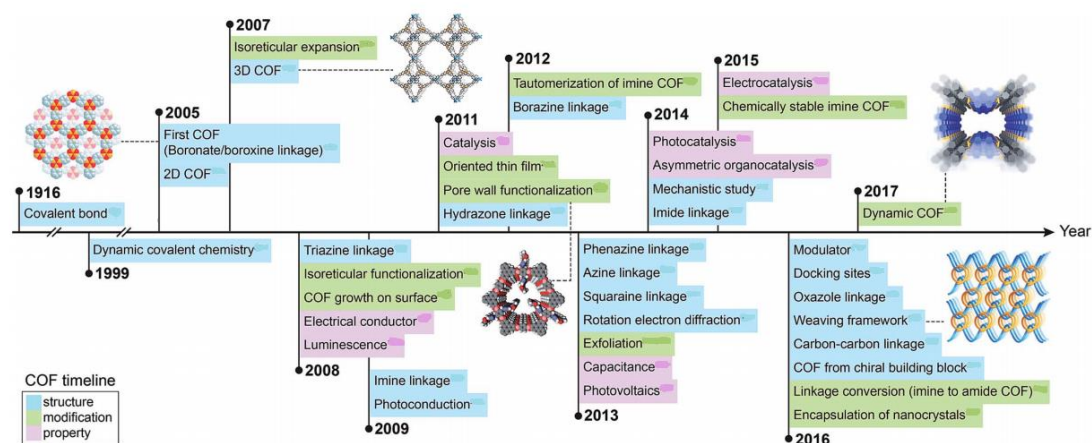
Figure 1.10. A general timeline on the history of COFs, as reproduced from[55].

Until now, there have been several different types of reversible reactions for the formation of COFs, as summarized in Figure 1.11. Recently, COFs have been proposed as promising candidates for CO_2 capture because of the fact that they process almost all the merits of MOFs having a high CO_2 adsorption capacity, great CO_2 selectivity over other gases, structural diversities, high permanent porosities, low density as well as high thermal and chemical stabilities. Since the first report on COFs for CO_2 adsorption in 2009,[56] great efforts have been made to improve the CO_2 capture performance of this type of materials and rapid research progress has been achieved. The benchmark COF for CO_2 adsorption at low pressure is claimed to be PPF-1, which exhibits the CO_2 uptake of 136 cm^3/g (5.99 mmol/g) at 273 K and 1 bar,[57] relatively lower than that of MOFs and CTFs, while COF-105 represents the benchmark COF for H_2 storage (10 wt% at 77 K and 80 bar).[53, 56] However, some aspects are necessary to obtain significant improvements in this area, including the construction of 3D COFs with high surface areas and pore volumes for high-pressure gas storage or precisely tuning the pore size and functionalities of COFs for efficient gas separation (e.g. CO_2/N_2, CO_2/CH_4 and C_3H_6/C_3H_8 etc.).

As stated in the review of Zhao et al.[58], taking all the parameters (e.g. gas adsorption and separation performance and chemical stability) into account, both imine and triazine-based COFs will tentatively have broader prospects for

the application of CO_2 capture. However, there is still a long but prospective way to go for their further applications in this area.
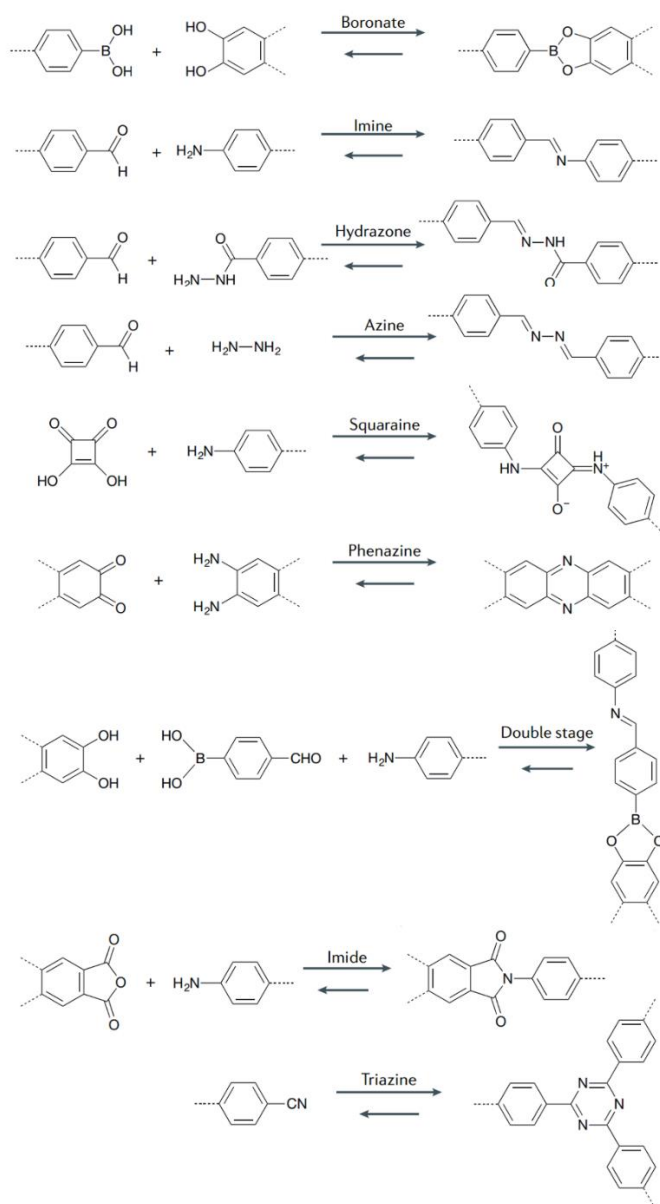
Figure 1.11. Diversity of linkages for the formation of COFs (Adapted from [59]).

1.3. Covalent Triazine Frameworks (CTFs)

1.3.1. Introduction of Covalent Triazine Frameworks

The polymerization of aromatic nitriles under Lewis acid assisted conditions can date back to 1960s reported by W. G. Toland and S. Rafael.[60] They reported on the trimerization of benonitrile and aromatic dinitriles to form

aromatic substituted triazines employing certain metal salts as catalysts, in which the catalysts, catalyst concentration as well as the reaction time and temperature have great influence on the polymerization process. In 1973, G. H. Miller (Texaco Inc.) employed several nitriles as monomers to obtain a set of highly stable crosslinked polymers and the approach of mixed-ligands was also applied in this study.[61] At that time the term of covalent triazine frameworks (CTFs) was not coined yet and researchers mainly focused on the process of polymerization without analyzing the potentially porous nature of the materials. It took this class of materials more than three decades to achieve the "scientific breakthrough" and regain attention by the scientific community. In 2008, the concept of CTFs was firstly adapted and reported by Kuhn, Thomas and Antonietti.[62] Targeting at the synthesis of polymers with tunable functionalities and intrinsic porosities, they developed CTFs as a high-performance class of materials with exceedingly high thermal and chemical stability, high porosity as well as numerous nitrogen-sites due to the presence of triazine functionalities within the structures. In this work they introduced five different monomers to prepare the CTF materials and the first covalent triazine framework, denoted as CTF-1, was prepared via dynamic trimerization of 1,4-dicyanobenzene (pDCB) in molten $ZnCl_2$ at 400 °C (Figure 1.12). The molten $ZnCl_2$ acts both as Lewis-acidic reaction medium with high solubility for the monomers and as catalyst for the trimerization reaction during synthesis.[62] Here in this thesis we will refer to CTFs as any porous materials which have been synthesized by the trimerization of aromatic nitriles.
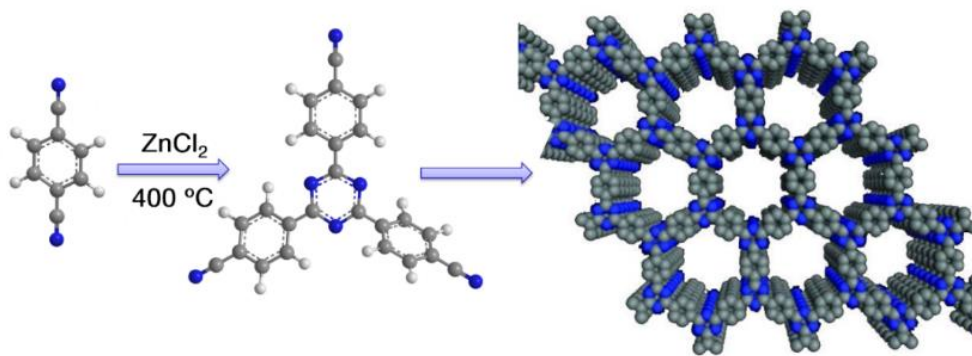
Figure 1.12. Idealized schematic formation of CTF-1 by trimerization of 1,4-dicyanobenzene in molten $ZnCl_2$ under ionothermal conditions.

In principle, a huge variety of monomers (building blocks) with varying aromatic structure elements can be used to give access to a broad range of materials with tunable properties in terms of steric effects or doping with different heteroatoms. In this manner, the properties of this type of materials including porosity, pore size, specific surface area, nitrogen content as well as the surface functionalities and polarities can be easily adjusted for the task-specific applications. In addition to these tunable physical and chemical properties, the exceptionally high stability of these materials in water, acid, base as well as common organic solvents make them promising candidates for numerous applications under harsh reaction conditions. Consequently, considerable efforts have been devoted to rationally design and synthesize various CTF materials and explore their possible applications. A summary of the building blocks which have been used for the preparation of CTFs in literature so far is shown in Figure 1.13.

Figure 1.13. An overview of the building blocks used for the construction of CTFs.

1.3.2. Synthesis Strategies of CTFs

For the preparation of triazine-based porous covalent organic polymers,

various synthesis approaches have been discussed and developed in literature,[63-64] however, based on the aim of this thesis, in the following we will mainly discuss the approaches of CTF preparation via trimerization of aromatic nitriles, including ionothermal synthesis, Brønsted acid synthesis and sulfur-mediated route (Figure 1.14).
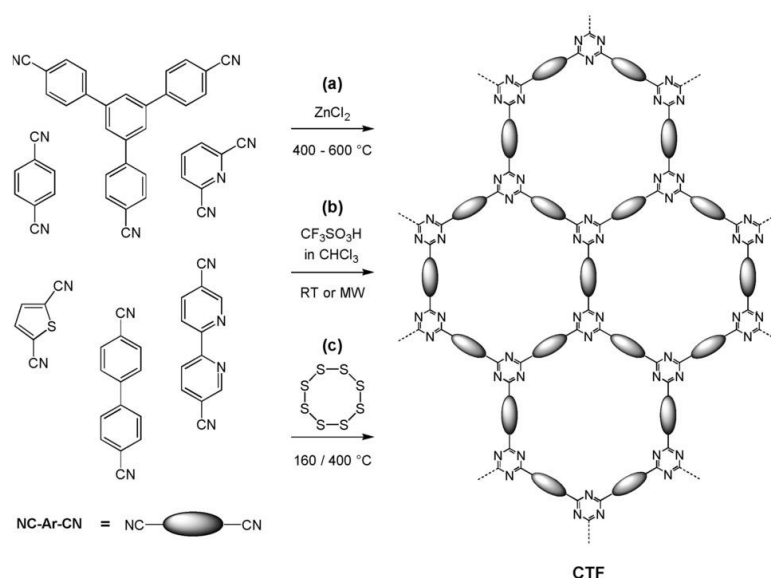
Figure 1.14. CTF synthesis procedures starting from various monomers, comprising (a) ionothermal synthesis, (b) Brønsted acid synthesis and (c) sulfur-mediated route (Adapted from[64]).

Ionothermal Synthesis

The concept of ionothermal synthesis was firstly reported by R. E. Morris in 2004 for the synthesis of zeolite analogues with an ionic liquid instead of water which acts both as the solvent and the structure directing agent at high temperature (400 °C) and pressure.[65] As reported in the first CTF publication by Antonietti et al., they developed the approach by dynamic trimerization of nitriles in molten $ZnCl_2$ at high temperature, triazine-based materials with high porosity properties can be obtained that are similar in performance to zeolites and $ZnCl_2$ acts as solvent and catalyst for the trimerization reaction.[62] Typically, the respective monomer and $ZnCl_2$ were transferred into an ampoule, which was evacuated, sealed and heated at 400 °C for 40/48 h and the black porous

CTF materials were obtained after further purification steps (Figure 1.15). It should be noted that most of the reported CTF materials prepared using this approach are amorphous except for CTF-0[66], CTF-1[62] and CTF-2[67], which are crystalline porous frameworks.
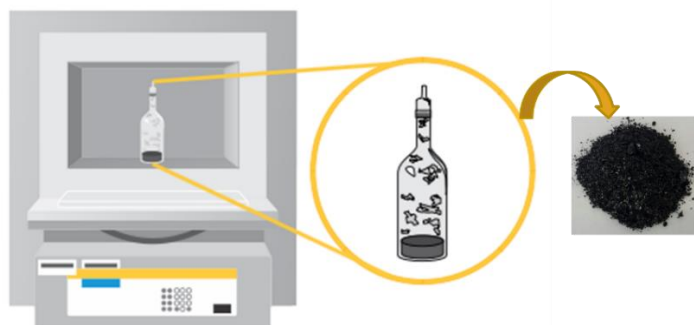
Figure 1.15. Representation of the preparation of the porous CTF materials.

In the following, a comprehensive overview of the influence of various reaction parameters such as the temperature and monomer concentration as well as the geometry and functionalities of the monomers on the outcome of the polymerization reaction in terms of chemical nature and porous properties of the materials is proposed by the same group.[68] As discussed in this study, high reaction temperature during the ionothermal synthesis can be employed to increase the porosity and surface area while it also comes at a cost: irreversible carbonization taking place leads to a loss of nitrogen, defects in the frameworks as well as rather undefined surface functionalities, thus the materials can better be described as nitrogen-doped carbons rather than triazine-based frameworks. In this manner, so far the highest reported specific surface area and pore volume for CTFs can reach up to 3300 m^2/g and 2.4 cm^3/g when a temperature of 600 °C was applied after a preformation step at 400 °C.[69]

Brønsted Acid Synthesis

In 2012, Cooper et al. reported an alternative approach for the synthesis of

CTFs.[70] They employed CF_3SO_3H as the catalyst to trimerize the aromatic nitriles under both room temperature and microwave conditions, which offered significant advantages by avoiding $ZnCl_2$ residual in the frameworks, decomposition of nitriles as well as carbonization of the materials. The resulting porous materials are typically pale yellow or brown in contrast to the black materials synthesized under ionothermal conditions, making them attractive for photocatalytic or sensing applications. Due to the mild reaction conditions, the Brønsted Acid approach can also be used to synthesize porous CTF membranes by spreading thin films of the acidic nitrile solution onto flat glass discs and heating it at 100 °C.[71] Nevertheless, some critical drawbacks of this methodology limit its widespread feasibility, such as high cost of the catalyst, low synthesis temperature required, unavailability for heteroatomic monomers, difficulty in handling the reaction due to corrosive and eye irritating carcinogenic chemicals involved as well as ice cold brine solution necessary for neutralization.[63]

Sulfur-mediated Route

Appart from the aforementioned two typical methods, more recently, the group of Coskun reported that CTFs can be prepared via a sulfur-mediated route without any catalysts or solvents.[72-73] Within this approach, CTFs are formed in the presence of elemental sulfur via in-situ vulcanization at 400 °C and the obtained CTFs show great potential as a cathode material for Lithium-Sulfur batteries. However, the limited possible applications of this type of obtained CTF materials hinder its widespread developments.

1.3.3. Applications of CTFs

Since the discovery of CTFs by the group of Thomas in 2008, this type of materials has been extensively exploited in a wide range of applications, including gas sorption and separation,[74-88] heterogeneous catalysis,[89-105] adsorption of toxic organic compounds (e.g. dyes,[106-107] aromatics,[108]

surfactants[109] or hazardous compounds[110]), sensing and detection (e.g. ammonia,[111] nitroaromatics[112-113]) as well as lithium batteries[72-73, 114-115] due to their remarkable surface area, low skeleton density, exceptional high thermal and chemical stability as well as enhanced tunability and functionality. Since the main aim of this thesis is designing novel CTF materials for the application of gas adsorption and separation, discussion of each application falls beyond the scope of this thesis. In the following we will mainly focus on the application of gas adsorption and separation and for other applications, the readers are referred to some critical reviews.[63-64, 116].

Gas Storage and Separation

As mentioned at the beginning of this chapter, CTFs have been recognized as promising platforms for gas storage and capture owing to the tunable modification of their pore size and functionalities by selecting the appropriate building blocks. From the view of the pore structures, it has been shown that ultramicropores are beneficial for selective CO_2 capture and for this reason tremendous efforts have been made to improve the gas adsorption capacities or selectivities of CTF materials. Lotsch et al. reported on a series of nitrogen-rich CTF materials as high-performance platforms for selective carbon capture and storage.[77] With the wide range of sorption data at hand, they proposed some general trends in the gas adsorption behavior within the CTF familiy and nitrogen-containing porous polymers in general, revealing the dominant role of the micropore volume for maximum CO_2 uptake, while the nitrogen content is a secondary effect enhancing the CO_2 adsorption performance. In contrast, the high CO_2 over N_2 selectivities are largely attributed to the nitrogen content. In the report of Zhong et al., a class of CTFs with ultramicropores and high nitrogen content were prepared for highly selective CO_2 capture. Especially, CTF-FUM-350 exhibited a significantly high CO_2/N_2 (102.4) and CO_2/CH_4 (20.5) selectivity at 298 K.[81] The approach of mixed-ligand for the preparation of

CTFs was reported by Janiak et al., in which the higher CO_2-accessible micropores volume and higher micropore volume fraction ($V_{0.1}/V_{tot.}$) was assigned to be the dominant factor for the enhanced CO_2 adsorption performance.[84] On the other hand, from the aspect of chemical composition, the incorporation of preferential CO_2-philic functionalities (e.g. nitrogen,[77, 86, 88] oxygen,[83, 117] fluorine,[74, 87, 118] et al.) into porous materials to induce strong electrostatic interactions between the CO_2 molecules and the material surface has been regarded as a useful route to improve their CO_2 adsorption capacities and selectivities. Jian et al., employed a series of N-heterocyclic phthalazinone monomers to prepare porous ether-linked phthalazinone-based CTFs (PHCTFs) with electron-rich N/O atoms (Figure 1.16) and one of the prepared CTFs (PHCTF-5) exhibited a significantly high CO_2/N_2 selectivity of 138.[117]
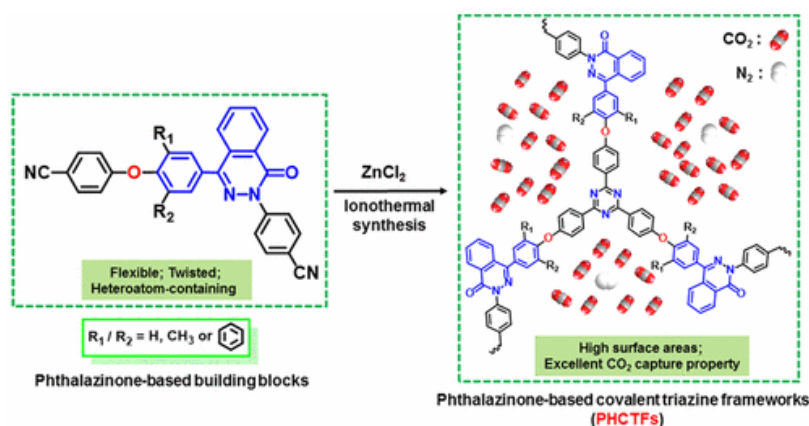
Figure 1.16. Preparation routes of the ideal phthalazinone-based covalent triazine frameworks (Adapted from[117]).

Very recently, Dai et al. reported on an in situ doping strategy for the preparation of hexaazatriphenylene-based conjugated triazine frameworks (Figure 1.17). The synergistic effects of ultrananoporosity and rich N/O codoped CO_2-philic sites bestow the framework (HAT-CTF-450/600) with an exceptionally high CO_2 uptake (6.3 mmol/g, 273 K and 1 bar), which represents the highest value for all the reported CTFs until now.[83] More importantly, this material can adsorb up to 3.0 mmol/g CO_2 at 0.15 bar/273 K, where the pressure is more relevant to practical carbon capture since flue gas contains

approximately 15% CO_2 at a total pressure of 1 bar.

Figure 1.17. Synthesis route of the proposed O-doped HAT-CTFs (Adapted from[83]).

In search of a particular functionality for some task-specific applications, fluorine groups have been regarded as a suitable candidate because of the fact that (1) the high electronegativity of F can further promote CO_2 adsorption through electrostatic interaction; (2) F groups can effectively reduce the micropore size to < 0.5 nm, thus facilitating CO_2 uptake and CO_2/N_2 separation by kinetic selectivity and (3) the hydrophobic C-F bonds can upgrade the materials tolerant to water. Along this line, Han et al. reported on the first perfluorinated covalent triazine-based framework (FCTF-1) for selective CO_2 capture by using tetrafluoroterephthalonitrile as the monomer (Figure 1.18).[74] Remarkably, the material of FCTF-1-600 exhibited a significantly high CO_2 uptake of 5.53 mmol/g at 273 K and 1 bar and an exceptional CO_2/N_2 selectivity of 77 under kinetic flow conditions.
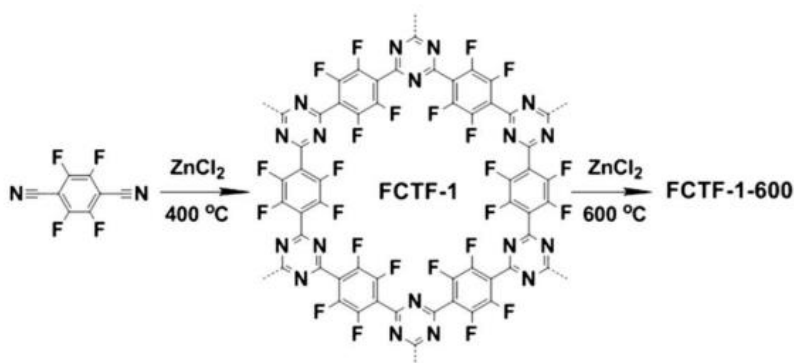
Figure 1.18. Reaction schemes and ideal structures of FCTF-1-600 synthesized through the trimerization of tetrafluoroterephthalonitrile (Reproduced from[74]).

Furthermore, Liu et al. reported on a set of fluorinated microporous organic polymers (F-MOPs), showing a twofold increase in the CO_2 adsorption capacity in comparison to the corresponding non-fluorinated MOPs due to the electrostatic interactions with the polar C-F bonds in the skeleton.[118] As a potential renewable and clean energy source, hydrogen storage remains challenging and the use of adsorbent materials for H_2 storage offers an appealing alternative to current H_2 transport technologies. Thomas et al., examined for the first time the H_2 storage potential of CTFs on DCBP (DCBP = 4,4'-biphenyldicarbonitrile) network, which can adsorb 1.55 wt% H_2 at 77 K and 1 bar.[62] Janiak et al., employed a novel tetranitrile as the monomer to obtain a porous CTF material (PCTF-1) with high surface area (2235 m^2/g) and significantly high H_2 uptake (1.86 wt% at 77 K and 1 bar).[119] A fluorene based covalent triazine framework (fl-CTF-400) with the H_2 adsorption capacity of 1.95 wt% was reported by Lotsch et al.[75], who reported later on a series of N-rich CTFs with exceptionally high H_2 uptake (2.1 wt% at 77 K and 1 bar).[77] In the report of Giambastiani et al., the synthesis and characterization of four CTF samples obtained from 1,3-dicyanobenzene (1,3-DCB) and 2,6-dicyanopyridine (2,6-DCP) at high temperatures were described (Figure 1.19) and more interestingly, the material of CTF-py[HT] exhibit the H_2 adsorption capacity of 2.63 wt% (13.02 mmol/g) at 77 K and 1 bar, which represents the highest value among all the CTF materials reported in literature up to now.[86]
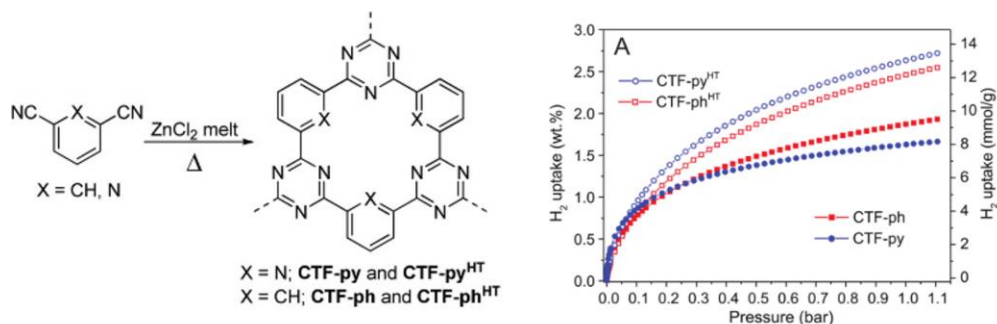
Figure 1.19. Schematic representation of the synthesis of CTFs (left); H_2 adsorption isotherms of the studied CTF materials measured at 77 K (right) (Adapted from[86]).

A systematical comparison of the gas adsorption capacities and selectivities

of the reported CTF materials in literature is summerized in Table 1.3.

Table 1.3. A summary of selected state-of-the-art CTF materials for carbon dioxide capture and separation (up to 1 bar).

Samples	S_{BET} (m²/g)	CO₂ uptake (mmol/g)		H₂ uptake (wt%)	Q_{st}^{max} (kJ/mol)	CO₂/N₂[a] Selectivity	CO₂/CH₄[a] Selectivity
		273K	298K	77 K			
HATCTF450/600	1090	6.3	4.8	-	27.1	126	-
F-DCBP-CTF-1	1574	5.98	3.82	1.77	33.1	31	-
CTF-py^{HT}	3040	5.97	4.22	2.63	27.1	29	-
Bipy-CTF-600	2479	5.58	2.95	2.1	34.4	37	-
HATN-CTF-2	1684	5.57	3.53	1.74	32.6	33	7.8
F-CTF-1-600	1535	5.53	3.41	-	32	19[b]	-
F-DCBP-CTF-2	1126	5.23	3.16	-	-	22	-
CTF-py	1239	5.08	3.79	1.63	35.1	45	-
CTF-BI-11	1549	4.93	2.63	-	-	34.3[b]	-
TPC-1	1940	4.9	2.47	2.02	32	38[b]	5[b]
MM2	1360	4.77	3.13	1.74	32	23[b]	5[b]
FCTF-1	662	4.67	3.21	-	35	31[c]	-
PCTF-4	1404	4.66	2.86	1.3	31.5	56	20[b]
lut-CTF400	968	4.55	2.72	1.36	37.5	63	-
CTF-ph	1991	4.54	3.05	1.87	33.2	20	-
FCTF-20-400	2060	4.54	2.67	1.88	29	21	5.6
CTF-ph^{HT}	2675	4.17	2.69	2.46	25.4	11	-
fl-CTF-400	2862	4.13	1.97	1.95	30.7	15	-
PHCTF1c	1845	3.89	2.27	1.92	16	12	12[b]
CTF-FUM-350	230	3.49	2.55	-	58.1	102.4	20.5
CTF-20-400	1458	3.48	2.09	1.5	22	19	-
bpim-CTF-400	786	2.85	2.46	-	31	32[b]	-
CTF-1	746	2.47	1.41	-	27.5	20[c]	-

a. The selectivity is calculated at 298 K by Henry Model; b. The selectivity is calculated by

Henry Model at 273 K; c. The selectivity is calculated by Ideal Adsorbed Solution Theory (IAST).

1.4. Aim of the Thesis

With the booming growth of economy, the global climate changes caused by burning of fossil fuels and emission of greenhouse gases (mainly CO_2) have become a severe problem. To address this issue and keep the CO_2 concentration at a safe level, exploring more cost-effective and scalable techniques for reducing CO_2 concentration is challenging and urgently required for human beings. As a new emerging class of advanced porous materials, CTFs have exhibited exceptionally high chemical and thermal stabilities under harsh conditions in addition to high surface areas, large pore volumes and diverse structural tunabilities and functionalities. Compared with other traditional adsorbents (e.g. zeolites or activated carbons), this type of materials have been regarded as promising and potential adsorbents for the application of carbon capture and separation. As reported in literature, incorporation of strong CO_2-philic sites (such as N, O and F) into the structures of porous materials is an efficient approach to achieve remarkable carbon capture and separation performances. Along this line, the overall aim of this thesis is adopting this efficient approach to prepare novel CTF materials by designing and synthesizing a set of unique nitrogen- or fluorine-rich building blocks and systematically investigates their gas adsorption and separation properties.

In **Chapter 2**, we aimed to synthesize a novel N-heteroaromatic tetranitrile as the building block for the preparation of nitrogen-rich CTF materials, which serve as high-performance platforms for carbon capture and separation. The influence of several parameters such as the $ZnCl_2$/monomer ratio and reaction temperature on the structure and porosity of the resulting frameworks were systematically examined. It is well known that the incorporation of fluorine groups into MOFs can significantly improve the materials' gas adsorption

performance and it has been extensively studied, however there are only limited few reports concerning fluorinated CTFs. In **Chapter 3**, we attempted to obtain a series of fluorine functionalized CTFs via the introduction of fluorine groups into the aforementioned tetranitrile building block to further improve the gas adsorption and separation properties of the obtained CTF materials. The aim of **Chapter 4** was to explore how the CO_2-philic sites (nitrogen sites) affect the materials' gas adsorption and separation performance. Thus, a novel nitrogen-rich hexaazatrinaphthalene-based nitrile was prepared for the first time as the building block for the synthesis of novel hexaazatrinaphthalene-based CTF materials, which were thoroughly characterized and examined for carbon capture and separation. In **Chapter 5**, we aimed to obtain a perfluorinated hydrophobic CTF materials by functionalization of the monomer of 4,4'-biphenyldicarbonitrile and the effects of fluorine groups on the gas adsorption and separation properties were studied in detail.

In **Chapter 6**, the most important results obtained in this thesis were highlighted and discussed. Suggestions for further research are proposed, including perspectives on improving the CO_2 adsorption and separation performances and possibility for practical and realistic applications.

1.5. References

1. Rochelle, G. T., Amine Scrubbing for CO_2 Capture. *Science* **2009**, *325* (5948), 1652.

2. Wang, Q.; Luo, J.; Zhong, Z.; Borgna, A., CO_2 capture by solid adsorbents and their applications: current status and new trends. *Energy Environ. Sci.* **2011**, *4* (1), 42-55.

3. Lin, Y.; Kong, C.; Zhang, Q.; Chen, L., Metal-Organic Frameworks for Carbon Dioxide Capture and Methane Storage. *Adv. Energy Mater.* **2017**, *7* (4), 1601296.

4. See the website:. *https://www.esrl.noaa.gov/gmd/ccgg/trends/* **2018**.

5. Yu, J.; Xie, L.-H.; Li, J.-R.; Ma, Y.; Seminario, J. M.; Balbuena, P. B., CO_2 Capture and Separations Using MOFs: Computational and Experimental Studies. *Chem. Rev.* **2017**.

6. Zou, L.; Sun, Y.; Che, S.; Yang, X.; Wang, X.; Bosch, M.; Wang, Q.; Li, H.; Smith, M.; Yuan, S.; Perry, Z.; Zhou, H. C., Porous Organic Polymers for Post-Combustion Carbon Capture. *Adv Mater* **2017**, *29* (37), 1700229-n/a.

7.   Cuéllar-Franca, R. M.; Azapagic, A., Carbon capture, storage and utilisation technologies: A critical analysis and comparison of their life cycle environmental impacts. *J. CO₂ Util.* **2015,** *9,* 82-102.

8.   Haszeldine, R. S., Carbon Capture and Storage: How Green Can Black Be? *Science* **2009,** *325* (5948), 1647.

9.   Carbon capture and utilization. *http://co2chem.co.uk/.*

10.   D'Alessandro, D. M.; Smit, B.; Long, J. R., Carbon Dioxide Capture: Prospects for New Materials. *Angew. Chem. Int. Ed.* **2010,** *49* (35), 6058-6082.

11.   Liang, Z.; Fu, K.; Idem, R.; Tontiwachwuthikul, P., Review on current advances, future challenges and consideration issues for post-combustion CO_2 capture using amine-based absorbents. *Chin. J. Chem. Eng.* **2016,** *24* (2), 278-288.

12.   Stowe, H. M.; Hwang, G. S., Fundamental Understanding of CO_2 Capture and Regeneration in Aqueous Amines from First-Principles Studies: Recent Progress and Remaining Challenges. *Ind. Eng. Chem. Res.* **2017,** *56* (24), 6887-6899.

13.   Danckwerts, P. V., The reaction of CO_2 with ethanolamines. *Chem. Eng. Sci.* **1979,** *34* (4), 443-446.

14.   Caplow, M., Kinetics of carbamate formation and breakdown. *J. Am. Chem. Soc.* **1968,** *90* (24), 6795-6803.

15.   Gouedard, C.; Picq, D.; Launay, F.; Carrette, P. L., Amine degradation in CO_2 capture. I. A review. *Int. J. Green h. Gas Control* **2012,** *10,* 244-270.

16.   Blanchard, L. A.; Hancu, D.; Beckman, E. J.; Brennecke, J. F., Green processing using ionic liquids and CO_2. *Nature* **1999,** *399,* 28.

17.   Xu, J.; Wang, S.; Yu, W.; Xu, Q.; Wang, W.; Yin, J., Molecular Dynamics Simulation for the Binary Mixtures of High Pressure Carbon Dioxide and Ionic Liquids. *Chin. J. Chem. Eng.* **2014,** *22* (2), 153-163.

18.   MacDowell, N.; Florin, N.; Buchard, A.; Hallett, J.; Galindo, A.; Jackson, G.; Adjiman, C. S.; Williams, C. K.; Shah, N.; Fennell, P., An overview of CO_2 capture technologies. *Energy Environ. Sci.* **2010,** *3* (11), 1645-1669.

19.   Jovancicevic, V.; Ramachandran, S.; Prince, P., Inhibition of Carbon Dioxide Corrosion of Mild Steel by Imidazolines and Their Precursors. *CORROSION* **1999,** *55* (5), 449-455.

20.   Trickett, C. A.; Helal, A.; Al-Maythalony, B. A.; Yamani, Z. H.; Cordova, K. E.; Yaghi, O. M., The chemistry of metal–organic frameworks for CO_2 capture, regeneration and conversion. *Nat. Rev. Mater.* **2017,** *2,* 17045.

21.   Qiu, S.; Xue, M.; Zhu, G., Metal-organic framework membranes: from synthesis to separation application. *Chem. Soc. Rev.* **2014,** *43* (16), 6116-6140.

22.   Robeson, L. M., Correlation of separation factor versus permeability for polymeric membranes. *J. Membr. Sci.* **1991,** *62* (2), 165-185.

23. Robeson, L. M., The upper bound revisited. *J J. Membr. Sci.* **2008,** *320* (1), 390-400.

24. Li, H.; Eddaoudi, M.; Groy, T. L.; Yaghi, O. M., Establishing Microporosity in Open Metal–Organic Frameworks: Gas Sorption Isotherms for Zn(BDC) (BDC = 1,4-Benzenedicarboxylate). *J. Am. Chem. Soc.* **1998,** *120* (33), 8571-8572.

25. Hermes, S.; Schröder, F.; Chelmowski, R.; Wöll, C.; Fischer, R. A., Selective Nucleation and Growth of Metal–Organic Open Framework Thin Films on Patterned COOH/CF₃-Terminated Self-Assembled Monolayers on Au(111). *J. Am. Chem. Soc.* **2005,** *127* (40), 13744-13745.

26. Rui, Z.; James Joshua, B.; Kasik, A.; Lin, Y. S., Metal ' organic framework membrane process for high purity CO_2 production. *AIChE J.* **2016,** *62* (11), 3836-3841.

27. Zacher, D.; Shekhah, O.; Woll, C.; Fischer, R. A., Thin films of metal-organic frameworks. *Chem. Soc. Rev.* **2009,** *38* (5), 1418-1429.

28. Bétard, A.; Fischer, R. A., Metal–Organic Framework Thin Films: From Fundamentals to Applications. *Chem. Rev.* **2012,** *112* (2), 1055-1083.

29. Shah, M.; McCarthy, M. C.; Sachdeva, S.; Lee, A. K.; Jeong, H.-K., Current Status of Metal–Organic Framework Membranes for Gas Separations: Promises and Challenges. *Ind. Eng. Chem. Res.* **2012,** *51* (5), 2179-2199.

30. Yao, J.; Wang, H., Zeolitic imidazolate framework composite membranes and thin films: synthesis and applications. *Chem. Soc. Rev.* **2014,** *43* (13), 4470-4493.

31. Seoane, B.; Coronas, J.; Gascon, I.; Benavides, M. E.; Karvan, O.; Caro, J.; Kapteijn, F.; Gascon, J., Metal-organic framework based mixed matrix membranes: a solution for highly efficient CO_2 capture? *Chem. Soc. Rev.* **2015,** *44* (8), 2421-2454.

32. Boot-Handford, M. E.; Abanades, J. C.; Anthony, E. J.; Blunt, M. J.; Brandani, S.; Mac Dowell, N.; Fernandez, J. R.; Ferrari, M.-C.; Gross, R.; Hallett, J. P.; Haszeldine, R. S.; Heptonstall, P.; Lyngfelt, A.; Makuch, Z.; Mangano, E.; Porter, R. T. J.; Pourkashanian, M.; Rochelle, G. T.; Shah, N.; Yao, J. G.; Fennell, P. S., Carbon capture and storage update. *Energy Environ. Sci.* **2014,** *7* (1), 130-189.

33. Choi, S.; Drese Jeffrey, H.; Jones Christopher, W., Adsorbent Materials for Carbon Dioxide Capture from Large Anthropogenic Point Sources. *ChemSusChem* **2009,** *2* (9), 796-854.

34. Yu, C.-H.; Huang, C.-H.; Tan, C.-S., A Review of CO_2 Capture by Absorption and Adsorption. *Aerosol Sci. Technol.* **2012,** *12* (5), 745-769.

35. Spigarelli, B. P.; Kawatra, S. K., Opportunities and challenges in carbon dioxide capture. *J. CO₂ Util.* **2013,** *1*, 69-87.

36. Chen, Z.; Deng, S.; Wei, H.; Wang, B.; Huang, J.; Yu, G., Activated carbons and amine-modified materials for carbon dioxide capture — a review. *Front. Environ. Sci. & Eng.* **2013,** *7* (3), 326-340.

37. Ben-Mansour, R.; Habib, M. A.; Bamidele, O. E.; Basha, M.; Qasem, N. A. A.; Peedikakkal, A.; Laoui, T.; Ali, M., Carbon capture by physical adsorption: Materials, experimental investigations and numerical modeling and simulations – A review. *Appl. Energ.* **2016,** *161,* 225-255.

38. Yaghi, O. M.; Li, G.; Li, H., Selective binding and removal of guests in a microporous metal–organic framework. *Nature* **1995,** *378,* 703.

39. Cook, T. R.; Zheng, Y.-R.; Stang, P. J., Metal–Organic Frameworks and Self-Assembled Supramolecular Coordination Complexes: Comparing and Contrasting the Design, Synthesis, and Functionality of Metal–Organic Materials. *Chem. Rev.* **2013,** *113* (1), 734-777.

40. Bao, Z.; Yu, L.; Ren, Q.; Lu, X.; Deng, S., Adsorption of CO_2 and CH_4 on a magnesium-based metal organic framework. *J. Colloid Interface Sci.* **2011,** *353* (2), 549-556.

41. Furukawa, H.; Ko, N.; Go, Y. B.; Aratani, N.; Choi, S. B.; Choi, E.; Yazaydin, A. Ö.; Snurr, R. Q.; O'Keeffe, M.; Kim, J.; Yaghi, O. M., Ultrahigh Porosity in Metal-Organic Frameworks. *Science* **2010,** *329* (5990), 424.

42. Tian, T.; Zeng, Z.; Vulpe, D.; Casco, M. E.; Divitini, G.; Midgley, P. A.; Silvestre-Albero, J.; Tan, J.-C.; Moghadam, P. Z.; Fairen-Jimenez, D., A sol–gel monolithic metal–organic framework with enhanced methane uptake. *Nature Mater.* **2017,** *17,* 174.

43. Zhang, Y.; Sunarso, J.; Liu, S.; Wang, R., Current status and development of membranes for CO_2/CH_4 separation: A review. *Int. J. Green h. Gas Control* **2013,** *12,* 84-107.

44. Li, J.-R.; Ma, Y.; McCarthy, M. C.; Sculley, J.; Yu, J.; Jeong, H.-K.; Balbuena, P. B.; Zhou, H.-C., Carbon dioxide capture-related gas adsorption and separation in metal-organic frameworks. *Coord. Chem. Rev.* **2011,** *255* (15-16), 1791-1823.

45. Herm, Z. R.; Bloch, E. D.; Long, J. R., Hydrocarbon Separations in Metal-Organic Frameworks. *Chem. Mater.* **2014,** *26* (1), 323-338.

46. Adil, K.; Belmabkhout, Y.; Pillai, R. S.; Cadiau, A.; Bhatt, P. M.; Assen, A. H.; Maurin, G.; Eddaoudi, M., Gas/vapour separation using ultra-microporous metal-organic frameworks: insights into the structure/separation relationship. *Chem. Soc. Rev.* **2017,** *46* (11), 3402-3430.

47. Yu, J.; Xie, L.-H.; Li, J.-R.; Ma, Y.; Seminario, J. M.; Balbuena, P. B., CO_2 Capture and Separations Using MOFs: Computational and Experimental Studies. *Chem. Rev.* **2017,** *117* (14), 9674-9754.

48. Morris, R. E.; Wheatley, P. S., Gas storage in nanoporous materials. *Angewandte Chemie-International Edition* **2008,** *47* (27), 4966-4981.

49. Murray, L. J.; Dinca, M.; Long, J. R., Hydrogen storage in metal-organic frameworks. *Chem. Soc. Rev.* **2009,** *38* (5), 1294-1314.

50. Svec, F.; Germain, J.; Frechet, J. M. J., Nanoporous Polymers for Hydrogen Storage. *Small* **2009,** *5* (10), 1098-1111.

51. Hu, Y. H.; Zhang, L., Hydrogen Storage in Metal-Organic Frameworks. *Adv. Mater.* **2010,**

22 (20), 117-130.

52. Lin, X.; Champness, N. R.; Schroeder, M., Hydrogen, Methane and Carbon Dioxide Adsorption in Metal-Organic Framework Materials. Top. Curr. Chem. 2010; 293, 35.

53. García-Holley, P.; Schweitzer, B.; Islamoglu, T.; Liu, Y.; Lin, L.; Rodriguez, S.; Weston, M. H.; Hupp, J. T.; Gómez-Gualdrón, D. A.; Yildirim, T.; Farha, O. K., Benchmark Study of Hydrogen Storage in Metal–Organic Frameworks under Temperature and Pressure Swing Conditions. *ACS Energy Letters* **2018,** *3* (3), 748-754.

54. Côté, A. P.; Benin, A. I.; Ockwig, N. W.; Keeffe, M.; Matzger, A. J.; Yaghi, O. M., Porous, Crystalline, Covalent Organic Frameworks. *Science* **2005,** *310* (5751), 1166.

55. Rungtaweevoranit, B.; Diercks, C. S.; Kalmutzki, M. J.; Yaghi, O., Spiers Memorial Lecture: Progress and prospects of reticular chemistry. *Faraday Discuss.* **2017,** *201* (0), 9-45.

56. Furukawa, H.; Yaghi, O. M., Storage of Hydrogen, Methane, and Carbon Dioxide in Highly Porous Covalent Organic Frameworks for Clean Energy Applications. *J. Am. Chem. Soc.* **2009,** *131* (25), 8875-8883.

57. Zhu, Y.; Long, H.; Zhang, W., Imine-Linked Porous Polymer Frameworks with High Small Gas (H_2, CO_2, CH_4, C_2H_2) Uptake and CO_2/N_2 Selectivity. *Chem. Mater.* **2013,** *25* (9), 1630-1635.

58. Zeng, Y.; Zou, R.; Zhao, Y., Covalent Organic Frameworks for CO_2 Capture. *Adv. Mater.* **2016,** *28* (15), 2855-2873.

59. Huang, N.; Wang, P.; Jiang, D., Covalent organic frameworks: a materials platform for structural and functional designs. *Nat. Rev. Mater.* **2016,** *1*, 16068.

60. W. G. Toland, S. R., *US3060179* **1962.**

61. G. H. Miller (Texaco Inc.) US 3775380. 1973.

62. Kuhn, P.; Antonietti, M.; Thomas, A., Porous, Covalent Triazine-Based Frameworks Prepared by Ionothermal Synthesis. *Angew. Chem. Int. Ed.* **2008,** *47* (18), 3450-3453.

63. Puthiaraj, P.; Lee, Y.-R.; Zhang, S.; Ahn, W.-S., Triazine-based covalent organic polymers: design, synthesis and applications in heterogeneous catalysis. *J. Mater. Chem. A* **2016,** *4* (42), 16288-16311.

64. Artz, J., Covalent Triazine-based Frameworks-Tailor-made Catalysts and Catalyst Supports for Molecular and Nanoparticulate Species. *ChemCatChem* **2018,** *10* (8), 1753-1771.

65. Cooper, E. R.; Andrews, C. D.; Wheatley, P. S.; Webb, P. B.; Wormald, P.; Morris, R. E., Ionic liquids and eutectic mixtures as solvent and template in synthesis of zeolite analogues. *Nature* **2004,** *430*, 1012.

66. Katekomol, P.; Roeser, J.; Bojdys, M.; Weber, J.; Thomas, A., Covalent Triazine Frameworks Prepared from 1,3,5-Tricyanobenzene. *Chem. Mater.* **2013,** *25* (9), 1542-1548.

67. Bojdys, M. J.; Jeromenok, J.; Thomas, A.; Antonietti, M., Rational Extension of the Family

of Layered, Covalent, Triazine-Based Frameworks with Regular Porosity. *Adv. Mater.* **2010,** *22* (19), 2202-2205.

68. Kuhn, P.; Thomas, A.; Antonietti, M., Toward Tailorable Porous Organic Polymer Networks: A High-Temperature Dynamic Polymerization Scheme Based on Aromatic Nitriles. *Macromolecules* **2009,** *42* (1), 319-326.

69. Kuhn, P.; Forget, A.; Su, D.; Thomas, A.; Antonietti, M., From Microporous Regular Frameworks to Mesoporous Materials with Ultrahigh Surface Area: Dynamic Reorganization of Porous Polymer Networks. *J. Am. Chem. Soc.* **2008,** *130* (40), 13333-13337.

70. Ren, S.; Bojdys, M. J.; Dawson, R.; Laybourn, A.; Khimyak, Y. Z.; Adams, D. J.; Cooper, A. I., Porous, Fluorescent, Covalent Triazine-Based Frameworks Via Room-Temperature and Microwave-Assisted Synthesis. *Adv. Mater.* **2012,** *24* (17), 2357-2361.

71. Zhu, X.; Tian, C.; Mahurin, S. M.; Chai, S.-H.; Wang, C.; Brown, S.; Veith, G. M.; Luo, H.; Liu, H.; Dai, S., A Superacid-Catalyzed Synthesis of Porous Membranes Based on Triazine Frameworks for CO_2 Separation. *J. Am. Chem. Soc.* **2012,** *134* (25), 10478-10484.

72. Talapaneni, S. N.; Hwang, T. H.; Je, S. H.; Buyukcakir, O.; Choi, J. W.; Coskun, A., Elemental-Sulfur-Mediated Facile Synthesis of a Covalent Triazine Framework for High-Performance Lithium-Sulfur Batteries. *Angew. Chem. Int. Ed.* **2016,** *55* (9), 3106-3111.

73. Je, S. H.; Kim, H. J.; Kim, J.; Choi, J. W.; Coskun, A., Perfluoroaryl-Elemental Sulfur SNAr Chemistry in Covalent Triazine Frameworks with High Sulfur Contents for Lithium–Sulfur Batteries. *Adv. Funct. Mater.* **2017,** *27* (47), 1703947-n/a.

74. Zhao, Y.; Yao, K. X.; Teng, B.; Zhang, T.; Han, Y., A perfluorinated covalent triazine-based framework for highly selective and water-tolerant CO_2 capture. *Energy Environ. Sci.* **2013,** *6* (12), 3684-3692.

75. Hug, S.; Mesch, M. B.; Oh, H.; Popp, N.; Hirscher, M.; Senker, J.; Lotsch, B. V., A fluorene based covalent triazine framework with high CO_2 and H_2 capture and storage capacities. *J. Mater. Chem. A* **2014,** *2* (16), 5928-5936.

76. Gu, C.; Liu, D.; Huang, W.; Liu, J.; Yang, R., Synthesis of covalent triazine-based frameworks with high CO_2 adsorption and selectivity. *Polym. Chem.* **2015,** *6* (42), 7410-7417.

77. Hug, S.; Stegbauer, L.; Oh, H.; Hirscher, M.; Lotsch, B. V., Nitrogen-Rich Covalent Triazine Frameworks as High-Performance Platforms for Selective Carbon Capture and Storage. *Chem. Mater.* **2015,** *27* (23), 8001-8010.

78. Saleh, M.; Baek, S. B.; Lee, H. M.; Kim, K. S., Triazine-Based Microporous Polymers for Selective Adsorption of CO_2. *J. Phys. Chem C* **2015,** *119* (10), 5395-5402.

79. Dey, S.; Bhunia, A.; Esquivel, D.; Janiak, C., Covalent triazine-based frameworks (CTFs) from triptycene and fluorene motifs for CO_2 adsorption. *J. Mater. Chem. A* **2016,** *4* (17), 6259-6263.

80. Tao, L.; Niu, F.; Wang, C.; Liu, J.; Wang, T.; Wang, Q., Benzimidazole functionalized covalent triazine frameworks for CO_2 capture. *J. Mater. Chem. A* **2016,** *4* (30), 11812-11820.

81. Wang, K.; Huang, H.; Liu, D.; Wang, C.; Li, J.; Zhong, C., Covalent Triazine-Based Frameworks with Ultramicropores and High Nitrogen Contents for Highly Selective CO_2 Capture. *Environ. Sci. Technol.* **2016,** *50* (9), 4869-4876.

82. Yuan, K.; Liu, C.; Han, J.; Yu, G.; Wang, J.; Duan, H.; Wang, Z.; Jian, X., Phthalazinone structure-based covalent triazine frameworks and their gas adsorption and separation properties. *RSC Adv.* **2016,** *6* (15), 12009-12020.

83. Zhu, X.; Tian, C.; Veith, G. M.; Abney, C. W.; Dehaudt, J.; Dai, S., In Situ Doping Strategy for the Preparation of Conjugated Triazine Frameworks Displaying Efficient CO_2 Capture Performance. *J. Am. Chem. Soc.* **2016,** *138* (36), 11497-11500.

84. Dey, S.; Bhunia, A.; Breitzke, H.; Groszewicz, P. B.; Buntkowsky, G.; Janiak, C., Two linkers are better than one: enhancing CO_2 capture and separation with porous covalent triazine-based frameworks from mixed nitrile linkers. *J. Mater. Chem. A* **2017,** *5* (7), 3609-3620.

85. Park, K.; Lee, K.; Kim, H.; Ganesan, V.; Cho, K.; Jeong, S. K.; Yoon, S., Preparation of covalent triazine frameworks with imidazolium cations embedded in basic sites and their application for CO_2 capture. *J. Mater. Chem. A* **2017,** *5* (18), 8576-8582.

86. Tuci, G.; Pilaski, M.; Ba, H.; Rossin, A.; Luconi, L.; Caporali, S.; Pham-Huu, C.; Palkovits, R.; Giambastiani, G., Unraveling Surface Basicity and Bulk Morphology Relationship on Covalent Triazine Frameworks with Unique Catalytic and Gas Adsorption Properties. *Adv. Funct. Mater.* **2017,** *27* (7), 1605672-n/a.

87. Wang, G.; Leus, K.; Jena, H. S.; Krishnaraj, C.; Zhao, S.; Depauw, H.; Tahir, N.; Liu, Y.-Y.; Van Der Voort, P., A fluorine-containing hydrophobic covalent triazine framework with excellent selective CO_2 capture performance. *J. Mater. Chem. A* **2018,** *6* (15), 6370-6375.

88. Wang, G.; Leus, K.; Zhao, S.; Van Der Voort, P., Newly Designed Covalent Triazine Framework Based on Novel N-Heteroaromatic Building Blocks for Efficient CO_2 and H_2 Capture and Storage. *ACS Appl. Mater. Interfaces* **2018,** *10* (1), 1244-1249.

89. Buyukcakir, O.; Je, S. H.; Talapaneni, S. N.; Kim, D.; Coskun, A., Charged Covalent Triazine Frameworks for CO_2 Capture and Conversion. *ACS Appl. Mater. Interfaces* **2017,** *9* (8), 7209-7216.

90. Bavykina, A. V.; Olivos-Suarez, A. I.; Osadchii, D.; Valecha, R.; Franz, R.; Makkee, M.; Kapteijn, F.; Gascon, J., Facile Method for the Preparation of Covalent Triazine Framework coated Monoliths as Catalyst Support: Applications in C1 Catalysis. *ACS Appl. Mater. Interfaces* **2017,** *9* (31), 26060-26065.

91. Bavykina, A. V.; Mautscke, H. H.; Makkee, M.; Kapteijn, F.; Gascon, J.; Xamena, F., Base free transfer hydrogenation using a covalent triazine framework based catalyst. *CrystEngComm* **2017,** *19* (29), 4166-4170.

92. Álvarez, A.; Bansode, A.; Urakawa, A.; Bavykina, A. V.; Wezendonk, T. A.; Makkee, M.; Gascon, J.; Kapteijn, F., Challenges in the Greener Production of Formates/Formic Acid, Methanol, and DME by Heterogeneously Catalyzed CO_2 Hydrogenation Processes. *Chem. Rev.* **2017,** *117* (14), 9804-9838.

93. Yoshioka, T.; Iwase, K.; Nakanishi, S.; Hashimoto, K.; Kamiya, K., Electrocatalytic Reduction of Nitrate to Nitrous Oxide by a Copper-Modified Covalent Triazine Framework. *J. Phys. Chem C* **2016,** *120* (29), 15729-15734.

94. Wang, Z. F.; Liu, C. B.; Huang, Y.; Hu, Y. C.; Zhang, B., Covalent triazine framework-supported palladium as a ligand-free catalyst for the selective double carbonylation of aryl iodides under ambient pressure of CO. *Chem. Commun.* **2016,** *52* (14), 2960-2963.

95. Puthiaraj, P.; Lee, Y. R.; Zhang, S. Q.; Ahn, W. S., Triazine-based covalent organic polymers: design, synthesis and applications in heterogeneous catalysis. *J. Mater. Chem. A* **2016,** *4* (42), 16288-16311.

96. Pilaski, M.; Artz, J.; Islam, H.-U.; Beale, A. M.; Palkovits, R., N-containing covalent organic frameworks as supports for rhodium as transition-metal catalysts in hydroformylation reactions. *Microporous Mesoporous Mater.* **2016,** *227*, 219-227.

97. Li, L. Y.; Fang, W.; Zhang, P.; Bi, J. H.; He, Y. H.; Wang, J. Y.; Su, W. Y., Sulfur-doped covalent triazine-based frameworks for enhanced photocatalytic hydrogen evolution from water under visible light. *J. Mater. Chem. A* **2016,** *4* (32), 12402-12406.

98. Kamai, R.; Kamiya, K.; Hashimoto, K.; Nakanishi, S., Oxygen-Tolerant Electrodes with Platinum-Loaded Covalent Triazine Frameworks for the Hydrogen Oxidation Reaction. *Angew. Chem. Int. Ed.* **2016,** *55* (42), 13184-13188.

99. Bavykina, A. V.; Rozhko, E.; Goesten, M. G.; Wezendonk, T.; Seoane, B.; Kapteijn, F.; Makkee, M.; Gascon, J., Shaping Covalent Triazine Frameworks for the Hydrogenation of Carbon Dioxide to Formic Acid. *ChemCatChem* **2016,** *8* (13), 2217-2221.

100. Iwase, K.; Yoshioka, T.; Nakanishi, S.; Hashimoto, K.; Kamiya, K., Copper-Modified Covalent Triazine Frameworks as Non-Noble-Metal Electrocatalysts for Oxygen Reduction. *Angew. Chem. Int. Ed.* **2015,** *54* (38), 11068-11072.

101. He, T.; Liu, L.; Wu, G. T.; Chen, P., Covalent triazine framework-supported palladium nanoparticles for catalytic hydrogenation of N-heterocycles. *J. Mater. Chem. A* **2015,** *3* (31), 16235-16241.

102. Chan-Thaw, C. E.; Villa, A.; Wang, D.; Dal Santo, V.; Biroli, A. O.; Veith, G. M.; Thomas, A.; Prati, L., PdHx Entrapped in a Covalent Triazine Framework Modulates Selectivity in Glycerol Oxidation. *ChemCatChem* **2015,** *7* (14), 2149-2154.

103. Bi, J. H.; Fang, W.; Li, L. Y.; Wang, J. Y.; Liang, S. J.; He, Y. H.; Liu, M. H.; Wu, L., Covalent Triazine-Based Frameworks as Visible Light Photocatalysts for the Splitting of Water. *Macromol. Rapid Commun.* **2015,** *36* (20), 1799-1805.

104. Kamiya, K.; Kamai, R.; Hashimoto, K.; Nakanishi, S., Platinum-modified covalent triazine frameworks hybridized with carbon nanoparticles as methanol-tolerant oxygen reduction electrocatalysts. *Nat. Commun.* **2014,** *5*.

105. Chan-Thaw, C. E.; Villa, A.; Katekomol, P.; Su, D. S.; Thomas, A.; Prati, L., Covalent Triazine Framework as Catalytic Support for Liquid Phase Reaction. *Nano Lett.* **2010,** *10* (2),

537-541.

106. Wang, T.; Kailasam, K.; Xiao, P.; Chen, G.; Chen, L.; Wang, L.; Li, J.; Zhu, J., Adsorption removal of organic dyes on covalent triazine framework (CTF). *Microporous Mesoporous Mater.* **2014,** *187,* 63-70.

107. Zhang, W.; Liang, F.; Li, C.; Qiu, L.-G.; Yuan, Y.-P.; Peng, F.-M.; Jiang, X.; Xie, A.-J.; Shen, Y.-H.; Zhu, J.-F., Microwave-enhanced synthesis of magnetic porous covalent triazine-based framework composites for fast separation of organic dye from aqueous solution. *J. Hazard. Mater.* **2011,** *186* (2), 984-990.

108. Liu, J.; Chen, H.; Zheng, S.; Xu, Z., Adsorption of 4,4ʹ -(Propane-2,2-diyl)diphenol from Aqueous Solution by a Covalent Triazine-Based Framework. *J. Chem. Eng. Data* **2013,** *58* (12), 3557-3562.

109. Bhunia, A.; Dey, S.; Bous, M.; Zhang, C. Y.; von Rybinski, W.; Janiak, C., High adsorptive properties of covalent triazine-based frameworks (CTFs) for surfactants from aqueous solution. *Chem. Commun.* **2015,** *51* (3), 484-486.

110. Wang, B.; Lee, L. S.; Wei, C.; Fu, H.; Zheng, S.; Xu, Z.; Zhu, D., Covalent triazine-based framework: A promising adsorbent for removal of perfluoroalkyl acids from aqueous solution. *Environ. Pollut.* **2016,** *216,* 884-892.

111. Tao, L.-M.; Niu, F.; Zhang, D.; Wang, T.-M.; Wang, Q.-H., Amorphous covalent triazine frameworks for high performance room temperature ammonia gas sensing. *New J. Chem.* **2014,** *38* (7), 2774-2777.

112. Karmakar, A.; Kumar, A.; Chaudhari Abhijeet, K.; Samanta, P.; Desai Aamod, V.; Krishna, R.; Ghosh Sujit, K., Bimodal Functionality in a Porous Covalent Triazine Framework by Rational Integration of an Electron ʹ Rich and ʹ Deficient Pore Surface. *Chem. Eur. J.,* *22* (14), 4931-4937.

113. Bhunia, A.; Esquivel, D.; Dey, S.; Fernandez-Teran, R.; Goto, Y.; Inagaki, S.; Van der Voort, P.; Janiak, C., A photoluminescent covalent triazine framework: CO_2 adsorption, light-driven hydrogen evolution and sensing of nitroaromatics. *J. Mater. Chem. A* **2016,** *4* (35), 13450-13457.

114. Deng, W.; Li, Y.; Zheng, S.; Liu, X.; Li, P.; Sun, L.; Yang, R.; Wang, S.; Wu, Z.; Bao, X., Conductive Microporous Covalent Triazine ʹ Based Framework for High ʹ Performance Electrochemical Capacitive Energy Storage. *Angew. Chem. Int. Ed.* 2018 , 57,7992 –7996

115. Bhanja, P.; Bhunia, K.; Das, S. K.; Pradhan, D.; Kimura, R.; Hijikata, Y.; Irle, S.; Bhaumik, A., New Triazine-Based Covalent Organic Framework for High-Performance Capacitive Energy Storage. *ChemSusChem* **2017,** *10* (5), 921-929.

116. Cheng, Z.; Pan, H.; Zhong, H.; Xiao, Z.; Li, X.; Wang, R., Porous Organic Polymers for Polysulfide Trapping in Lithium–Sulfur Batteries. *Adv. Funct. Mater. 2018,* 1707597.

117. Yuan, K.; Liu, C.; Zong, L.; Yu, G.; Cheng, S.; Wang, J.; Weng, Z.; Jian, X., Promoting and Tuning Porosity of Flexible Ether-Linked Phthalazinone-Based Covalent Triazine Frameworks

Utilizing Substitution Effect for Effective CO_2 Capture. *ACS Appl. Mater. Interfaces* **2017**, *9* (15), 13201-13212.

118. Yang, Z.-Z.; Zhao, Y.; Zhang, H.; Yu, B.; Ma, Z.; Ji, G.; Liu, Z., Fluorinated microporous organic polymers: design and applications in CO_2 adsorption and conversion. *Chem. Commun.* **2014,** *50* (90), 13910-13913.

119. Bhunia, A.; Vasylyeva, V.; Janiak, C., From a supramolecular tetranitrile to a porous covalent triazine-based framework with high gas uptake capacities. *Chem. Commun.* **2013,** *49* (38), 3961-3963.

CHAPTER 2

Newly Designed Covalent Triazine Framework Based on Novel N-heteroaromatic Building Blocks for Efficient CO$_2$ and H$_2$ Capture and Storage

The results of this chapter were published in:

Abstract
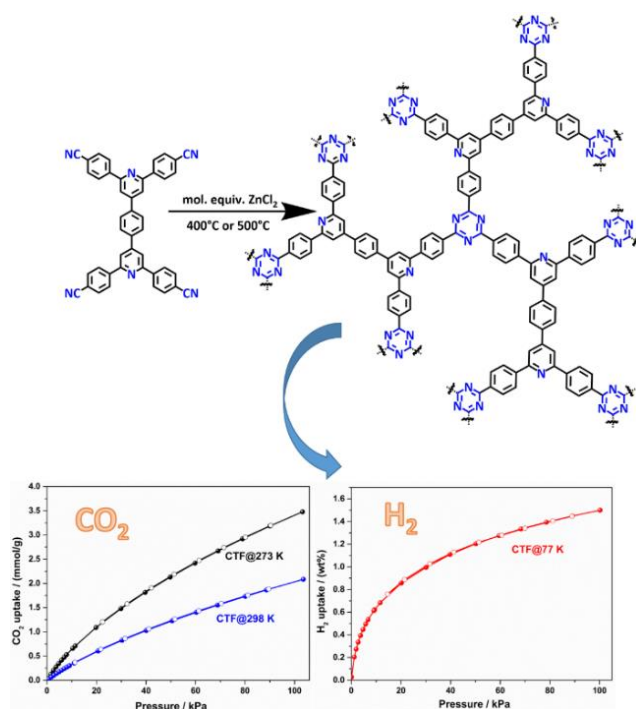
In this chapter, a set of novel CTF materials have been designed and prepared via trimerization of 4,4 ′ ,4 ″ ,4‴-(1,4-phenylenebis(pyridine-4,2,6-triyl))-tetrabenzonitrile in molten $ZnCl_2$ under ionothermal conditions. The influence of several parameters such as the $ZnCl_2$/monomer ratio and reaction temperatures on the structure and porosity of the resulting frameworks was systematically examined. After a thorough characterization, their performance in CO_2 and H_2 adsorption as well as their selectivity of CO_2 over N_2 was assessed. Notably, the CTF obtained using 20 molar equiv. of $ZnCl_2$ at the reaction temperature of 400 °C (CTF-20-400) exhibits an excellent CO_2 adsorption capacity of 3.48 mmol/g at 1 bar and 273 K as well as a significantly high H_2 uptake of 1.5 wt % at 1 bar and 77 K. In addition, one of the obtained CTFs (CTF-5-400) also presents a relatively high CO_2/N_2 selectivity (up to 36 at 298 K), making it promising adsorbents for gas sorption and separation.

2.1. Introduction

Carbon dioxide, mainly produced from human activities including, but not limited to, the burning of fossil fuels (e.g. coal, petroleum and natural gas), has been widely accepted to be the primary contributor to global warming.[1-2] Considering that fossil fuels will still be the dominant source of energy for humans in the foreseeable future, it is beyond all doubt that exploring more cost-effective and sustainable materials for carbon capture from emission sources remains challenging and urgently required.[3-5] In terms of gas adsorption and separation applications, an ideal porous material should exhibit a significantly high CO_2 uptake and selectivity at low pressures as well as an excellent resistance to water and acid gases.[6] To address the issue of carbon capture, a new advanced class of porous and tunable materials including MOFs[7-9] and COFs[10-11] have demonstrated promising potential because of their high surface area, intrinsic porosity, low mass density, high physicochemical stability as well as diverse structural tunability. However, the poor chemical stability of most MOFs limits their practical applications.[12-13] In contrast, a subclass of COFs, namely CTFs, have emerged as promising candidates for gas capture and storage due to their high stability and porosity in addition to their high intrinsic nitrogen content.[2, 14-16] Generally, CTFs can be prepared via trimerization of aromatic nitriles either under ionothermal conditions using $ZnCl_2$ as the catalyst[17] or using strong Brønsted acid (CF_3SO_3H)[18]. However, the strong Brønsted acid approach cannot be applied to all types of monomers and for this reason its widespread application is limited. Since the pioneering work of Thomas et al. in 2008, who developed the first CTF materials, namely CTF-1, tremendous efforts have been made to design and synthesize CTF materials with the goal of enhanced gas capture (CO_2) and storage $(CH_4$ and $H_2)$.[19-20] From the view of pore structures, it has been proven that ultramicropores are beneficial for selective CO_2 capture. In the report of Lotsch et al., a series of nitrogen-rich CTFs were synthesized and the gas adsorption

results revealed the dominant role of ultramicropores for efficient and selective CO_2 capture.[14] From the aspect of the building blocks of CTFs, the incorporation of preferential CO_2-philic sites (e.g. N, O and F) into the frameworks to induce strong electrostatic interactions between CO_2 molecules and the material surface is expected to significantly improve their CO_2 adsorption performance. With the aforementioned consideration in mind, we present in this chapter the use of a novel heteroaromatic tetranitrile, 4,4',4'',4'''-(1,4-phenylenebis(pyridine-4,2,6-triyl))tetrabenzonitrile as the building block to synthesize a set of stable porous CTFs by varying the $ZnCl_2$/monomer ratio and synthesis temperature. The influence of several parameters such as the $ZnCl_2$/monomer ratio and reaction temperature on the structure and porosity of the resulting frameworks was systematically examined. After a thorough characterization, the obtained CTFs were explored for their CO_2 and H_2 adsorption properties. In addition, their selectivity of CO_2 over N_2 was also assessed for potential gas separation applications.

2.2. Results and Discussion

The CTF materials were typically prepared under ionothermal conditions using molten $ZnCl_2$ both as the Lewis acidic trimerization catalyst and reaction medium.[17] As previous reports already demonstrated, the $ZnCl_2$/monomer ratio as well as the reaction temperature have great influence on the structural and porous properties of such networks.[21-22] Therefore, in the present study, we followed the typical ionothermal procedure using 4,4',4'',4'''-(1,4-phenylenebis(pyridine-4,2,6-triyl))tetrabenzonitrile as the monomer to prepare a series of CTFs by varying the reaction temperature and the amount of employed $ZnCl_2$ (Figure 2.1). The obtained CTFs are denoted as, CTF-mol equiv. $ZnCl_2$-temperature, in the following (e.g. CTF-5-400 is prepared at 400 °C with 5 mol equiv. $ZnCl_2$).
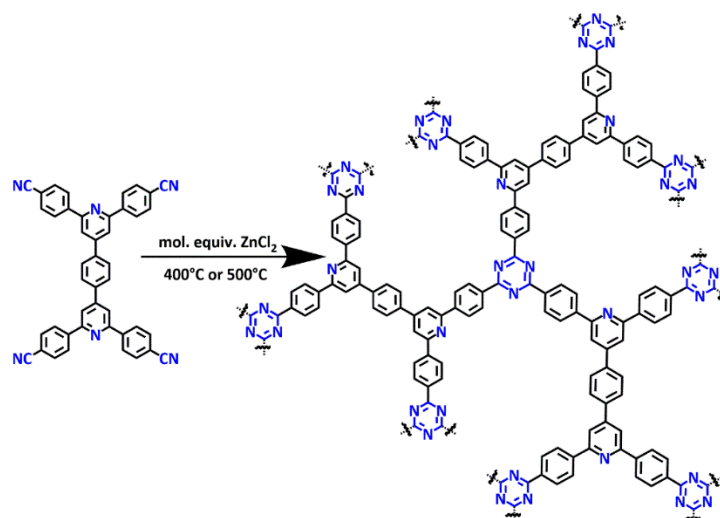
Figure 2.1. Schematic illustration of the ideal synthesis of the CTF materials discussed in this work.

The crystallinity of all the synthesized materials was examined by means of powder X-ray diffraction (Figure 2.2). As expected, all the CTF materials are amorphous. A broad peak at $2\theta = 24°$ is observed for the samples synthesized at 500 °C, indicating a generally amorphous structure along with a few graphitic two-dimensional layers.[23]
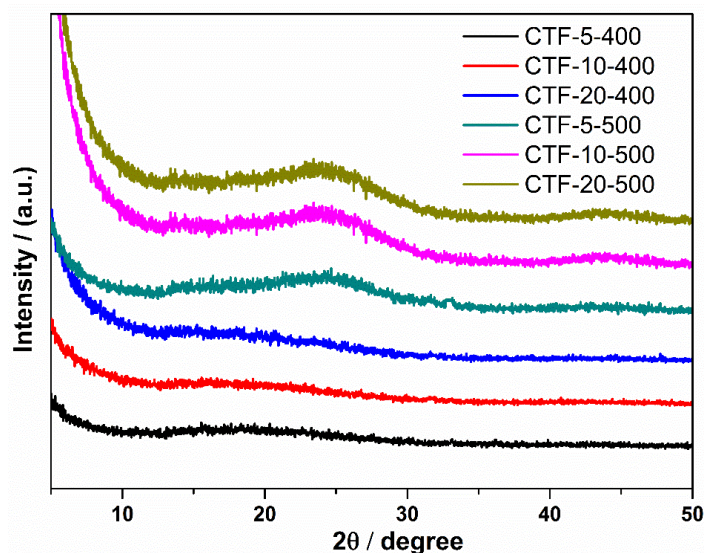
Figure 2.2. Powder X-ray diffraction measurements of the present CTFs, indicating that all the CTFs are amorphous.

The successful trimerization reaction was confirmed by FT-IR measurements (Figure 2.3). For the CTF-5-400 and CTF-10-400, the characteristic band of cyano group at 2230 cm^{-1} can be clearly observed, indicating a low degree of

trimerization. This might be attributed to the high mass of the monomer and the employed amount of $ZnCl_2$ is not sufficient enough in such a reaction mixture to completely dissolve the monomer and the produced oligomers. In contrast, when 20 mol equiv. $ZnCl_2$ was used or the reaction temperature was increased to 500 °C, the carbonitrile band at 2230 cm^{-1} completely disappears, indicating the successful completion of the trimerization. At a synthesis temperature of 400 °C, the characteristic bands for the triazine rings at 1548 cm^{-1} and 1360 cm^{-1} are visible, while at a higher reaction temperature (500 °C) these vibrations are rather featureless, which might be attributed to the partial carbonization of the materials.[14-15]
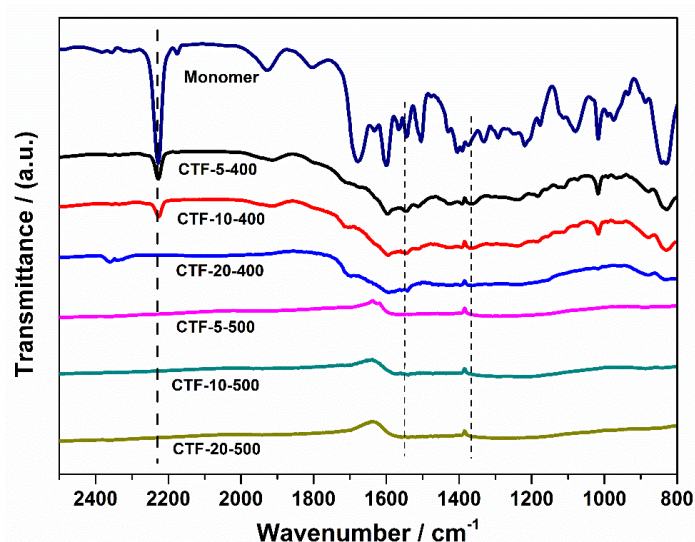
Figure 2.3. FT-IR spectra of the monomer and all the obtained CTFs discussed in this work.

Elemental analysis results indicate a relatively lower nitrogen content in comparison to the theoretically expected values for all the obtained CTFs. It is mainly due to the carbonization process and formation of irreversible C-C bonds during the synthesis reactions. Additionally, a significantly enhanced C/N ratio was observed when the reaction temperature and the amount of the employed $ZnCl_2$ was increased (Table 2.1), which can be attributed to the higher nitriles cleavages in the structure as well as to the decomposition of the triazine rings during the trimerization process at higher reaction temperature or high $ZnCl_2$ concentration which is in accordance with previous studies.[14, 22-]

[24] It should be noted that the total amount of elements (C, H, N) determined by element analysis is always lower than 100%, the deviation might be due to the trapped metal salts and water molecules in the pores, which could not be completely removed.[25-26]

Table 2.1. Elemental Analysis results of all the obtained CTFs.

Materials	Calculated (%)				Found (%)			
	C	H	N	C/N	C	H	N	C/N
CTF-5-400	83.02	3.77	13.21	6.28	78.29	3.59	5.15	15.2
CTF-10-400	83.02	3.77	13.21	6.28	82.14	3.69	5.33	15.4
CTF-20-400	83.02	3.77	13.21	6.28	82.33	3.02	4.07	20.2
CTF-5-500	83.02	3.77	13.21	6.28	78.34	1.95	4.18	18.7
CTF-10-500	83.02	3.77	13.21	6.28	84.22	1.91	4.16	20.2
CTF-20-500	83.02	3.77	13.21	6.28	87.21	1.44	3.46	25.2

The SEM images, presented in Figure 2.4, showed that all the CTFs display the general morphology of aggregates of irregular lump having different sizes.
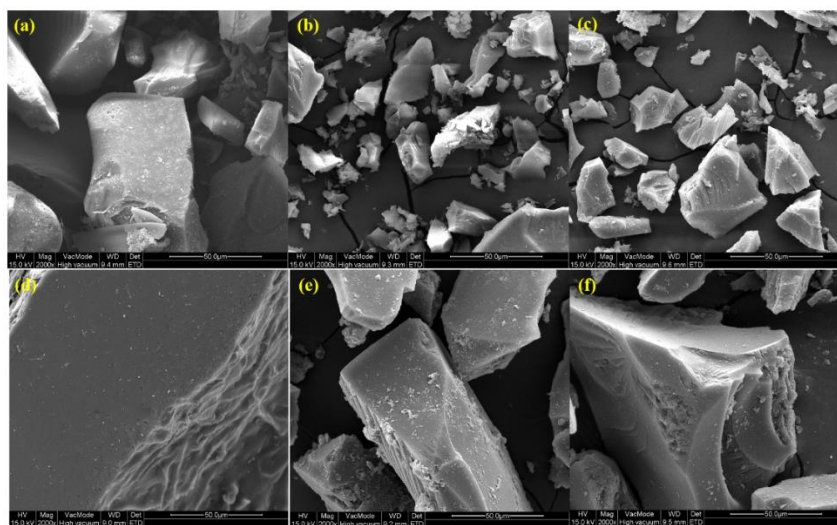
Figure 2.4. SEM images of (a) CTF-5-400; (b) CTF-10-400; (c) CTF-20-400; (d) CTF-5-500; (e) CTF-10-500; (f) CTF-20-500.

The thermal stability of the obtained CTFs was confirmed by TGA analysis under air atmosphere (Figure 2.5). For the samples synthesized at 400 °C, the framework starts to decompose at around 440 °C, while the CTFs prepared at a higher temperature are stable up to 500 °C, demonstrating their high thermal

stability.
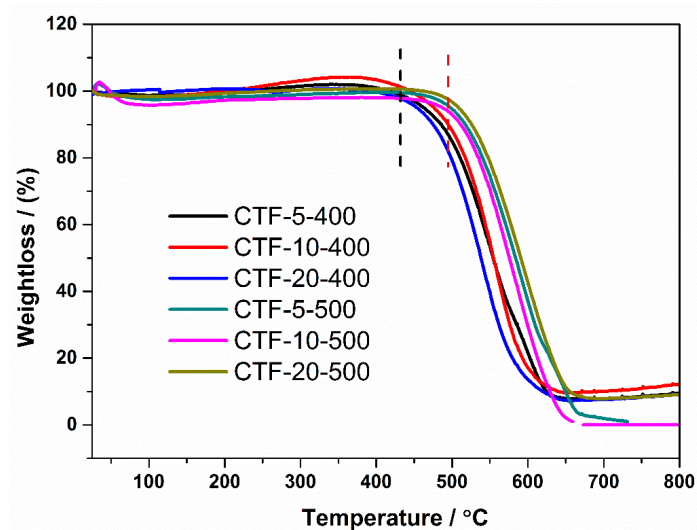
Figure 2.5. TGA curves of all the obtained CTF materials measured at a heating rate of 10 °C/min under an air flow.

Gas sorption properties.

The permanent porosity properties of all the obtained CTFs were studied by N_2 sorption measurements at 77 K (Figure 2.6).
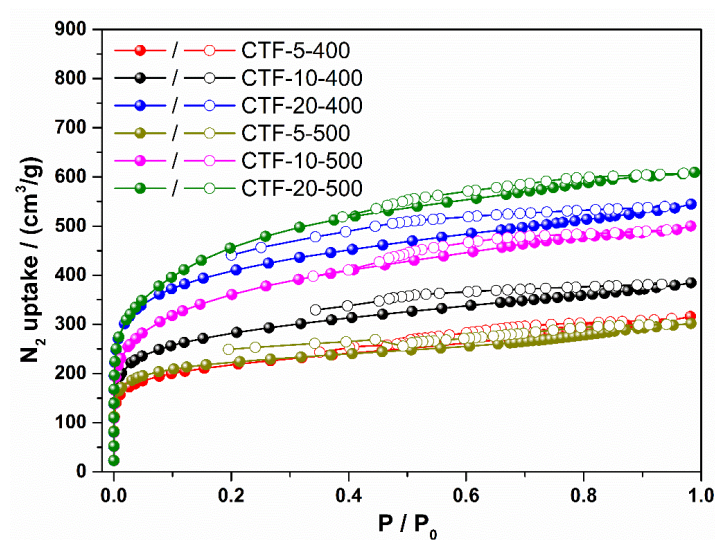
Figure 2.6. N_2 adsorption (closed symbols) and desorption (open symbols) isotherms of all the studied CTF materials measured at 77 K.

All the studied samples were activated at 150 °C for 3 hours under vacuum prior to the measurements. As can be seen from Figure 2.6, all the CTFs show a steep increase of N_2 uptake in the low P/P_0 region, indicating the microporous character of the materials and the existence of a slight hysteresis

loop of the isotherms suggests the presence of mesopores. More specifically, with the increase of the reaction temperature and the amount of $ZnCl_2$, the Brunauer-Emmett-Teller (BET) surface area and pore volume of the CTF materials increased from 802 m^2/g and 0.48 cm^3/g for CTF-5-400 to 1563 m^2/g and 0.94 cm^3/g for CTF-20-500, respectively. The higher porosity of the latter samples might be assigned to the presence of extra defects in the structure created at higher temperatures or when more $ZnCl_2$ is used.[15, 19] The detailed porosity parameters for all the CTF materials are presented in Table 2.2.

Table 2.2. BET surface areas, pore volumes, CO_2 and H_2 adsorption uptakes, CO_2 adsorption of isosteric heat (Q_{st}) and CO_2/N_2 selectivities of the presented CTFs

Sample	S_{BET}[a] (m^2/g)	V_{micro}[b] (cm^3/g)	V_{tot}[c] (cm^3/g)	CO_2 uptake (mmol/g)		H_2 uptake (wt%)	Q_{st} for CO_2 (kJ/mol)	CO_2/N_2[d] Selectivity
				273 K	298 K			
CTF-5-400	802	0.37	0.48	2.25	1.51	0.98	25.5	24
CTF-10-400	1033	0.50	0.59	2.90	1.68	1.21	27.9	14
CTF-20-400	1458	0.73	0.84	3.48	2.09	1.50	22.1	19
CTF-5-500	853	0.34	0.47	3.02	1.91	1.13	26.4	36
CTF-10-500	1251	0.7	0.78	3.20	1.90	1.34	25.7	18
CTF-20-500	1563	0.82	0.94	3.21	1.92	1.48	25.4	20

[a] BET surface area was calculated over the relative pressure range of 0.01-0.05 at 77 K; [b] V_{micro}, micropore volume was calculated by N_2 adsorption isotherm using t-plot method; [c] V_{tot}, total pore volume was calculated at P/P_0 = 0.98; [d] The selectivity was calculated by Henry Model.

The unique N-heteroatom framework, the high surface area as well as the microporous nature of the studied CTF materials prompted us to further explore their gas sorption properties at atmospheric pressure. To this aim, CO_2 adsorption isotherms were recorded at 273 K and 298 K (Figure 2.7 and Figure 2.8). As shown in both figures, when using the same equiv. of $ZnCl_2$, increasing the synthesis temperature from 400 °C to 500 °C results in the materials exhibiting a higher CO_2 uptake, while at the same synthesis temperature (400 °C), applying more equiv. of $ZnCl_2$ results in CTFs having a higher CO_2

adsorption capacity. Nevertheless, when the synthesis temperature is 500 °C, the amount of employed $ZnCl_2$ has little effect on the material's CO_2 adsorption capacity as the CO_2 uptake is almost the same for all the samples obtained at 500 °C.
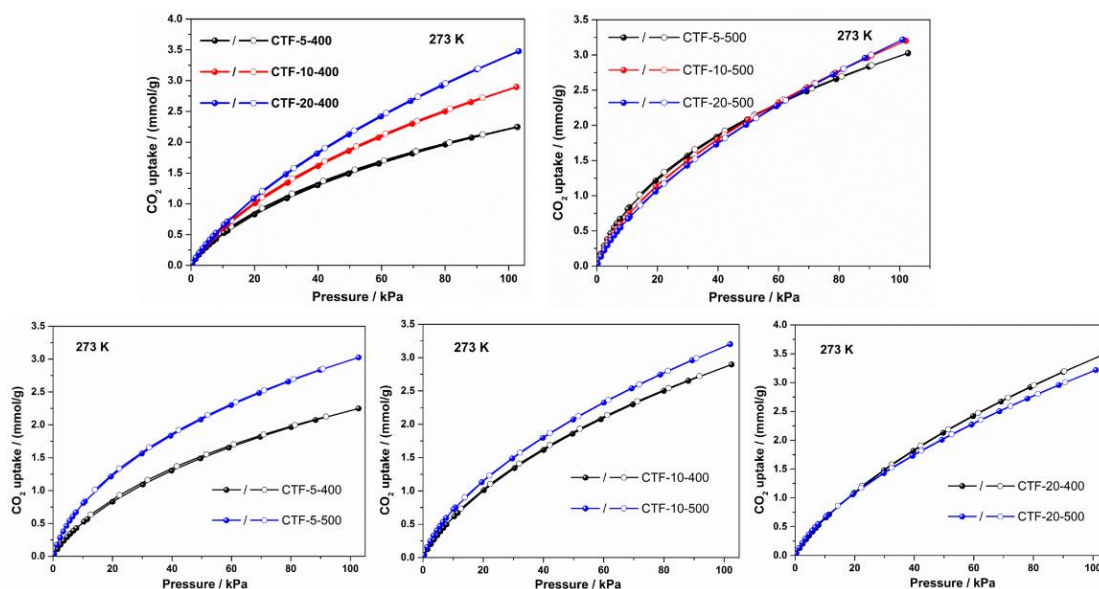
Figure 2.7. CO_2 adsorption (closed symbols) and desorption (open symbols) isotherms of the studied CTF materials measured up to 1 bar at 273 K.
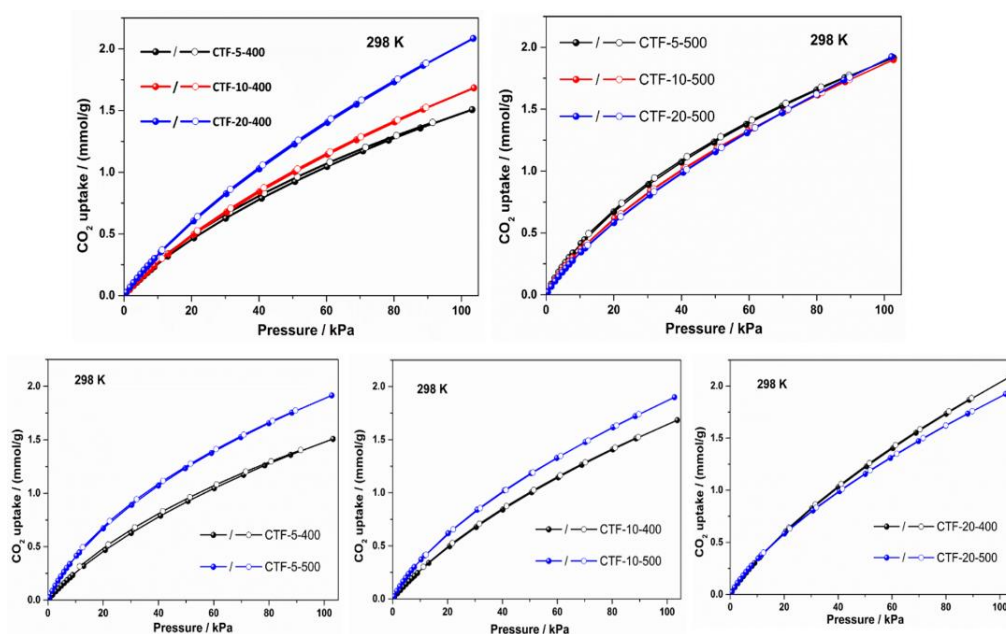
Figure 2.8. CO_2 adsorption (closed symbols) and desorption (open symbols) isotherms of the studied CTF materials measured up to 1 bar at 298 K.

Among all the obtained CTFs, CTF-20-400 exhibits the highest CO_2 adsorption

uptake of 3.48 and 2.09 mmol/g at 273 K and 298 K, respectively. The CO_2 uptake of CTF-20-400 is much higher in comparison to numerous CTFs measured at 273 K such as CTF-1 (2.47 mmol/g)[2], CTF-DCN-500 (2.7 mmol/g)[15], PCTF-1 to 3 (2.02-3 mmol/g)[27] and CTF-0 (1.54-2.34 mmol/g)[19]. The isosteric heat of CO_2 adsorption (Q_{st}) is considered as a rough estimate of the interaction energies. Thus, to get a better insight in the CO_2 adsorption of the CTFs, we calculated the Q_{st} for all the CTFs by employing the Clausius-Clapeyron equation to fit the CO_2 adsorption isotherms at 273 K and 298 K and plotted the Q_{st} as a function of the adsorbed CO_2 uptake (Figure 2.9). At low CO_2 coverage, the Q_{st} values are calculated to be 22-28 kJ/mol, which is much higher than the heat of liquefaction of bulk CO_2 (17 kJ/mol)[28] and similar to the isosteric heat of CO_2 adsorption on activated carbon.[29] These results indicate relatively strong interactions between CO_2 molecules and the network, explaining the overall high CO_2 uptakes of the CTFs.
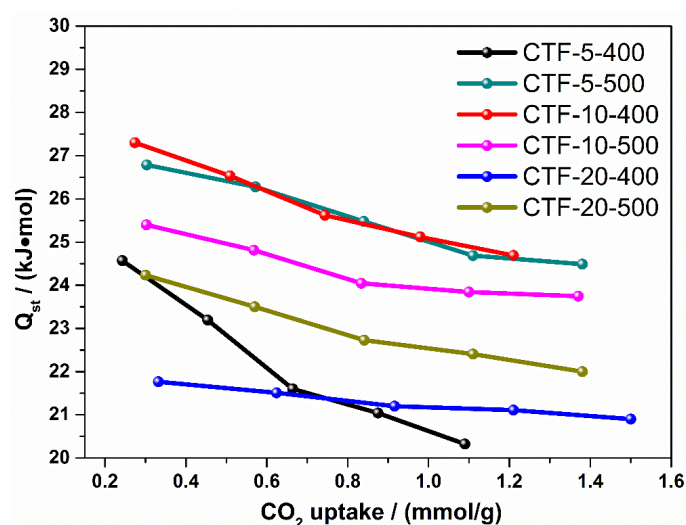
Figure 2.9. Isosteric heat of CO_2 adsorption (Q_{st}) of all the studied CTF materials.

Moreover, the incorporation of nitrogen sites into CTFs not only afforded significant CO_2 uptakes but also resulted in more preferential CO_2 adsorption over N_2, i.e., higher CO_2/N_2 selectivity, another crucial factor for realistic carbon capture. Thus we further calculated the CO_2/N_2 selectivity at 298 K of all the studied CTFs using the Henry model based on the CO_2 and N_2 adsorption

isotherms (Figure 2.10) and the detailed values are listed in Table 2.2. The highest CO_2/N_2 selectivity was observed for CTF-5-500 (36 at 298 K), which is in line with the fact that smaller pores are more favorable for CO_2 adsorption.
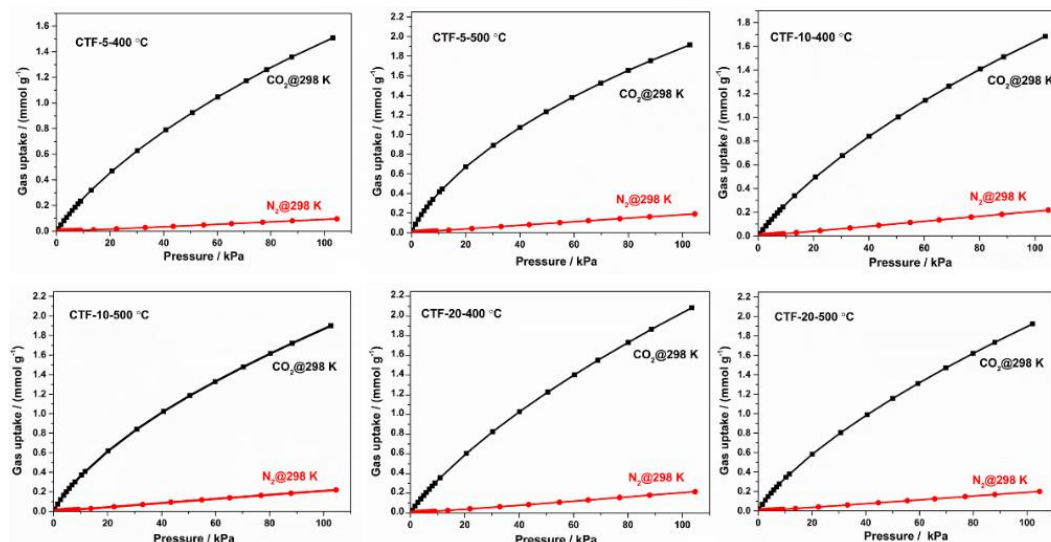
Figure 2.10. CO_2 and N_2 adsorption isotherms measured on all the presented CTF samples up to 1 bar at 298 K.

As a potential renewable and clean alternative to current fossil fuels, hydrogen storage remains the major obstacle for its widespread applications and the development of safe and efficient ways of H_2 storage remains urgent and challengeable. Recently, adsorptive hydrogen storage in MOFs and COFs has been explored as a plausible approach for hydrogen storage.[30-31] Thus, we further carried out H_2 adsorption measurements on all the obtained CTFs up to 1 bar at 77 K (Figure 2.11). In contrast to CO_2 adsorption, H_2 uptakes mainly depend on the materials' surface area and the H_2 adsorption capacities varied from 0.98 to 1.5 wt % (Table 2.2). The highest H_2 adsorption capacity was found for CTF-20-400 (1.5 wt%), this value is comparable to that reported for DCBP-CTF (1.55 wt%)[17] and is only slightly lower than PCTF-1 (1.86 wt%)[32] and fl-CTF-400 (1.95 wt%)[33].
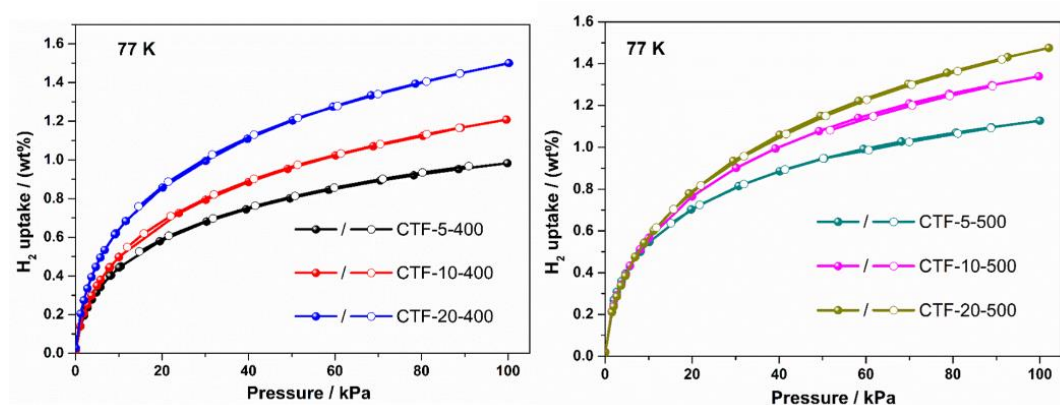
Figure 2.11. H_2 adsorption (solid symbols) and desorption (open symbols) isotherms for the CTFs synthesized at 400 °C (left) and 500 °C (right) measured at 77 K.

2.3. Conclusion

In conclusion, in this chapter we have employed a novel heteroaromatic building block to prepare a set of highly microporous and nitrogen-rich CTFs as high-performance platforms for gas sorption and storage. The effects of several synthesis parameters including the reaction temperature and molar ratios of $ZnCl_2$ on the structure and porosity properties of such networks was comprehensively studied. Notably, the microporosity together with the rich CO_2-philic N sites results in the framework with excellent CO_2 (3.48 mmol/g, at 273 K and 1 bar) and H_2 (1.5 wt%, 77 K and 1 bar) uptakes. These values are among the top levels for all the reported CTFs measured under identical conditions. In addition, the obtained CTFs also exhibit relatively high CO_2/N_2 selectivities (up to 36) as calculated by Henry Model at 298 K. These properties together with their good thermal and chemical stability render the studied CTFs promising candidates as prospective carbon capture and hydrogen storage materials.

2.4. Experimental Section

Materials and analytical techniques. All the chemicals were bought from commercial suppliers and used as such without further purifications. Powder-X-ray diffraction (PXRD) patterns were recorded on a Thermo Scientific ARL

X'Tra diffractometer (Cu-Kα radiation (λ = 1.5406 Å) at 40 kV and 30 mA). Fourier Transform Infrared Spectroscopy (FT-IR) measurements were carried out on a Thermo Nicolet 6700 FT-IR spectrometer using a KBr beam splitter and a MCT detector. Elemental analysis were obtained using a Thermo Scientific Flash 2000 CHNS-O analyzer. Thermogravimetric analysis (TGA) curves were recorded under an air flow with a heating rate of 10 °C/min in the range of 25-800 °C on a Netzsch STA-449 F3 Jupiter-simultaneous TG-DSC analyzer. The Scanning Electron Microscopy (SEM) images of the CTFs materials were recorded on a JEOL JSM 7600F FEG/SEM. A Belsorp Mini instrument was employed to obtain the N_2 adsorption isotherms at 77 K, whereas for the CO_2 and H_2 isotherms, an iSorb-HP gas sorption analyzer (Quantachrome) was used. All the materials were dried at 150 °C under vacuum for 3 h before the gas adsorption measurements were performed.

Synthesis of CTFs. The monomer, 4,4',4'',4'''-(1,4-phenylenebis(pyridine-4,2,6-triyl))tetrabenzonitrile, was synthesized following the procedure reported by Zhang et al.[34] In a typical CTF material synthesis, the ampoule was charged with the monomer (318 mg, 0.5 mmol) and various amounts of anhydrous $ZnCl_2$ (ranging from 340 mg, 2.5 mmol to 1360 mg, 10 mmol) in the glovebox. Hereafter, the ampoule was evacuated, flame-sealed and slowly heated to the desired temperatures (400 °C or 500 °C) with the heating step of 1 °C/min for 48 h. Hereafter, at room temperature, the ampoule was opened and the crude material was grounded and stirred in water for 6 h, filtrated and washed thoroughly with distillated water. Afterwards, the obtained black solid was stirred in HCl (1M) overnight, followed by successive washing with water, THF and acetone. Hereafter, the resulting CTF materials was activated at 150 °C under vacuum overnight prior to further analysis.

2.5. References

1. Davis, S. J.; Caldeira, K.; Matthews, H. D., Future CO_2; Emissions and Climate Change

from Existing Energy Infrastructure. *Science* **2010,** *329* (5997), 1330.

2.   Zhao, Y.; Yao, K. X.; Teng, B.; Zhang, T.; Han, Y., A perfluorinated covalent triazine-based framework for highly selective and water-tolerant CO_2 capture. *Energy Environ. Sci.* **2013,** *6* (12), 3684-3692.

3.   Rochelle, G. T., Amine Scrubbing for CO_2 Capture. *Science* **2009,** *325* (5948), 1652.

4.   D'Alessandro, D. M.; Smit, B.; Long, J. R., Carbon Dioxide Capture: Prospects for New Materials. *Angew. Chem. Int. Ed.* **2010,** *49* (35), 6058-6082.

5.   Ferey, G.; Serre, C.; Devic, T.; Maurin, G.; Jobic, H.; Llewellyn, P. L.; De Weireld, G.; Vimont, A.; Daturi, M.; Chang, J.-S., Why hybrid porous solids capture greenhouse gases? *Chem. Soc. Rev.* **2011,** *40* (2), 550-562.

6.   Wang, J.; Huang, L.; Yang, R.; Zhang, Z.; Wu, J.; Gao, Y.; Wang, Q.; O'Hare, D.; Zhong, Z., Recent advances in solid sorbents for CO_2 capture and new development trends. *Energy Environ. Sci.* **2014,** *7* (11), 3478-3518.

7.   Furukawa, H.; Cordova, K. E.; O'Keeffe, M.; Yaghi, O. M., The Chemistry and Applications of Metal-Organic Frameworks. *Science* **2013,** *341* (6149).

8.   Li, B.; Wen, H.-M.; Cui, Y.; Zhou, W.; Qian, G.; Chen, B., Emerging Multifunctional Metal–Organic Framework Materials. *Adv. Mater.* **2016,** *28* (40), 8819-8860.

9.   Zhou, H.-C.; Long, J. R.; Yaghi, O. M., Introduction to Metal–Organic Frameworks. *Chem. Rev.* **2012,** *112* (2), 673-674.

10. Ding, S.-Y.; Wang, W., Covalent organic frameworks (COFs): from design to applications. *Chem. Soc. Rev.* **2013,** *42* (2), 548-568.

11. Zeng, Y.; Zou, R.; Zhao, Y., Covalent Organic Frameworks for CO_2 Capture. *Adv. Mater.* **2016,** *28* (15), 2855-2873.

12. Leus, K.; Bogaerts, T.; De Decker, J.; Depauw, H.; Hendrickx, K.; Vrielinck, H.; Van Speybroeck, V.; Van Der Voort, P., Systematic study of the chemical and hydrothermal stability of selected "stable" Metal Organic Frameworks. *Microporous Mesoporous Mater.* **2016,** *226,* 110-116.

13. Zhang, Z. J.; Yao, Z. Z.; Xiang, S. C.; Chen, B. L., Perspective of microporous metal-organic frameworks for CO_2 capture and separation. *Energy Environ. Sci.,* 2014; 7, 2868-2899.

14. Hug, S.; Stegbauer, L.; Oh, H.; Hirscher, M.; Lotsch, B. V., Nitrogen-Rich Covalent Triazine Frameworks as High-Performance Platforms for Selective Carbon Capture and Storage. *Chem. Mater.* **2015,** *27* (23), 8001-8010.

15. Wang, K.; Huang, H.; Liu, D.; Wang, C.; Li, J.; Zhong, C., Covalent Triazine-Based Frameworks with Ultramicropores and High Nitrogen Contents for Highly Selective CO_2 Capture. *Environ. Sci. Technol.* **2016,** *50* (9), 4869-4876.

16. Tuci, G.; Pilaski, M.; Ba, H.; Rossin, A.; Luconi, L.; Caporali, S.; Pham-Huu, C.; Palkovits, R.; Giambastiani, G., Unraveling Surface Basicity and Bulk Morphology Relationship on

Covalent Triazine Frameworks with Unique Catalytic and Gas Adsorption Properties. *Adv. Funct. Mater.* **2017,** *27* (7), 1605672.

17. Kuhn, P.; Antonietti, M.; Thomas, A., Porous, Covalent Triazine-Based Frameworks Prepared by Ionothermal Synthesis. *Angew. Chem. Int. Ed.* **2008,** *47* (18), 3450-3453.

18. Ren, S.; Bojdys, M. J.; Dawson, R.; Laybourn, A.; Khimyak, Y. Z.; Adams, D. J.; Cooper, A. I., Porous, Fluorescent, Covalent Triazine-Based Frameworks Via Room-Temperature and Microwave-Assisted Synthesis. *Adv. Mater.* **2012,** *24* (17), 2357-2361.

19. Katekomol, P.; Roeser, J.; Bojdys, M.; Weber, J.; Thomas, A., Covalent Triazine Frameworks Prepared from 1,3,5-Tricyanobenzene. *Chem. Mater.* **2013,** *25* (9), 1542-1548.

20. Park, K.; Lee, K.; Kim, H.; Ganesan, V.; Cho, K.; Jeong, S. K.; Yoon, S., Preparation of covalent triazine frameworks with imidazolium cations embedded in basic sites and their application for CO₂ capture. *J. Mater. Chem. A* **2017,** *5* (18), 8576-8582.

21. Kuhn, P.; Thomas, A.; Antonietti, M., Toward Tailorable Porous Organic Polymer Networks: A High-Temperature Dynamic Polymerization Scheme Based on Aromatic Nitriles. *Macromolecules* **2009,** *42* (1), 319-326.

22. Kuhn, P.; Forget, A.; Su, D.; Thomas, A.; Antonietti, M., From Microporous Regular Frameworks to Mesoporous Materials with Ultrahigh Surface Area: Dynamic Reorganization of Porous Polymer Networks. *J. Am. Chem. Soc.* **2008,** *130* (40), 13333-13337.

23. Park, K.; Lee, K.; Kim, H.; Ganesan, V.; Cho, K.; Jeong, S. K.; Yoon, S., Preparation of covalent triazine frameworks with imidazolium cations embedded in basic sites and their application for CO₂ capture. *J. Mater. Chem. A* **2017,** *5* (18), 8576-8582.

24. Hug, S.; Tauchert, M. E.; Li, S.; Pachmayr, U. E.; Lotsch, B. V., A functional triazine framework based on N-heterocyclic building blocks. *J. Mater. Chem.* **2012,** *22* (28), 13956-13964.

25. Dey, S.; Bhunia, A.; Boldog, I.; Janiak, C., A mixed-linker approach towards improving covalent triazine-based frameworks for CO₂ capture and separation. *Microporous Mesoporous Mater.* **2017,** *241*, 303-315.

26. Dey, S.; Bhunia, A.; Esquivel, D.; Janiak, C., Covalent triazine-based frameworks (CTFs) from triptycene and fluorene motifs for CO₂ adsorption. *J. Mater. Chem. A* **2016,** *4* (17), 6259-6263.

27. Gu, C.; Liu, D.; Huang, W.; Liu, J.; Yang, R., Synthesis of covalent triazine-based frameworks with high CO₂ adsorption and selectivity. *Polym. Chem.* **2015,** *6* (42), 7410-7417.

28. Keskin, S.; van Heest, T. M.; Sholl, D. S., Can Metal–Organic Framework Materials Play a Useful Role in Large-Scale Carbon Dioxide Separations? *ChemSusChem* **2010,** *3* (8), 879-891.

29. Himeno, S.; Komatsu, T.; Fujita, S., High-Pressure Adsorption Equilibria of Methane and Carbon Dioxide on Several Activated Carbons. *Journal of Chemical & Engineering Data* **2005,** *50* (2), 369-376.

30. Sculley, J.; Yuan, D.; Zhou, H.-C., The current status of hydrogen storage in metal-organic frameworks-updated. *Energy Environ. Sci.* **2011,** *4* (8), 2721-2735.

31. Schlapbach, L.; Zuttel, A., Hydrogen-storage materials for mobile applications. *Nature* **2001,** *414* (6861), 353-358.

32. Bhunia, A.; Vasylyeva, V.; Janiak, C., From a supramolecular tetranitrile to a porous covalent triazine-based framework with high gas uptake capacities. *Chem. Commun.* **2013,** *49* (38), 3961-3963.

33. Hug, S.; Mesch, M. B.; Oh, H.; Popp, N.; Hirscher, M.; Senker, J.; Lotsch, B. V., A fluorene based covalent triazine framework with high CO_2 and H_2 capture and storage capacities. *J. Mater. Chem. A* **2014,** *2* (16), 5928-5936.

34. Wang, J.-H.; Zhang, Y.; Li, M.; Yan, S.; Li, D.; Zhang, X.-M., Solvent-Assisted Metal Metathesis: A Highly Efficient and Versatile Route towards Synthetically Demanding Chromium Metal–Organic Frameworks. *Angew. Chem. Int. Ed.* **2017,** *56* (23), 6478-6482.

CHAPTER 3

Highly Enhanced Gas Adsorption Performance in a Fluorinated Microporous Covalent Triazine Framework
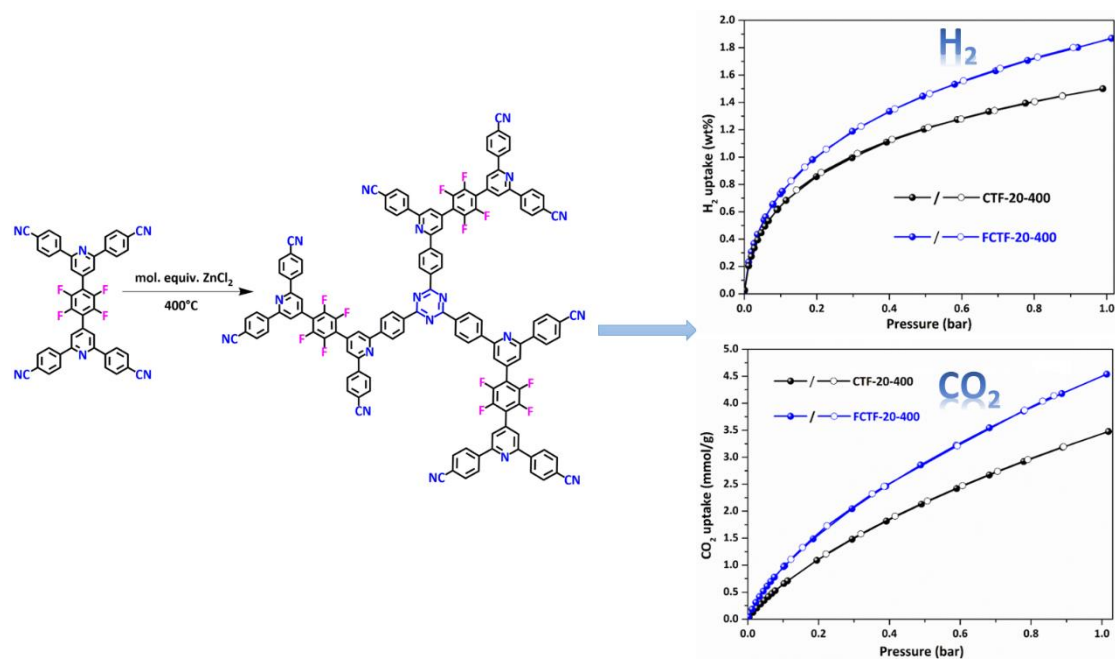
The results of this chapter were published in:

Abstract

In this chapter, a new fluorinated microporous CTF material has been synthesized via straightforward incorporation of fluorine groups into the building block. The resulting fluorinated CTFs show nitrogen- and fluorine-rich environments, significantly high surface area (up to 2060 m^2/g) and pore volume of 1.06 cm^3/g as well as high physiochemical stability, exhibiting excellent promise for efficient CO_2 capture and H_2 storage. Remarkably, the CO_2 adsorption capacity of F-CTF-20-400 can reach up to 4.54 mmol/g at 273 K and 1 bar, which is much higher than that of corresponding non-functionalized CTF (3.48 mmol/g) and higher than most of other reported CTF materials except few examples. Furthermore, the material of F-CTF-20-400 also exhibits superior H_2 adsorption capacity of 1.88 wt%, which surpasses most of the reported CTF materials in literature. Additionally, the fluorinated CTFs also feature quite high CO_2 selectivity over N_2 (28) and CH_4 (5.6) at room temperature.

3.1. Introduction

In chapter 2, we have reported on a novel N-heteroaromatic-based covalent triazine framework, which was evaluated as platforms for efficient CO_2 and H_2 adsorption.[1] The gas adsorption capacities of the studied materials were higher than lots of reported CTF materials,[2-4] however, there is still room for improvement, compared with the benchmark CTF materials.[5-6] Incorporation of functional groups into the frameworks of porous materials is considered as an efficient approach for improving their gas adsorption performance[3, 7] and in search of a particular functionality for the application of gas adsorption and separation, fluorine groups are regarded as a suitable candidate owing to the strong electronegativity of F and hydrophobicity of the fluorine groups.[8-10] Han et al. reported a perfluorinated covalent triazine framework (FCTF-1) by using tetrafluoroterephthalonitrile as the building block. Remarkably, the material of FCTF-1 exhibits a significantly high CO_2 uptake of 4.67 mmol/g at 273 K and 1 bar, which is much higher than that of non-functionalized CTF-1 (2.47mmol/g under identical conditions).[11]

In this chapter, we report on the fluorination of the aforementioned tetranitrile, which is then employed as the building block to prepare a set of fluorinated CTF materials. The presence of fluorine and corresponding fluorine content in the obtained CTF materials was determined by TEM and EDX mapping and F1s XPS measurements. Afterwards, the gas adsorption and separation performances on all the obtained fluorinated CTFs were systematically evaluated.

3.2. Results and Discussion

The synthesis of the fluorinated CTFs is carried out under the typical ionothermal conditions through $ZnCl_2$ catalyzed trimerization of the nitriles (Figure 3.1). Generally, the trimerization of the fluorinated tetranitrile with

$ZnCl_2$/monomer ratio of 5, 10 and 20 at 400 °C yielded FCTF-5-400, FCTF-10-400 and FCTF-20-400, respectively.
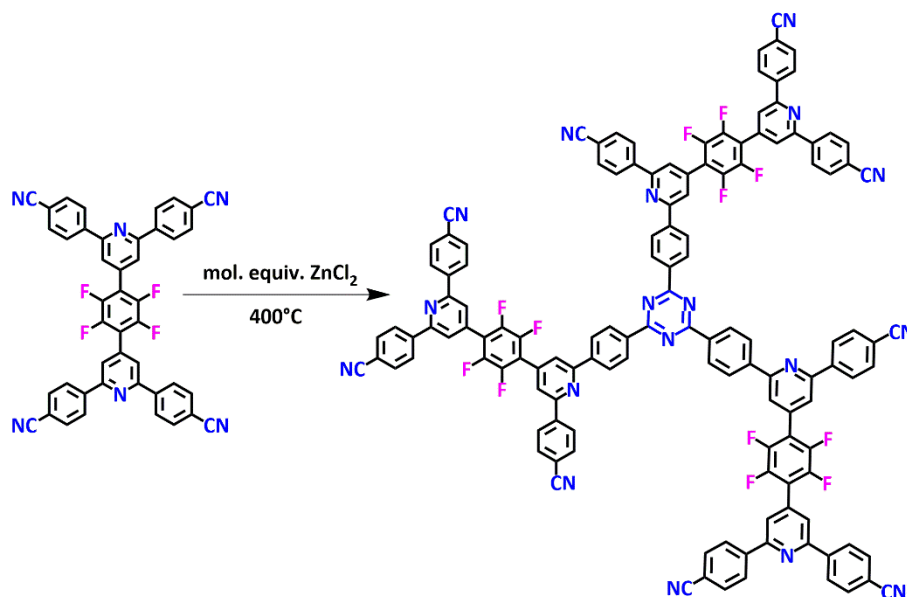
Figure 3.1. Schematic representation of the ideal structure of the FCTF materials.

The obtained black powders are not soluble in water, acids, bases and organic solvents, indicating that fully condensed networks were formed. The synthesized materials were evaluated with respect to their crystallinity by powder X-ray diffraction (Figure S3.1). As expected, all the samples were amorphous. FT-IR measurements were carried out to confirm whether the trimerization reaction was completed or not.
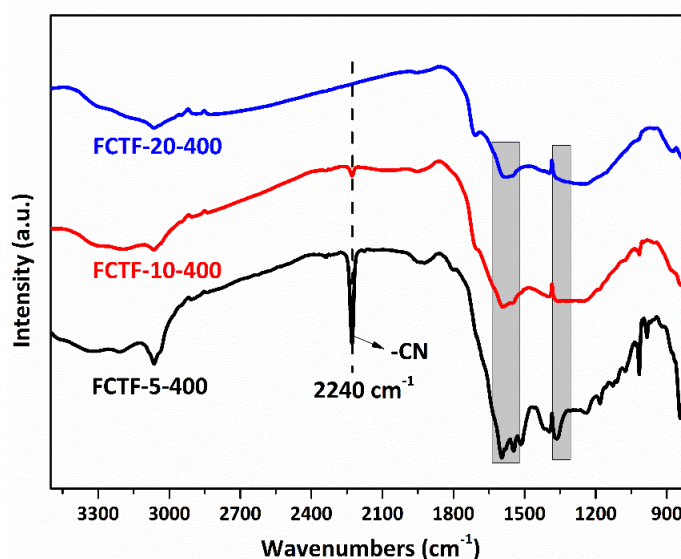
Figure 3.2. FT-IR spectra of the studied fluorinated CTF materials.

As shown in Figure 3.2, the characteristic band of nitriles for FCTF-5-400 and FCTF-10-400 at 2240 cm^{-1} can be clearly observed, suggesting the incomplete trimerization process, which is mainly attributed to the high mass of the monomer and the employed amount of $ZnCl_2$ for both synthesis is not enough to catalyze the trimerization reactions,[1] while the trimerization is completed for FCTF-20-400, as the characteristic peak of the nitrile groups is absent. The triazine moieties can be assigned to the bands around 1540 and 1360 cm^{-1} (highlighted grey).[3, 12] To obtain a more detailed picture of the composition of the resulting CTF materials, elemental analysis was performed on all the studied samples. As shown in Table 3.1, with the increase of the $ZnCl_2$/monomer ratio from 5 to 20, the content of C gradually increased, while the content of H and N was noted to the opposite tendency. The overall lower absolute nitrogen and carbon content compared to the theoretical values is likely caused by the residual water and metal salts entrapped in the pores that can't be completely removed even after extensive washing.[12-13]

Table 3.1. Elemental analysis and pore characteristics of the studied fluorinated CTFs.

Sample	Elemental analysis (%)				S_{BET}[a] (m^2/g)	$V_{micro.}$[b] (cm^3/g)	$V_{tot.}$[c] (cm^3/g)
	C	H	N	F [d]			
FCTF-5-400	73.6	3.18	9.78	1.44	987	0.46	0.52
FCTF-10-400	75.4	2.83	7.98	0.87	1897	0.89	0.93
FCTF-20-400	80.8	2.40	7.62	0.45	2060	0.96	1.06
Theoretical value	74.57	2.84	11.86	10.72	-	-	-

a. BET surface area calculated over the pressure range 0.01-0.05 P/P_0 at 77 K; b. V_{micro}, pore volume at $P/P_0 = 0.1$ at 77 K; c. V_{tot}, total pore volume calculated at $P/P_0 = 0.98$; d. determined by XPS.

The presence of fluorine groups in the materials was confirmed by high angle annular dark field scanning-transmission electron microscopy (HAADF-STEM) and corresponding energy dispersive X-ray spectroscopy (EDX) mapping images (Figure 3.3 and Figure S3.2-S3.3). It is clear that C, N and F elements are well dispersed and homogeneously distributed throughout the materials. It should be noted that the theoretical fluorine content is much lower than that of carbon and nitrogen and the defluorination process is inevitable during the

synthesis, resulting in almost complete fluorine loss for the samples of FCTF-FCTF-20-400 (0.45 % out of theoretical value of 10.72 %, determined by XPS measurements), this observation is in accordance with previous reports and explains the almost absence of F species in FCTF-20-400.[11, 14] The defluorination process and created defects of the frameworks possibly accounts for the generation of extra micropores, resulting in higher surface areas.
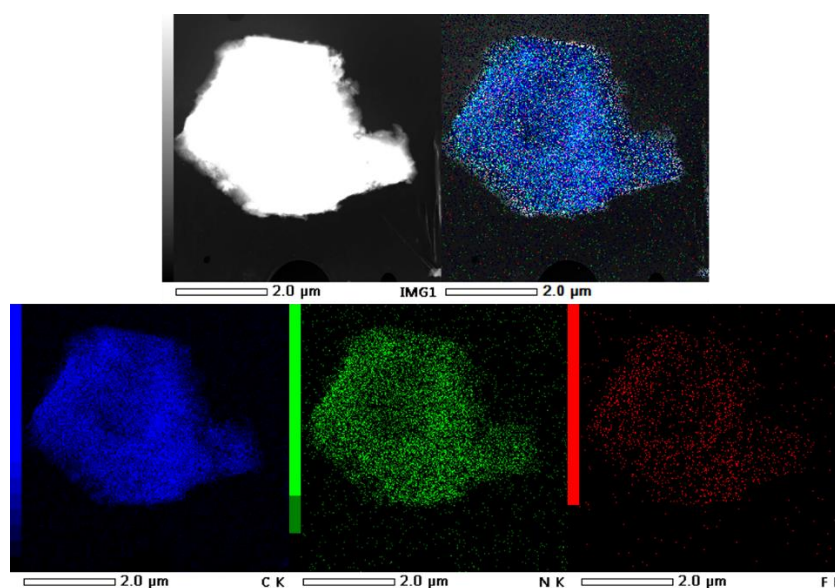
Figure 3.3. High angle annular dark field scanning-transmission electron microscopy (HAADF-STEM) and corresponding energy dispersive X-ray spectroscopy (EDX) mapping images of carbon (blue), nitrogen (green) and fluorine (red) for the sample of FCTF-5-400.

Additionally, X-ray photoelectron spectroscopy (XPS) measurements were performed to further investigate the chemical state of various elements in the adsorbents. XPS C1s spectra of all the fluorinated CTFs were fitted using five peaks with the binding energies of 285.00 ± 0.05 eV (C-C), 286.30 ± 0.05 eV (C-O/C-N), 287.70 ± 0.05 eV (C≡N), 289.10 ± 0.05 eV (O-C=O) and 291.20 ± 0.05 eV (C-F). The results show that the deconvolution of the N1s peak can be divided into four peaks: pyridinic (398.8 ± 0.1 eV), pyrrolic (400.2 ± 0.1 eV), quaternary (401.3 ± 0.1 eV) and oxidized N-O (403.4 ± 0.2 eV) (Figure 3.4). It can be clearly see that the higher $ZnCl_2$/monomer ratio will lead to the formation of more pyrrolic products (5-ring aromatics) and less pyridinic products (6-ring

aromatics) due to the presence of more defects in the structure. The N-O chemical shift appears mainly because of the exposure of the samples in the open air or the existence of water or other solvents in the as-synthesized monomer, which are too difficult to be completely removed.
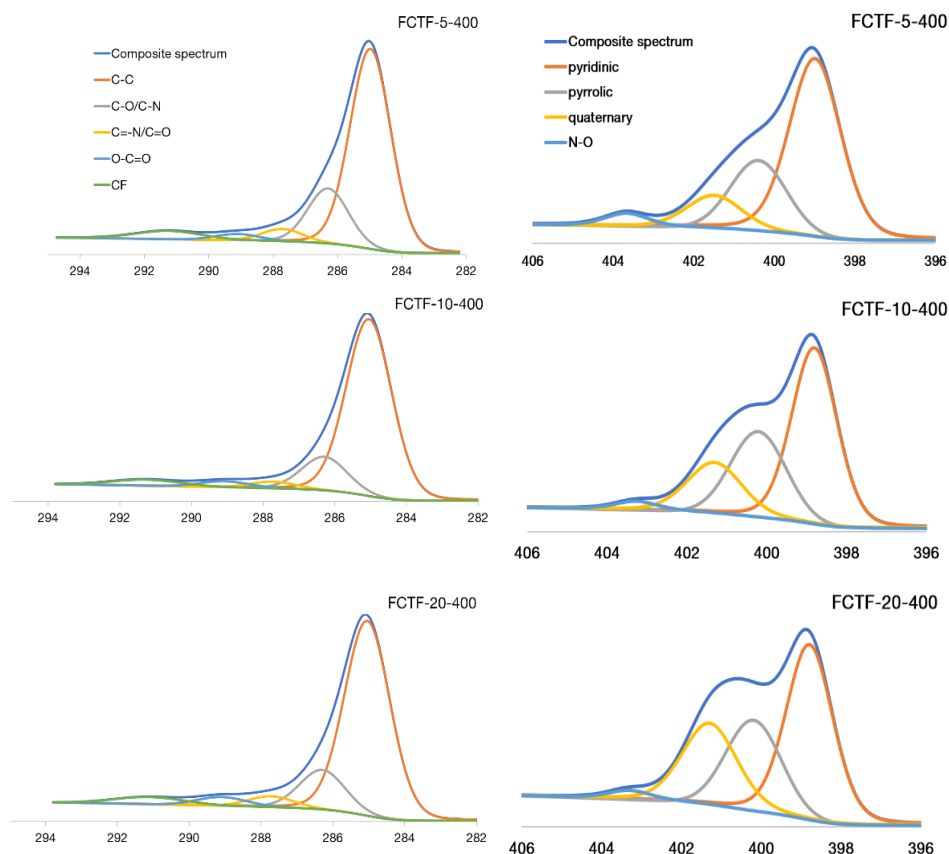
Figure 3.4. Deconvoluted C1s (left) and N1s (right) spectra of the FCTF materials.

The single peak at 687.8 eV in the F 1s spectra of the FCTF materials corresponds to the aromatic C-F species[10] (Figure 3.5). It should be noted that, for the samples of FCTF-10-400 and FCTF-20-400, this typical peak is too weak to distinguish and it is mainly because of the fact that $ZnCl_2$ is able to induce and accelerate the defluorination process,[7] thus resulting in the prominent loss of the fluorine groups, which is also in accordance with the observation from TEM and EDX mapping images. The content of fluorine calculated from XPS measurements ranged from 1.44 % for FCTF-5-400 to only 0.45 % for FCTF-20-400 (out of theoretical value of 10.72 %). The detailed chemical composition obtained from XPS survey scans for all the CTF

materials is summarized in Table S3.1. Thermogravimetric analysis (TGA) measured under air flow indicated that the all the samples are stable up to 400 ℃ (Figure S3.4).
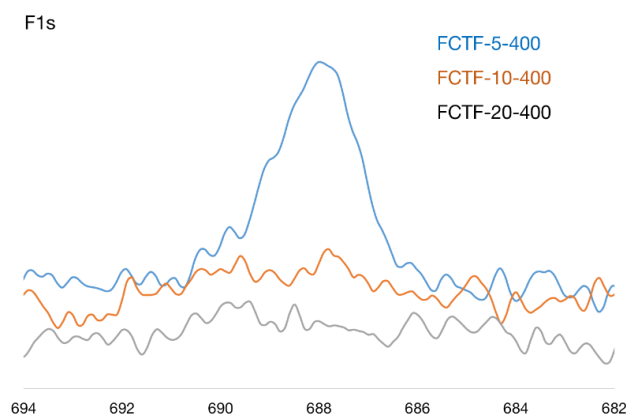
Figure 3.5. Deconvoluted F1s spectra of all the studied FCTF materials.
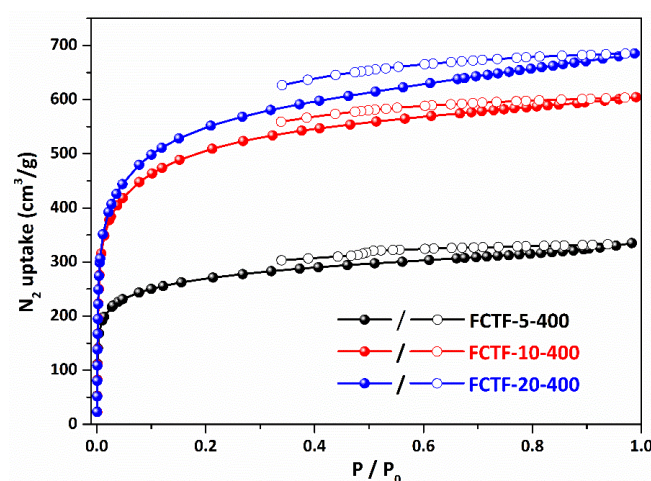
Figure 3.6. N_2 adsorption and desorption isotherms of the studied fluorinated CTF materials.

The permanent porosity of all the studied fluorinated CTFs is investigated by nitrogen adsorption measurements at 77 K, after activation at 150 ℃ for 3 h (Figure 3.6). As shown in Figure 3.6, all the N_2 adsorption isotherms exhibit typical type I behavior, characteristic of microporous materials and with the increase of $ZnCl_2$/monomer ratio, the materials exhibit higher N_2 uptakes, indicating its significantly larger porosity. The Brunauer-Emmett-Teller (BET) surface area and pore volume of FCTF-20-400 can reach up to 2060 m^2/g and 1.06 cm^3/g, which is much higher than that of CTF-20-400 (1458 m^2/g and 0.84

cm^3/g, respectively)[1]. The detailed calculated surface areas and pore volumes of all the materials were summarized in table 3.1.

Given the high porosity as well as the nitrogen- and fluorine-rich features of the FCTF materials, single-component CO_2, CH_4 and N_2 gas adsorption isotherms were recorded up to 1 bar at different temperatures to evaluate their performance in selective gas adsorption (Figure 3.7).
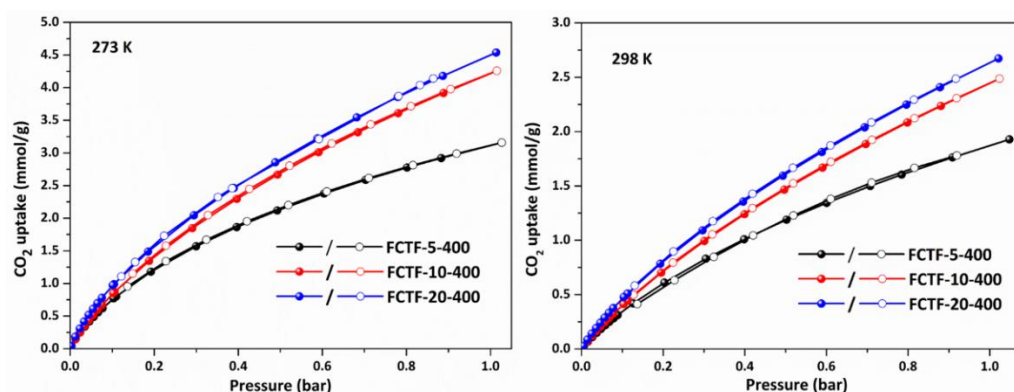
Figure 3.7. CO_2 adsorption isotherms of all the studied materials measured at 273K and 298K up to 1 bar, respectively.

As shown in Figure 3.7, at both 273 K and 298 K, CO_2 uptakes in these studied materials increase gradually with the increase of the $ZnCl_2$/monomer ratio from 5 to 20, without saturation in uptake observed in the studied pressure region. The CO_2 adsorption capacity for these fluorinated CTFs at 273 K and 298 K and 1 bar ranges from 3.15 and 1.92 mmol/g (FCTF-5-400) to 4.54 and 2.67 mmol/g (FCTF-20-400).
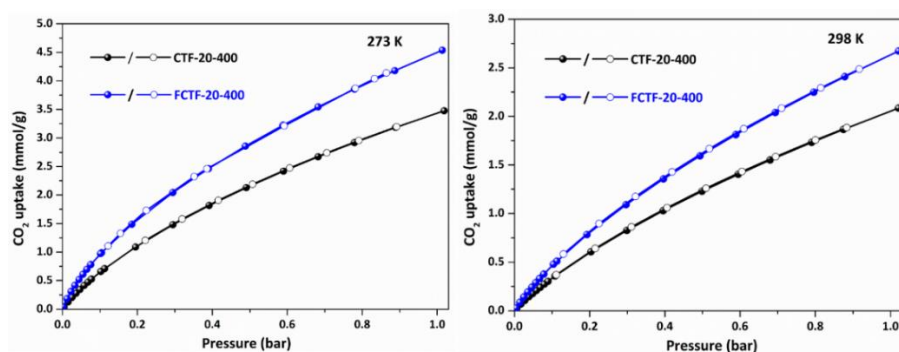
Figure 3.8. Comparison of the CO_2 adsorption isotherms of CTF-20-400 and FCTF-20-400 measured at 273K and 298K, respectively.

Table 3.2. Summary and comparison of the gas adsorption performance of the studied fluorinated CTFs and some of the reported CTF materials.

Sample	CO_2 uptake (mmol/g)		H_2 uptake (wt%)	CO_2/N_2 Selectivity	CO_2/CH_4 Selectivity	Q_{st} kJ/mol	Ref.
	273K	298K	77 K	298K	298K		
FCTF-5-400	3.15	1.92	1.30	28	5.6	29.5	This work
FCTF-10-400	4.25	2.48	1.86	19	4.7	25.0	
FCTF-20-400	4.54	2.67	1.88	21	5.1	27.5	
PCTF-1	3.21	1.84[a]	1.86	-	3[a]	-	15
FCTF-1	4.67	3.21	-	31[b]	-	35.0	11
lut-CTF400	4.55	2.72	1.36	63	-	37.5	12
CTF-5-400	2.25	1.51	0.98	24	-	25.5	1
CTF-10-400	2.90	1.68	1.21	14	-	27.9	1
CTF-20-400	3.48	2.09	1.50	19	-	22.1	1

a. Gas uptake at 293K; b. CO_2/N_2 selectivity was calculated by Ideal Adsorption Solution Theory (IAST).

Notably, the CO_2 adsorption uptake is much higher than that of the pristine CTFs.[1] For example, the CO_2 adsorption capacity is found to be 3.48 mmol/g for CTF-20-400, while FCTF-20-400 exhibits the CO_2 uptake of 4.54 mmol/g under the same conditions (Figure 3.8 and Table 3.2), which outperforms most of the reported CTF materials (Table 1.3). The isosteric heat of CO_2 adsorption (Q_{st}) for all the FCTF materials was calculated from fitting the isotherms by Clausius-Clapeyron equation and the values were found to be 25-29.5 kJ/mol for the FCTF materials (Figure S3.5), slightly higher than that of non-functionalized CTFs (22.1-27.9 kJ/mol). These findings indicate the strong interactions between the framework and the CO_2 molecules. In sharp contrast to the high CO_2 adsorption capacities, CH_4 and N_2 adsorption capacities of the FCTF samples are much lower and in view of the significant differences of the CO_2, CH_4 and N_2 adsorption performance of the studied materials, we further estimated their potential for the separation of CO_2/CH_4 and CO_2/N_2. Thus, the corresponding selectivities were calculated by the henry model according to their corresponding single gas adsorption isotherms (Figure 3.9).
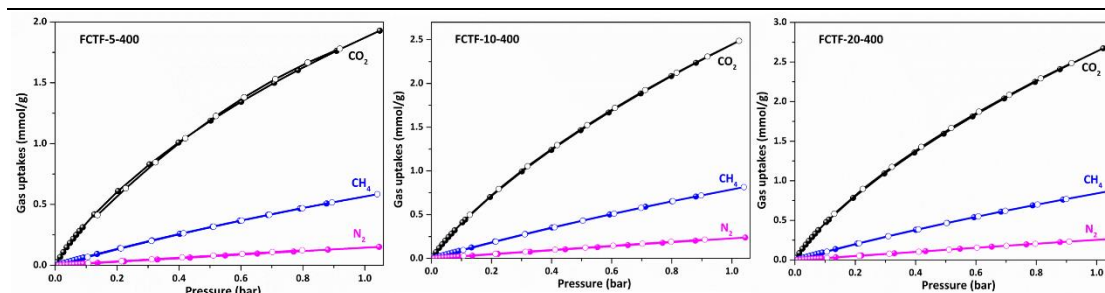
Figure 3.9. CO_2, CH_4 and N_2 adsorption isotherms of the studied FCTF materials measured at 298K.

The detailed values for all the samples were listed in Table 3.2. The highest adsorption selectivity of CO_2/CH_4 (5.6) and CO_2/N_2 (28) was found for FCTF-5-400, and for all the fluorinated CTFs, significant improvement was observed compared with those of non-functionalized CTFs. All the observed results indicate that incorporation of fluorine groups into the frameworks of CTFs exhibit great benefits not only for improving gas adsorption capacities, but also for enhancing the selectivity of CO_2 over CH_4 and N_2 in the low pressure region.

To further examine the effect of fluorine groups on the materials' gas adsorption performance, we performed hydrogen storage measurements of all the studied materials and compared with the non-functionalized CTF materials. Figure 3.10 shows the H_2 adsorption isotherms recorded at 77 K up to 1 bar and the detailed H_2 uptakes are summarized in Table 3.2. Typically, the higher surface area of the samples, the higher H_2 adsorption capacity. In line with the general claim for CO_2 adsorption, FCTF-20-400 exhibits the highest H_2 uptake. Noteworthy, the H_2 adsorption uptakes for the fluorinated CTFs were significantly enhanced compared with those of non-functionalized ones. For example, CTF-20-400 exhibited the H_2 adsorption capacity of 1.5 wt% at 77 K and 1 bar, while this value was observed to be 1.88 wt% for FCTF-20-400, which is higher than most of the reported CTF materials, comparable to that of PCTF-1 (1.86 wt%)[15] and only slightly lower than that of the benchmark CTF (fl-CTF-400) synthesized at 400 ℃ (1.95 wt%).[16]
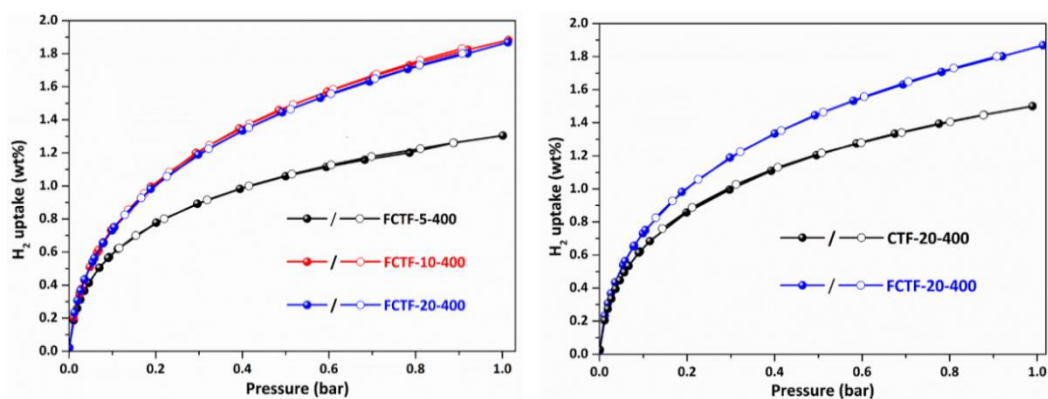
Figure 3.10. H_2 adsorption isotherms of all the studied FCTF materials and comparison of the H_2 adsorption isotherms of CTF-20-400 and FCTF-20-400.

3.3. Conclusion

In conclusion, we have succeeded in the preparation of a set of fluorinated CTF materials. The presence of fluorine groups in the materials was confirmed by TEM and EDX mapping measurements, while only 10% of theoretical fluorine groups was reserved in the frameworks due to the defluorination process determined by XPS measurements. Interestingly, compared with the non-functionalized CTFs, the fluorinated CTF materials exhibit much higher CO_2 adsorption capacities (4.54 mmol/g versus 3.48 mmol/g at 273 K and 1 bar) and exceptionally high H_2 adsorption uptakes (1.88 wt% versus 1.50 wt% at 77 K and 1 bar). This approach not only enables superior CO_2 adsorption and separation performance but also facilitates new possibilities for the rational design and synthesis of porous CTF materials.

3.4. Experimental Section

The ^1H and ^{19}F NMR spectra of the monomer were recorded on a Bruker Advance 300 MHz/500 MHz spectrometer using mesitylene or trifluorotoluene as the internal standard. Powder X-ray diffraction (PXRD) patterns were collected on a Thermo Scientific ARL X'Tra diffractometer, operated at 40 kV, 30 mA using Cu-K$_\alpha$ radiation (λ = 1.5406 Å). Fourier Transform Infrared Spectroscopy (FT-IR) in the region of 4000-800 cm^{-1} were performed with a

Thermo Nicolet 6700 FT-IR spectrometer equipped with a nitrogen-cooled MCT detector and a KBr beam splitter. Elemental analyses (C, H, N) were carried out on a Thermo Scientific Flash 2000 CHNS-O analyzer equipped with a TCD detector. Thermogravimetric analysis (TGA) were performed on a Netzsch STA-449 F3 Jupiter-simultaneous TG-DSC analyzer in a temperature range of 20 - 800 °C under air atmosphere and a heating rate of 5 °C/min. High angle annular dark field scanning-transmission electron microscopy (HAADF-STEM) and corresponding energy dispersive X-ray spectroscopy (EDX) mapping measurements was performed on a JEOL JEM-2200FS high resolution scanning transmission electron microscope equipped with an EDX spectrometer with a spatial resolution of 0.13 nm, image lens spherical aberration corrector, electron energy loss spectrometer (filter) and an emission field gun (FEG) operating at 200 KeV. X-ray photoelectron spectroscopy (XPS) measurements were performed using a Thermo Scientific K-Alpha+ X-ray Photoelectron Spectrometer. All samples were analyzed using a microfocused, monochromated Al K α X-ray source (1486.68 eV; 400 μm spot size). The K-Alpha+ charge compensation system was employed during analysis to prevent any localized charge buildup. The samples were mounted on conductive carbon tape and resulting spectra analyzed using the Avantage software from Thermo Scientific. N_2 adsorption isotherms were obtained using a Belsorp Mini apparatus measured at 77 K, whereas CO_2 CH_4 and H_2 adsorption measurements were carried out on a Quantachrome iSorb-HP gas sorption analyzer. Water adsorption isotherms were measured on a Quantachrome Autosorb-iQ-TPX machine at 298 K. Prior to all the gas sorption measurements, the materials were activated by slowly heating up the samples with a heating rate of 5 °C/min up to 150 °C under vacuum for 3 h.

Synthesis of the building block. Generally, a solution of p-cyanacetophenon (20mmol), 2,3,5,6-tetrafluoro-1,4-Benzenedicarboxaldehyde (5 mmol) and NaOH (20 mmol) in 60 mL ethanol was stirred for 16h at room temperature

after which aqueous ammonia (20 mL) was slowly added and stirred at room temperature for another 24 h. The obtained solid was filtered and thoroughly washed with ethanol. The targeted orange color product was obtained after drying under vacuum at 80 °C overnight. ^{1}H-NMR (DMSO-d_6, 300MHz):δ 8.07-8.09 (8H), δ 8.38-8.41(4H), δ 8.50-8.54 (8H) (Figure S3.6); ^{19}F NMR (DMSO-d_6, 500MHz), δ = -141.9 ppm (s,4F) (Figure S3.7); FT-IR spectrum: (KBr, cm^{-1}): 2240 (s), 1683 (s), 1595 (s), 1544 (s), 1480 (s), 1389 (s) (Figure S3.8).

Synthesis of CTFs. The CTF materials were synthesized according to previously reported procedure with slight modification.[13] Typically, the quartz ampoule was charged with the monomer (354 mg, 0.5 mmol) and different ratios of anhydrous $ZnCl_2$ (5-20 equiv.) in the glovebox under N_2 atmosphere. Afterwards, the ampoule was evacuated, flame-sealed and heated to 400 °C with a heating rate of 1 °C/min for 48 h. After cooling down to room temperature, the obtained crude product was grounded and washed thoroughly with water to remove the residual salt. Afterwards, the crude material was stirred in diluted HCl overnight and then stirred in THF for another 24 h at room temperature. The resulting black powder was successively washed with water and acetone and then dried under vacuum at 150 °C overnight.

3.5. Supplementary Information

The supplementary figures and tables appeared in this chapter are listed in this section.
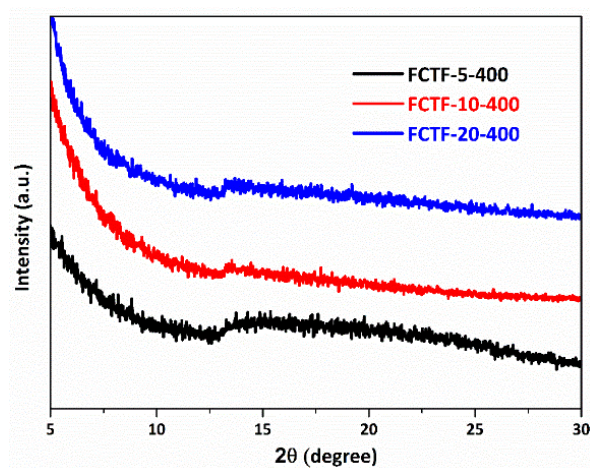
Figure S3.1. PXRD patterns of all the studied fluorinated CTF materials.
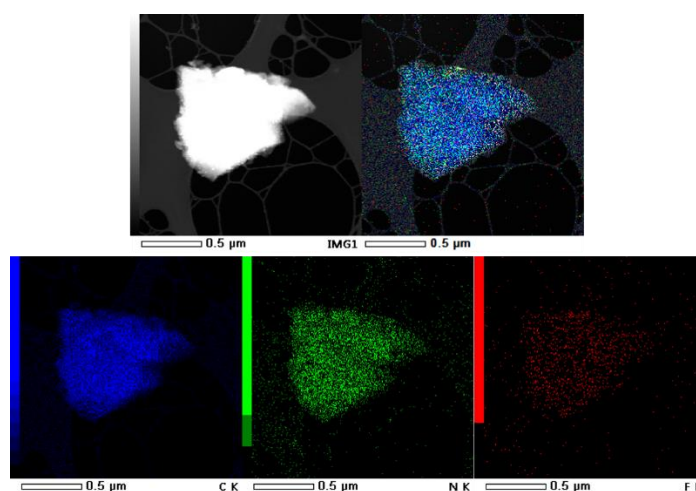
Figure S3.2. High angle annular dark field scanning-transmission electron microscopy (HAADF-STEM) and corresponding energy dispersive X-ray spectroscopy (EDX) mapping images of carbon (blue), nitrogen (green) and fluorine (red) for the sample of FCTF-10-400.
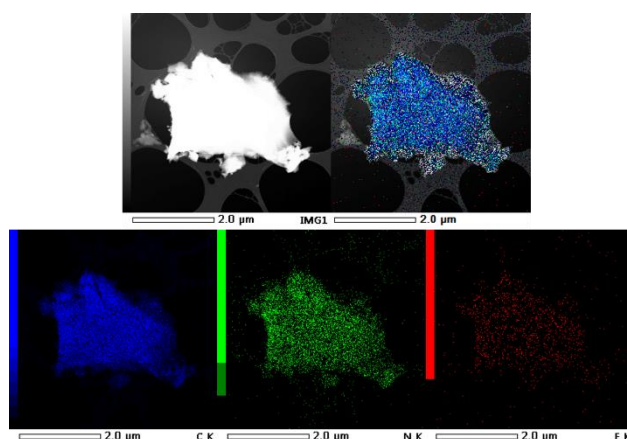
Figure S3.3. High angle annular dark field scanning-transmission electron microscopy (HAADF-STEM) and corresponding energy dispersive X-ray spectroscopy (EDX) mapping images of carbon (blue), nitrogen (green) and fluorine (red) for the sample of FCTF-20-400.

Table S3.1. Chemical composition obtained from XPS survey scans for the studied
FCTF materials.

Samples	C (at%)	O (at%)	N (at%)	F (at%)
FCTF-5-400	84.2	7.27	7.05	1.44
FCTF-10-400	87.3	4.14	7.69	0.87
FCTF-20-400	87.7	5.11	6.73	0.45
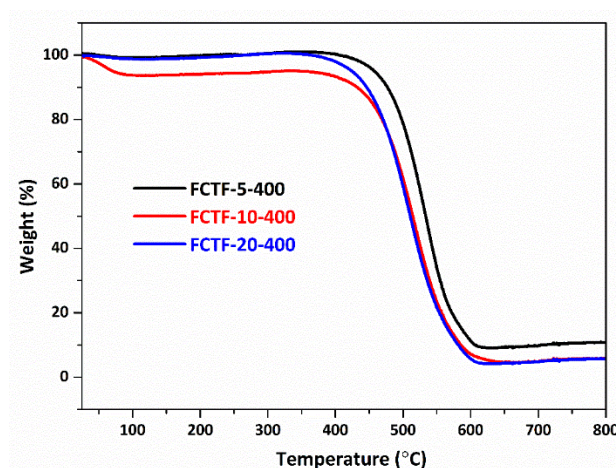
Figure S3.4. TGA curves of the studied CTF materials measured at a heating rate of 5
ºC/min under an air flow.
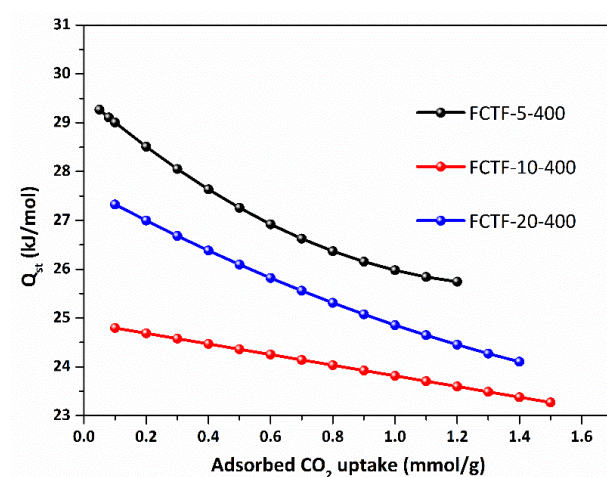
Figure S3.5. Isosteric heat of CO_2 adsorption (Q_{st}) for the studied FCTF materials.
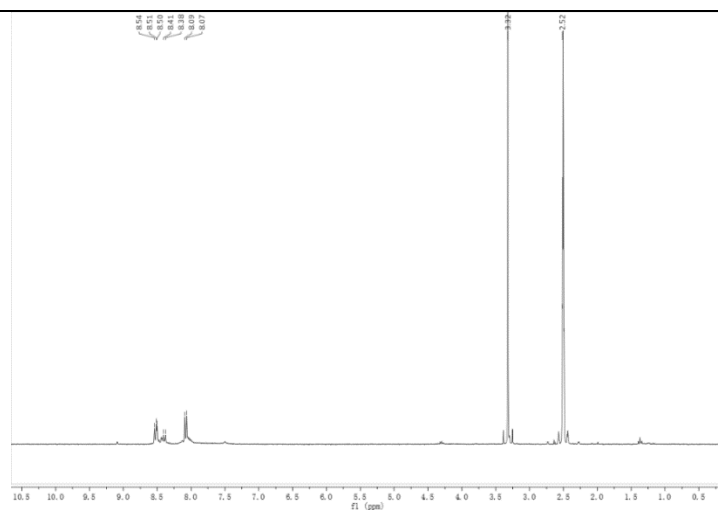
Figure S3.6. ^{1}H NMR spectrum of the building block.
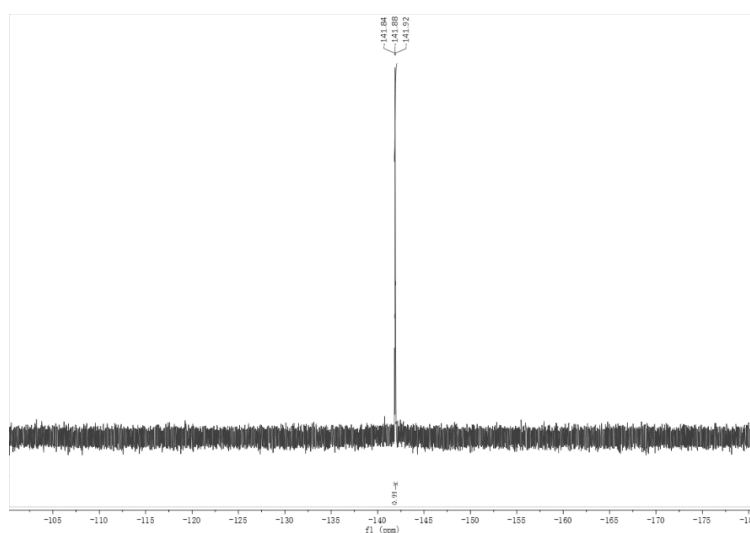
Figure S3.7. ^{19}F NMR spectrum of the building block.
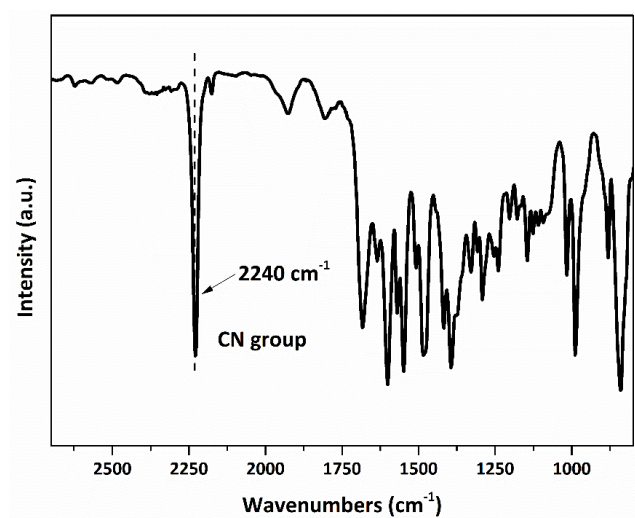
Figure S3.8. FT-IR spectrum of the monomer.

3.6. References

1.   Wang, G.; Leus, K.; Zhao, S.; Van Der Voort, P., Newly Designed Covalent Triazine Framework Based on Novel N-Heteroaromatic Building Blocks for Efficient CO_2 and H_2 Capture and Storage. *ACS Appl. Mater. Interfaces* **2018,** *10* (1), 1244-1249.

2.   Katekomol, P.; Roeser, J.; Bojdys, M.; Weber, J.; Thomas, A., Covalent Triazine Frameworks Prepared from 1,3,5-Tricyanobenzene. *Chem. Mater.* **2013,** *25* (9), 1542-1548.

3.   Wang, K.; Huang, H.; Liu, D.; Wang, C.; Li, J.; Zhong, C., Covalent Triazine-Based Frameworks with Ultramicropores and High Nitrogen Contents for Highly Selective CO_2 Capture. *Environ. Sci. Technol.* **2016,** *50* (9), 4869-4876.

4.   Dey, S.; Bhunia, A.; Boldog, I.; Janiak, C., A mixed-linker approach towards improving covalent triazine-based frameworks for CO_2 capture and separation. *Microporous Mesoporous Mater.* **2017,** *241*, 303-315.

5.   Zhu, X.; Tian, C.; Veith, G. M.; Abney, C. W.; Dehaudt, J.; Dai, S., In Situ Doping Strategy for the Preparation of Conjugated Triazine Frameworks Displaying Efficient CO_2 Capture Performance. *J. Am. Chem. Soc.* **2016,** *138* (36), 11497-11500.

6.   Tuci, G.; Pilaski, M.; Ba, H.; Rossin, A.; Luconi, L.; Caporali, S.; Pham-Huu, C.; Palkovits, R.; Giambastiani, G., Unraveling Surface Basicity and Bulk Morphology Relationship on Covalent Triazine Frameworks with Unique Catalytic and Gas Adsorption Properties. *Adv. Funct. Mater.* **2017,** *27* (7), 1605672-n/a.

7.   Dey, S.; Bhunia, A.; Breitzke, H.; Groszewicz, P. B.; Buntkowsky, G.; Janiak, C., Two linkers are better than one: enhancing CO_2 capture and separation with porous covalent triazine-based frameworks from mixed nitrile linkers. *J. Mater. Chem. A* **2017,** *5* (7), 3609-3620.

8.   Yu, H.-R.; Cho, S.; Bai, B. C.; Yi, K. B.; Lee, Y.-S., Effects of fluorination on carbon molecular sieves for CH_4/CO_2 gas separation behavior. *Int. J. Green h. Gas Control* **2012,** *10*, 278-284.

9.   Hu, X.-M.; Chen, Q.; Zhao, Y.-C.; Laursen, B. W.; Han, B.-H., Straightforward synthesis of a triazine-based porous carbon with high gas-uptake capacities. *J. Mater. Chem. A* **2014,** *2* (34), 14201-14208.

10.   Byun, J.; Patel, H. A.; Thirion, D.; Yavuz, C. T., Charge-specific size-dependent separation of water-soluble organic molecules by fluorinated nanoporous networks. *Nat. Commun.* **2016,** *7*, 13377.

11.   Zhao, Y.; Yao, K. X.; Teng, B.; Zhang, T.; Han, Y., A perfluorinated covalent triazine-based framework for highly selective and water-tolerant CO_2 capture. *Energy Environ. Sci.* **2013,** *6* (12), 3684-3692.

12.   Hug, S.; Stegbauer, L.; Oh, H.; Hirscher, M.; Lotsch, B. V., Nitrogen-Rich Covalent Triazine Frameworks as High-Performance Platforms for Selective Carbon Capture and Storage. *Chem. Mater.* **2015,** *27* (23), 8001-8010.

13. Kuhn, P.; Antonietti, M.; Thomas, A., Porous, Covalent Triazine-Based Frameworks Prepared by Ionothermal Synthesis. *Angew. Chem. Int. Ed.* **2008,** *47* (18), 3450-3453.

14. Nansé, G.; Papirer, E.; Fioux, P.; Moguet, F.; Tressaud, A., Fluorination of carbon blacks: An X-ray photoelectron spectroscopy study: I. A literature review of XPS studies of fluorinated carbons. XPS investigation of some reference compounds. *Carbon* **1997,** *35* (2), 175-194.

15. Bhunia, A.; Vasylyeva, V.; Janiak, C., From a supramolecular tetranitrile to a porous covalent triazine-based framework with high gas uptake capacities. *Chem. Commun.* **2013,** *49* (38), 3961-3963.

16. Hug, S.; Mesch, M. B.; Oh, H.; Popp, N.; Hirscher, M.; Senker, J.; Lotsch, B. V., A fluorene based covalent triazine framework with high CO_2 and H_2 capture and storage capacities. *J. Mater. Chem. A* **2014,** *2* (16), 5928-5936.

CHAPTER 4

Novel Hexaazatrinaphthalene-based Covalent Triazine Frameworks as High-Performance Platforms for Efficient Carbon Capture and Storage
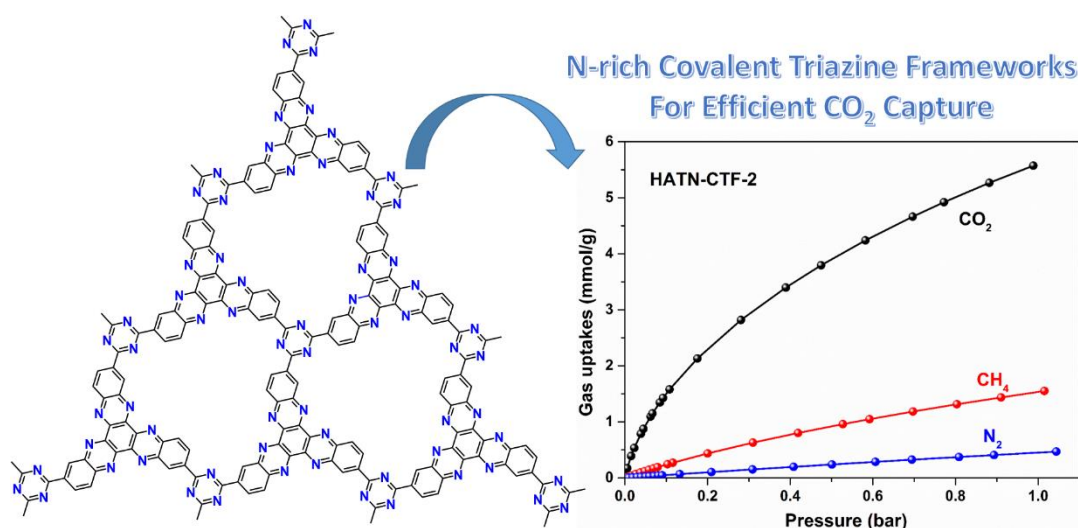
The results of this chapter were published in:

Abstract

In this chapter, we present for the first time the design and synthesis of a novel and nitrogen-rich hexaazatrinaphthalene-based CTF materials under typical ionothermal conditions. Notably, the synergistic effects of ultramicroporosity and rich CO_2-philic nitrogen sites empower the networks with superior CO_2 adsorption capacity (5.57 mmol/g at 273 K and 1 bar), outperforming most of the reported covalent triazine frameworks in literature and with significantly high CO_2/N_2 and CO_2/CH_4 selectivities at room temperature.

4.1. Introduction

In the field of carbon capture and separation, one of the most important criteria for adsorbents is the capacity and selectivity of CO_2 adsorption. To achieve higher CO_2 adsorption performance, the incorporation of CO_2-philic sites or functionalities into the skeleton of the adsorbents is considered as one of the most promising and efficient strategies. Along this line, the existence of nitrogen atoms in the porous skeleton or introduction of nitrogen functionalities into the networks have been proven to be beneficial to improving CO_2 adsorption capacities on the materials.[1-4] Recently, Dai et al. reported an in-situ doping strategy for the generation of a novel family of hexaazatriphenylene-based conjugated triazine frameworks. Interestingly, HAT-CTF-400 only exhibited the CO_2 uptake of 2.7 mmol/g at 273 K and 1 bar, while HAT-CTF-450/600 exhibited an exceptionally high CO_2 uptake of 6.3 mmol/g at the same conditions, which represents the highest value for all the reported CTF materials until now.[2] As a rigid and planar aza-based heteroaromatic scaffold, haxaazatrinaphthalene (HATN) derivatives exhibit excellent electron-deficient property and high π-π stacking tendency, which makes them ideal building blocks for the construction of supramolecular architectures and functional porous materials.[5] However, to the best of our knowledge, there are still no reports on this type of building blocks for the construction of porous materials.

In this chapter, we describe the rational design and synthesis of a novel covalent triazine framework with intrinsic ultramicropores and abundant surface CO_2-philic nitrogen sites for potential applications in gas adsorption and separation. More specifically, we for the first time prepared diquinoxalino[2,3-a:2',3'-c]phenazine-2,8,14-tricarbonitrile (HATN-3CN) as the building block for the construction of hexaazatrinaphthalene-based covalent triazine frameworks (HATN-CTFs) using the typical ionothermal synthesis

conditions (Figure 4.1). The resulting materials were characterized thoroughly and extensive gas adsorption studies were carried out and discussed on the obtained HATN-CTFs with the gases N_2, CO_2, CH_4 and H_2. Moreover, their CO_2/CH_4 and CO_2/N_2 selectivities were also assessed towards their potential use in gas adsorption and separation applications.
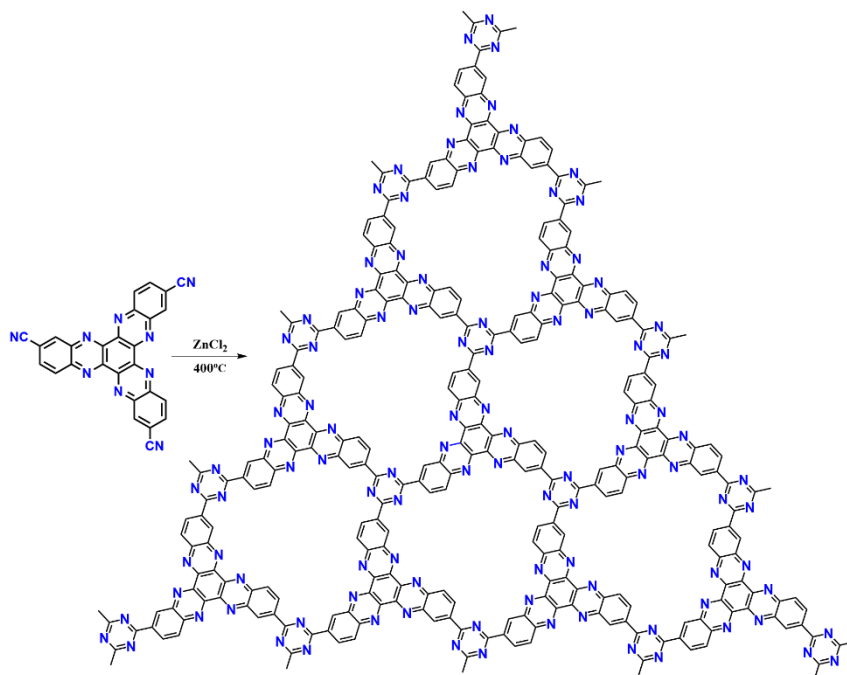
Figure 4.1. Schematic representation of the ideal structure of the HATN-CTF materials.

4.2. Results and Discussion

Trimerization of HATN-3CN under typical ionothermal conditions with $ZnCl_2$/monomer ratios of 5 and 10 at 400 °C yielded HATN-CTF-1 and HATN-CTF-2, respectively. The details of the synthesis are summarized in Table S4.1. The Fourier transform infrared spectroscopy (FT-IR) measurements were performed to evaluate the trimerization process (Figure S4.1). The weak band at 2240 cm^{-1} for HATN-CTF-1 revealed the incomplete trimerization of the nitrile groups due to the high mass of the monomer, while this characteristic band completely disappeared for HATN-CTF-2, indicating the completion of the trimerization reaction. It should be noted that the characteristic bands for

the triazine units are difficult to distinguish because of the partial carbonization of the CTFs, which is in accordance with previous reports.[6-7] As confirmed by the powder X-ray diffraction (PXRD) measurements, the studied HATN-CTFs were amorphous (Figure S4.2). Additionally, X-ray photoelectron spectroscopy (XPS) measurements were conducted to obtain more insights into the frameworks. XPS C1s spectra of HATN-CTF-1 and HATN-CTF-2 were fitted using four peaks (Figure 4.2) with the binding energies of 285.00 ± 0.05 eV (C-C), 286.40 ± 0.05 eV (C-O/C-N), 288.00 ± 0.05 eV (C≡N/C=O) and 289.20 ± 0.05 eV (O-C=O). The summary of the chemical states of C1s peak (Table S4.2) reveals two factors: (1) C-C bond is the main component of C1s peak (more than 80%) and (2) HATN-CTF-2 has less amount of ester and ether groups in comparison to HATN-CTF-1.
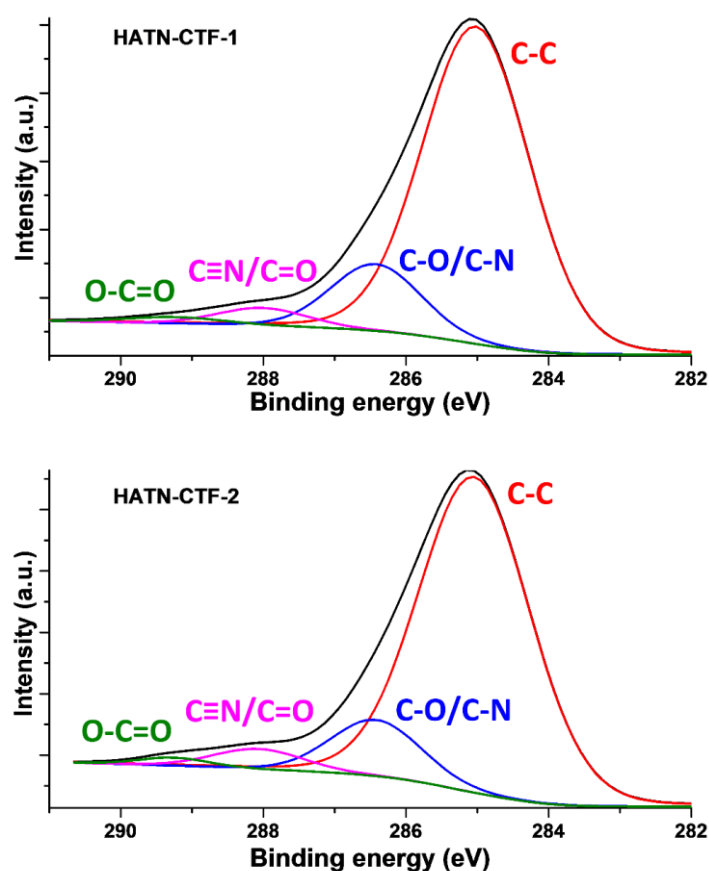
Figure 4.2. Deconvoluted C1s spectra of HATN-CTF-1 and HATN-CTF-2.

The results show that the deconvolution of the N1s peak can be done with the same set of four components: pyridinic (398.8 ± 0.1 eV), pyrrolic (400.2 ± 0.1 eV), quaternary (401.3 ± 0.1 eV) and oxidized N-O (403.70 ± 0.15 eV) (Figure 4.3).[2, 8] The pyridinic nitrogen species amount decreased by 3.5% (Table S4.3) for HATN-CTF-2 in comparison to HATN-CTF-1, while the pyrrolic compound demonstrated an opposite trend: as it increased by 3.2%. The quaternary and oxidized nitrogen also exhibit the same tendency that HATN-CTF-1 materials process more quaternary species and less oxidized nitrogen species with a difference of approximately 2%. The N-O chemical shift appears mainly due to the exposure of the samples to the open air and the possible existence of the trapped solvents in the newly synthesized building blocks. The detailed chemical composition obtained from XPS survey scans for both HATN-CTFs is summarized in Table S4.4.
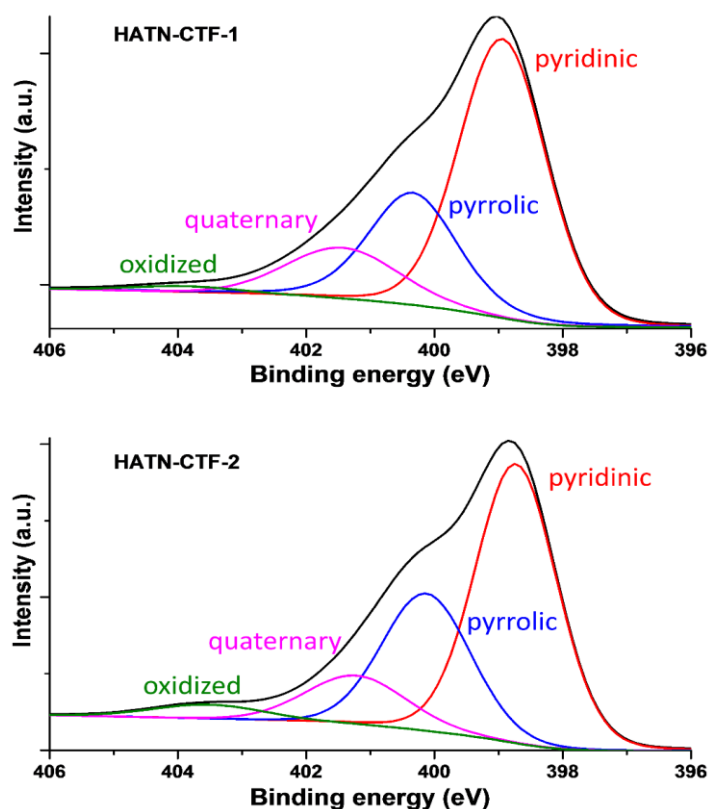
Figure 4.3. Deconvoluted N1s spectra of HATN-CTF-1 and HATN-CTF-2.

The elemental composition of the HATN-CTFs was also determined by means of Elemental Analysis (EA). As can be seen in Table 4.1, HATN-CTF-1 and HATN-CTF-2 have a nitrogen content up to 20.42% and 21.81 % respectively (out of theoretical value of 27.80 %), which is accordance with the XPS results that HATN-CTF-2 has slightly higher N content than HATN-CTF-1. The experimentally observed lower nitrogen content of the HATN-CTFs is mainly

Table 4.1. Elemental analysis and pore characteristics of the studied HATN-CTFs.

Sample	Elemental analysis (Experimental %)				$S_{BET}{}^{a}$ (m²/g)	$V_{micro.}{}^{b}$ (cm³/g)	$V_{tot.}{}^{c}$ (cm³/g)
	C	H	N	C/N			
HATN-CTF-1	58.91	2.44	20.42	2.88	575	0.24	0.25
HATN-CTF-2	63.45	2.70	21.81	2.91	1684	0.76	0.79
Calculated.	71.53	0.67	27.8	2.57	-	-	-

a). BET surface area calculated over the pressure range 0.01-0.05 P/P_0 at 77 K; b). V_{micro}, micropore volume was calculated by N_2 adsorption isotherms using the t-plot method; c). $V_{tot.}$, total pore volume calculated at P/P_0 = 0.98.

due to the elimination of the nitriles and the decomposition of the triazine units during the synthesis.[9] The high nitrogen content is supposed to be one of the preferential binding sites for the adsorption of more CO_2 molecules in the frameworks. It should be noted that the overall lower element contents compared to the theoretical values are likely because of the trapped metal salts and water molecules in the networks, which could not be completely removed.[1, 10] Thermogravimetric analysis (TGA) was performed to assess the thermal stability of the HATN-CTFs (Figure S4.3). As shown in Figure S4.3, the obtained HATN-CTFs exhibit remarkable thermal stability up to 400 °C, while the loss of the weight for HATN-CTF-1 below 200 °C is attributed to the loss of trapped water and solvents in the pores of the materials.
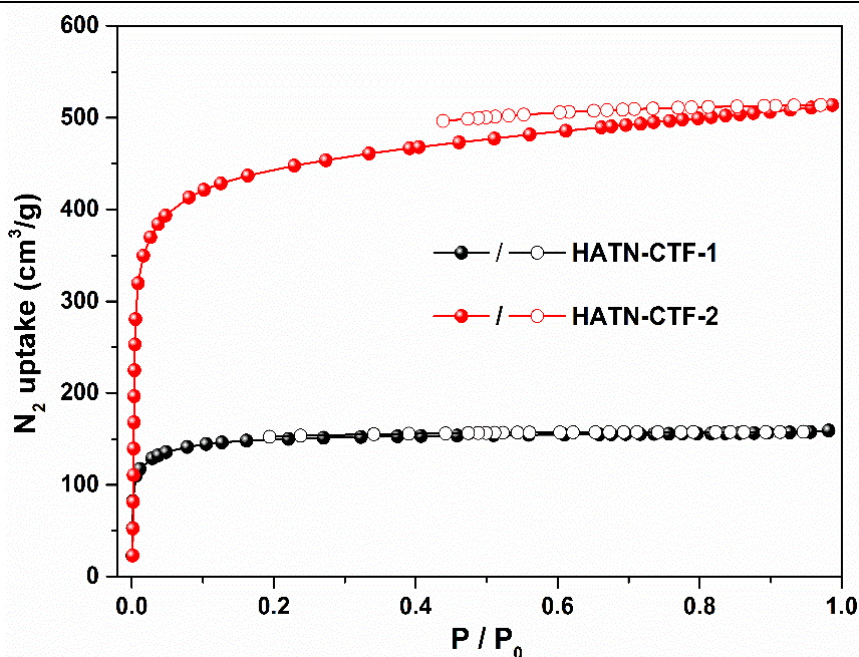
Figure 4.4. N_2 adsorption and desorption isotherms of HATN-CTF-1 (black) and HATN-CTF-2 (red) measured at 77K.

The N_2 adsorption isotherms of the synthesized HATN-CTF materials were subsequently recorded at 77 K to determine the permanent porosity of the networks. As shown in Figure 4.4, both HATN-CTF-1 and HATN-CTF-2 exhibit type I isotherms featuring sharp N_2 uptakes at low relative pressure, indicating the characteristic microporosity of the materials. The Brunauer-Emmett-Teller (BET) surface areas of HATN-CTF-1 and HATN-CTF-2 are calculated to be 575 m^2/g and 1684 m^2/g and their corresponding pore volumes are 0.25 cm^3/g and 0.79 cm^3/g, respectively (Table 4.1). Considering the high microporosity as well as the nitrogen-rich feature of the framework, they are expected to be promising candidates for selective carbon capture and separation. To verify this, single-component CO_2, N_2 and CH_4 adsorption isotherms were recorded at 273 K and 298 K up to 1 bar. (Figure 4.5a and Figure S4.4-S4.5).
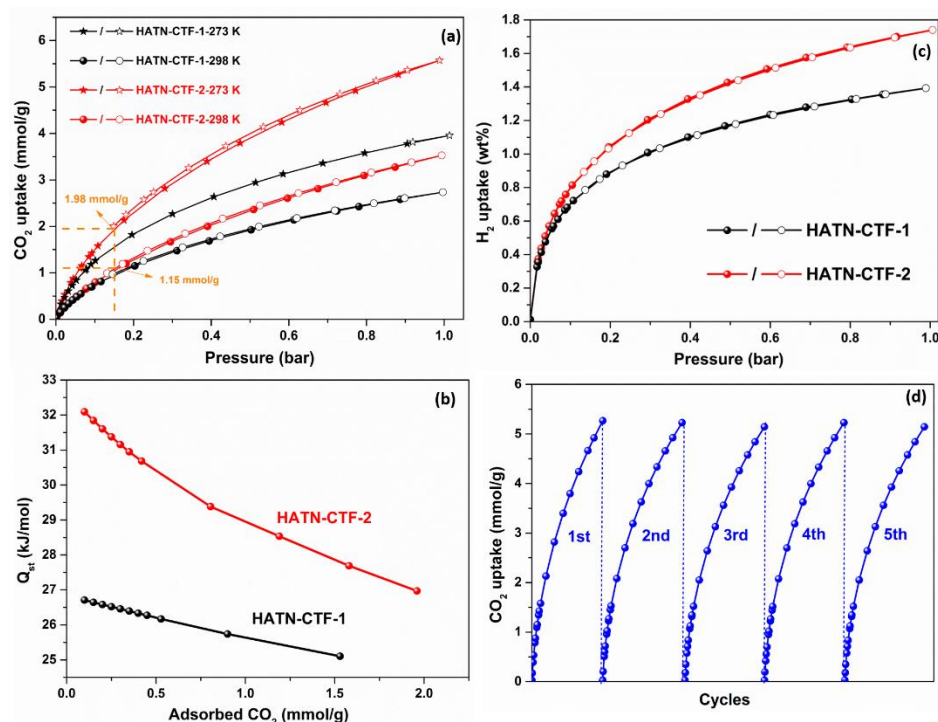
Figure 4.5. (a) CO_2 adsorption and desorption isotherms of HATN-CTF-1 and HATN-CTF-2 measured at 273 K and 298 K up to 1 bar; (b) The isosteric heat of CO_2 adsorption (Q_{st}) of HATN-CTF-1 and HATN-CTF-2; (c) H_2 adsorption isotherms of HATN-CTF-1 and HATN-CTF-2 measured at 77 K; (d) Five cycles of CO_2 adsorption measurements at 273 K on the HATN-CTF-2 sample.

As presented in Figure 4.5a, HATN-CTF-1 exhibits the CO_2 uptake of 3.95 and 2.73 mmol/g at 273 K and 298 K, respectively, while an impressively high CO_2 adsorption capacity is observed for HATN-CTF-2 reaching up to 5.57 mmol and 3.53 mmol/g under identical conditions. To the best of our knowledge, these values are amongst the highest ever reported in literature for the entire family of CTF materials, as summarized in Table 4.2. More importantly, the CO_2-philic N sites of the CTFs have much more significant effect on the CO_2 adsorption performance in the low-pressure region, where the adsorption process is more relevant to the practical CO_2 capture.[11] For example, HATN-CTF-2 exhibits remarkable CO_2 adsorption capacity of 1.98 mmol/g at 0.15 bar and 273 K. Moreover, the isosteric heats of CO_2 adsorption (Q_{st}) were calculated by fitting the CO_2 adsorption isotherms at 273 K and 298 K and applying the Clausius-Clapeyron equation to provide a better understanding

of the CO_2 adsorption performance (Figure 4b). The Q_{st} value at low coverage for HATN-CTF-1 (26.8 kJ/mol) is slightly lower than that of HATN-CTF-2 (32.6 kJ/mol), which is in accordance with the CO_2 adsorption results and also indicates the strong interactions between CO_2 molecules and the frameworks. Excellent reuse of the HATN-CTFs was demonstrated over five cycles of CO_2 adsorption and desorption measurements without significant changes in the CO_2 adsorption capacity for HATN-CTF-2, indicating complete desorption during each regeneration cycle and suggesting the high potential for its application in CO_2 capture (Figure 4d). By contrast, the CH_4 and N_2 uptakes of the HATN-CTFs are much lower (Figure S7-8), which encourages us to evaluate the potential of these materials for CO_2 separation over N_2 and CH_4. Accordingly, the CO_2/N_2 and CO_2/CH_4 selectivities of the studied HATN-CTFs were calculated by the ratio of the initial slopes of the respective CO_2, CH_4 and N_2 adsorption isotherms in the Henry region (Figure S4.6-4.9). The calculated CO_2/N_2 and CO_2/CH_4 selectivity of HATN-CTF-1 can reach up to 53 (39) and 9.8 (8) at 273 (298) K, respectively, while the corresponding CO_2/N_2 and CO_2/CH_4 selectivity of HATN-CTF-2 is calculated to be 46 (33) and 9.6 (7.8) at 273 (298) K. The high selectivity can be ascribed to the rich nitrogen sites in the framework, which may facilitate the interaction with the CO_2 molecules through dipole-quadrupole interactions.[12] As potential renewable and clean energy source, hydrogen storage remains challenging and solid adsorbents have been regarded as promising candidates. For this reason, the H_2 adsorption isotherms of the HATN-CTFs were recorded to explore their potential storage application. As shown in Figure 4c, the H_2 adsorption capacities of HATN-CTF-1 and HATN-CTF-2 can reach up to 1.38 and 1.74 wt% respectively at 77 K and 1 bar, which outperforms most of the reported CTFs and which are only slightly lower values than those of CTF-py[HT] (2.63 wt%)[13], Bipy-CTF-600 (2.1 wt%)[1], fl-CTF-400 (1.95 wt%)[14] and PCTF-1 (1.86 wt%)[15].

Table 4.2. Summary and comparison of the gas adsorption performance of the studied HATN-CTFs and some of the reported CTF materials.

Sample	CO_2 uptake (mmol/g)		H_2 uptake (wt%)	CH_4 uptake (mmol/g)		CO_2/N_2 Selectivity		CO_2/CH_4 Selectivity		Qst (kJ/mol)	Ref.
	273K	298K	77 K	273K	298K	273K	298K	273K	298K		
HATN-CTF-1	3.95	2.73	1.38	1.12	0.77	53	39	9.8	8	26.8	This work
HATN-CTF-2	5.57	3.53	1.74	1.55	0.96	46	33	9.6	7.8	32.6	This work
PCTF-1	3.21	1.84[a]	1.86	1.05	0.68[a]	13	-	5	3[a]	-	15
FCTF-1	4.67	3.21	-	-	-	-	31[b]	-	-	35.0	11
lut-CTF400	4.55	2.72	1.36	-	-	-	63	-	-	37.5	1
HAT-CTF-450/600	6.3	4.8	-	-	-	160	126	-	-	27.1	12

a. Gas uptake at 293K; b. CO_2/N_2 selectivity was calculated by Ideal Adsorption Solution Theory (IAST).

4.3. Conclusion

In summary, we have designed and synthesized a novel and nitrogen-rich hexaazatrinaphthalene-based covalent triazine framework for efficient CO_2 adsorption and separation. Remarkably, the CO_2 adsorption capacity of HATN-CTF-2 can reach up to 5.57 mmol/g at 273 K and 1 bar (1.98 mmol/g at 0.15 bar) due to the synergistic effects of ultramicroporosity and rich CO_2-philic N sites. Furthermore, HATN-CTF-2 also exhibits significantly high H_2 adsorption capacity of 1.74 wt% at 77 K and 1 bar. The CO_2/N_2 and CO_2/CH_4 selectivities of the studied HATN-CTFs were calculated by the Henry model and the CO_2/N_2 selectivity of HATN-CTF-1 can reach up to 39 at 298 K. These impressive results render the studied HATN-CTFs as promising candidates for efficient carbon capture and storage.

4.4. Experimental Section

Materials and methods. All the chemicals were obtained from commercial suppliers and used as received without further purification. The ^{1}H NMR analysis of the nitrile linker was performed on a Bruker Advance 300 MHz spectrometer using mesitylene as internal standard. Powder X-ray diffraction (PXRD) patterns were collected on a Thermo Scientific ARL X'Tra diffractometer, operated at 40 kV, 30 mA using Cu-K_α radiation (λ = 1.5406 Å). Fourier Transform Infrared Spectroscopy (FT-IR) in the region of 4000-800 cm^{-1} was performed with a Thermo Nicolet 6700 FT-IR spectrometer equipped with a nitrogen-cooled MCT detector and a KBr beam splitter. Elemental analyses (C, H, N) were carried out on a Thermo Scientific Flash 2000 CHNS-O analyzer equipped with a TCD detector. XPS measurements were performed on a PHI Versaprobe II spectrometer equipped with a monochromatic Al Kα X-ray source (hv = 1486.6 eV) with a beam size of 100 μm and operating at 25.8 W. Survey scans and detailed C1s and N1s spectra were recorded with a pass

energy of 187.85 eV and 23.5 eV respectively at a take-off angle of 45° relative to the sample surface in a vacuum of at least 10^{-6} Pa to identify and quantify the chemical composition and the different carbon/nitrogen groups respectively. The atomic elemental composition was calculated from XPS survey spectra using Multipak (v 9.6.1) software. A spectrum calibration (C-C: 285.0 eV) was done prior to analysis and an iterated Shirley background was applied to determine the elemental composition using the relative sensitivity factors supplied by the manufacturer. Curve peak fitting of the individual high-resolution peaks was also performed making use of Multipak software after applying a Savitzky-Golay smoothening procedure. Peaks were deconvoluted using Gaussian–Lorentzian peak shapes, keeping the FWHM below 1.8 and 2.0 eV and the χ^2 below 7 and 0.2 for C1s and N1s peaks respectively. Thermogravimetric analysis (TGA) was performed on a Netzsch STA-449 F3 Jupiter-simultaneous TG-DSC analyzer in a temperature range of 25 - 800 °C under air atmosphere and a heating rate of 5 °C/min. N_2 adsorption isotherms were obtained using a Belsorp Mini apparatus measured at 77 K, whereas all the other gas (CO_2, CH_4, N_2 and H_2) adsorption measurements at 273 K and 298 K were carried out on a Quantachrome iSorb-HP gas sorption analyzer. Prior to all the gas sorption measurements, the materials were activated by slowly heating up the samples under vacuum with a heating rate of 5 °C/min up to 150 °C for 3 h.

Diquinoxalino[2,3-a:2',3'-c]phenazine-2,8,14-tricarbonitrile (HATN-3CN) synthesis.

Typically, a mixture of hexaketocyclohexane octahydrate (312 mg, 1 mmol) and 3, 4-diaminobenzonitrile (532.6 mg, 4 mmol) in deoxygenated acetic acid (60 mL) was added into a Schlenk flask, which was purged by argon and equipped with a magnetic stir bar. The mixture was refluxed under argon for 40 h. After cooling down to room temperature, the mixture was poured into

water and the greenish yellow suspension was filtered and thoroughly washed with water to give the greenish yellow solid of HATN-3CN, which was dried under vacuum before further synthesis. ^{1}H NMR (300 MHz, DMSO d$_6$): δ = 8.48-8.52 (3H, Ar–H), 8.78-8.82 (3H, Ar–H), 9.28-9.30 (3H, Ar-H) (Figure S 4.10).

Synthesis of HATN-CTFs. In a typical CTF synthesis, the ampoule was charged with HATN-3CN (275.4 mg, 0.3 mmol) and different molar ratios of anhydrous ZnCl$_2$ (5 and10 equiv.) in a glovebox, then the ampoule was taken out and evacuated, flame-sealed and heated at 400 °C for 48 h. After cooling down to room temperature, the ampoule was opened and the crude material was grounded and thoroughly washed by water. Afterwards, the black material was subsequently stirred in 1M HCl and THF for 24 h, filtered and washed with water and acetone. Finally, the black powder was dried at 150 °C under vacuum overnight.

4.5. Supplementary Information

The supplementary figures and tables appeared in this chapter will be listed in this section.

Table S4.1. Overview of the detailed synthesis parameters used for the studied HATN-CTFs.

Samples	Monomer (mg)	ZnCl$_2$ (mg)	ZnCl$_2$/monomer molar ratio	Temperature (°C)	Time (h)
HATN-CTF-1	275.4	408	5	400	48
HATN-CTF-2	275.4	816	10	400	48
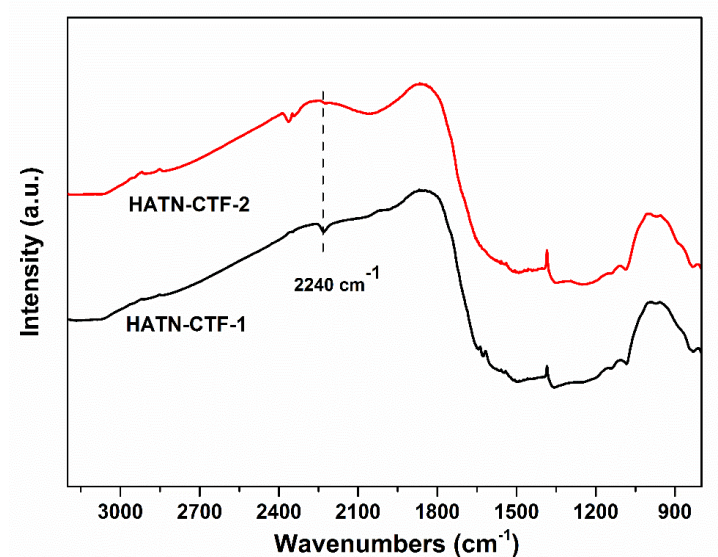
Figure S4.1. FT-IR spectra of HATN-CTF-1 and HATN-CTF-2
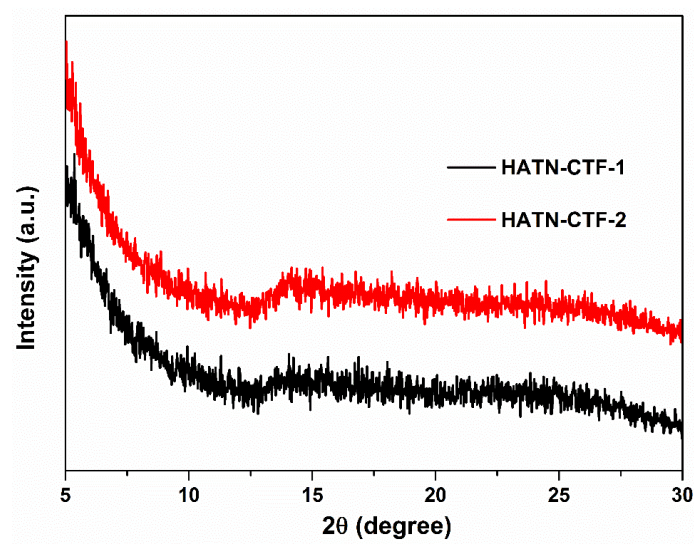
Figure S4.2. Powder X-ray diffraction patterns of the obtained HATN-CTFs, indicating the amorphous feature of the materials.

Table S4.2. Relative concentrations of the different carbon groups present on HATN-CTF-1 and HATN-CTF-2 as obtained from C1s curve fitting.

Samples	C-C (%)	C-O/C-N (%)	C≡N/C=O (%)	O-C=O (%)
HATN-CTF-1	80.3	14.3	3.8	1.5
HATN-CTF-2	82.4	11.9	4.3	1.4

Table S4.3. Relative concentrations of the different nitrogen groups present on HATN-CTF-1 and HATN-CTF-2 as obtained from N1s curve fitting.

Samples	Pyridinic (%)	Pyrrolic (%)	Quaternary (%)	N-O (%)
HATN-CTF-1	58.4	26.0	13.9	1.7
HATN-CTF-2	54.9	29.2	11.9	4.0

Table S4.4. Chemical composition obtained from XPS survey scans for the studied HATN-CTFs.

Samples	C (at%)	O (at%)	N (at%)
HATN-CTF-1	74.9	11.3	13.9
HATN-CTF-2	75.1	7.0	17.9
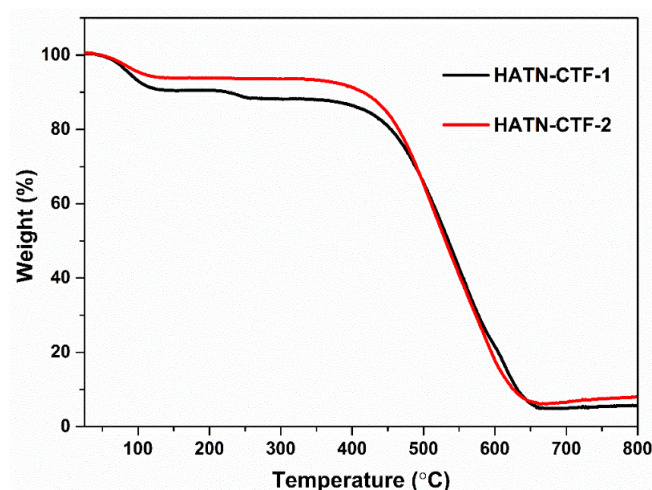
Figure S4.3. TGA curves of the studied HATN-CTFs measured at a heating rate of 5 K/min under an air flow.
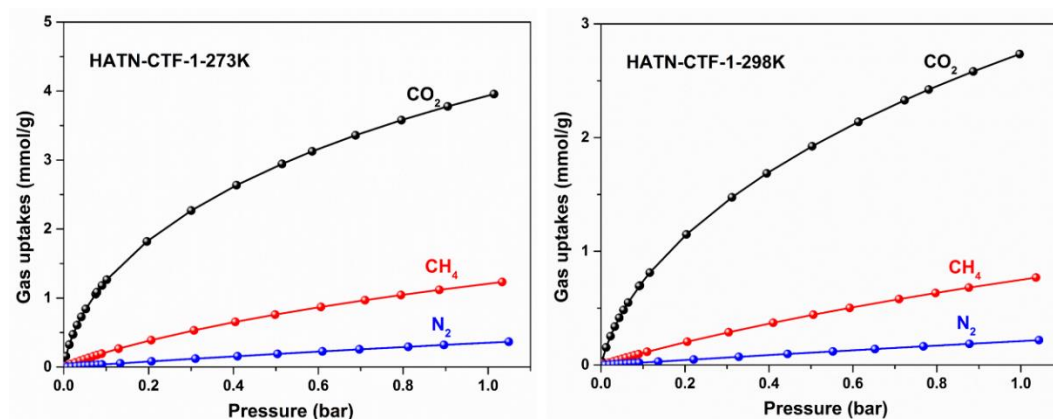
Figure S4.4. CO_2, CH_4 and N_2 adsorption isotherms of HATN-CTF-1 measured at 273 K and 298 K up to 1 bar.
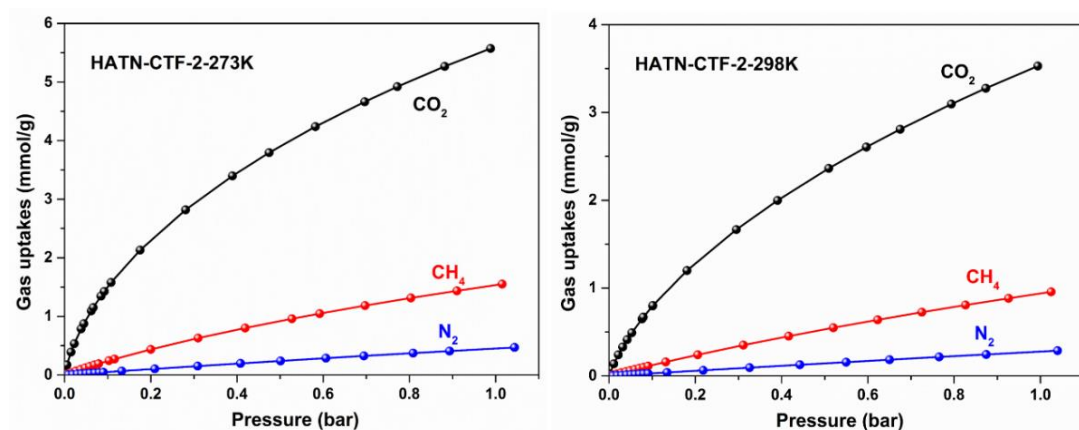
Figure S4.5. CO_2, CH_4 and N_2 adsorption isotherms of HATN-CTF-2 measured at 273 K and 298 K up to 1 bar.
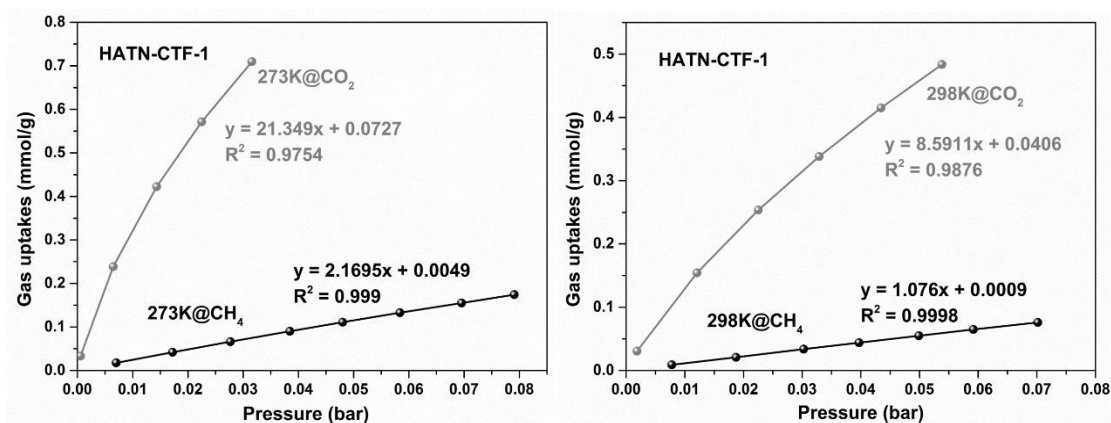
Figure S4.6. Henry plots of HATN-CTF-1 as obtained from CO_2 and CH_4 isotherms at 273 K and 298 K, respectively.
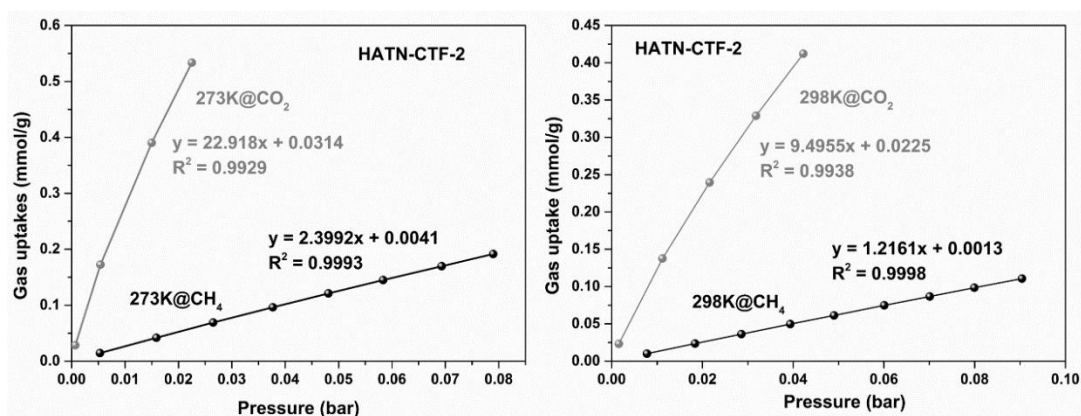
Figure S4.7. Henry plots of HATN-CTF-2 as obtained from CO_2 and CH_4 isotherms at 273 K and 298 K, respectively.
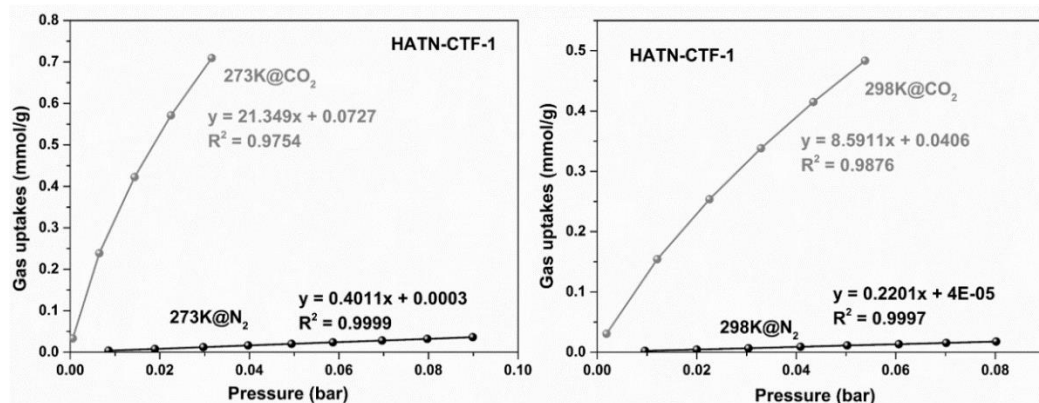
Figure S4.8. Henry plots of HATN-CTF-1 as obtained from CO_2 and N_2 isotherms at 273 K and 298 K, respectively.
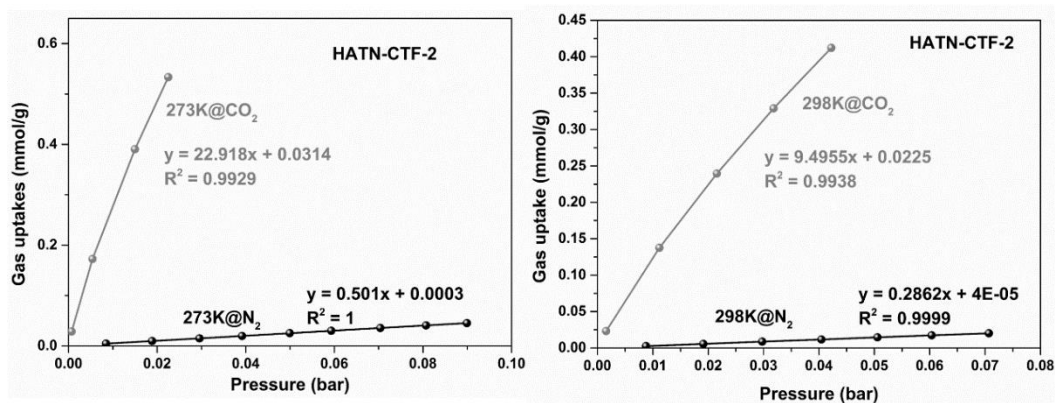
Figure S4.9. Henry plots of HATN-CTF-2 as obtained from CO_2 and N_2 isotherms at 273 K and 298 K, respectively.
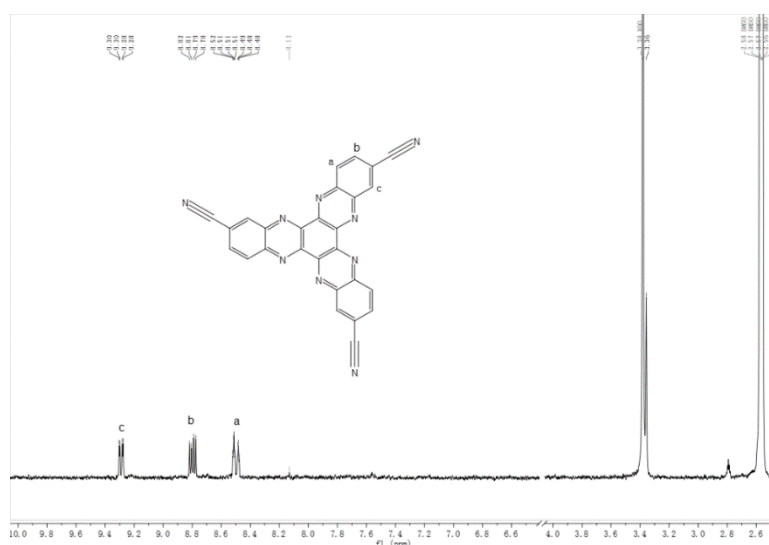
Figure S4.10. ^{1}H NMR spectrum of HATN-3CN.

4.6. References

1.   Hug, S.; Stegbauer, L.; Oh, H.; Hirscher, M.; Lotsch, B. V., Nitrogen-Rich Covalent Triazine Frameworks as High-Performance Platforms for Selective Carbon Capture and Storage. *Chem. Mater.* 2015, *27* (23), 8001-8010.

2.   Zhu, X.; Tian, C.; Veith, G. M.; Abney, C. W.; Dehaudt, J.; Dai, S., In Situ Doping Strategy for the Preparation of Conjugated Triazine Frameworks Displaying Efficient CO_2 Capture Performance. *J. Am. Chem. Soc.* 2016, *138* (36), 11497-11500.

3.   Xu, S.; He, J.; Jin, S.; Tan, B., Heteroatom-rich porous organic polymers constructed by benzoxazine linkage with high carbon dioxide adsorption affinity. *J. Colloid Interface Sci.* 2018, *509*, 457-462.

4.   Tao, L.; Niu, F.; Wang, C.; Liu, J.; Wang, T.; Wang, Q., Benzimidazole functionalized covalent triazine frameworks for CO_2 capture. *J. Mater. Chem. A* 2016, *4* (30), 11812-11820.

5.   Yan, X.-Y.; Lin, M.-D.; Zheng, S.-T.; Zhan, T.-G.; Zhang, X.; Zhang, K.-D.; Zhao, X., Recent advances of hexaazatriphenylene (HAT) derivatives: Their applications in self-assembly and porous organic materials. *Tetrahedron Letters* 2018, *59* (7), 592-604.

6.   Wang, K.; Huang, H.; Liu, D.; Wang, C.; Li, J.; Zhong, C., Covalent Triazine-Based Frameworks with Ultramicropores and High Nitrogen Contents for Highly Selective CO_2 Capture. *Environ. Sci. Technol.* 2016, *50* (9), 4869-4876.

7.   Wang, G.; Leus, K.; Zhao, S.; Van Der Voort, P., Newly Designed Covalent Triazine Framework Based on Novel N-Heteroaromatic Building Blocks for Efficient CO_2 and H_2 Capture and Storage. *ACS Appl. Mater. Interfaces* 2018, *10* (1), 1244-1249.

8.   Osadchii, D. Y.; Olivos-Suarez, A. I.; Bavykina, A. V.; Gascon, J., Revisiting Nitrogen Species in Covalent Triazine Frameworks. *Langmuir* 2017, *33* (50), 14278-14285.

9.   Kuhn, P.; Thomas, A.; Antonietti, M., Toward Tailorable Porous Organic Polymer Networks: A High-Temperature Dynamic Polymerization Scheme Based on Aromatic Nitriles. *Macromolecules* 2009, *42* (1), 319-326.

10. Kuhn, P.; Antonietti, M.; Thomas, A., Porous, Covalent Triazine-Based Frameworks Prepared by Ionothermal Synthesis. *Angew. Chem. Int. Ed.* 2008, *47* (18), 3450-3453.

11. Zhao, Y.; Yao, K. X.; Teng, B.; Zhang, T.; Han, Y., A perfluorinated covalent triazine-based framework for highly selective and water-tolerant CO_2 capture. *Energy Environ. Sci.* 2013, *6* (12), 3684-3692.

12. Zhu, X.; Tian, C. C.; Mahurin, S. M.; Chai, S. H.; Wang, C. M.; Brown, S.; Veith, G. M.; Luo, H. M.; Liu, H. L.; Dai, S., A Superacid-Catalyzed Synthesis of Porous Membranes Based on Triazine Frameworks for CO_2 Separation. *J. Am. Chem. Soc.* 2012, *134* (25), 10478-10484.

13. Tuci, G.; Pilaski, M.; Ba, H.; Rossin, A.; Luconi, L.; Caporali, S.; Pham-Huu, C.; Palkovits, R.; Giambastiani, G., Unraveling Surface Basicity and Bulk Morphology Relationship on

Covalent Triazine Frameworks with Unique Catalytic and Gas Adsorption Properties. *Adv. Funct. Mater.* **2017,** *27* (7), 1605672-n/a.

14. Hug, S.; Mesch, M. B.; Oh, H.; Popp, N.; Hirscher, M.; Senker, J.; Lotsch, B. V., A fluorene based covalent triazine framework with high CO_2 and H_2 capture and storage capacities. *J. Mater. Chem. A* **2014,** *2* (16), 5928-5936.

15. Bhunia, A.; Vasylyeva, V.; Janiak, C., From a supramolecular tetranitrile to a porous covalent triazine-based framework with high gas uptake capacities. *Chem. Commun.* **2013,** *49* (38), 3961-3963.

CHAPTER 5

A Fluorine-Containing Hydrophobic Covalent Triazine Framework with Excellent Selective CO$_2$ Capture Performance

The results of this chapter were published in:

Abstract
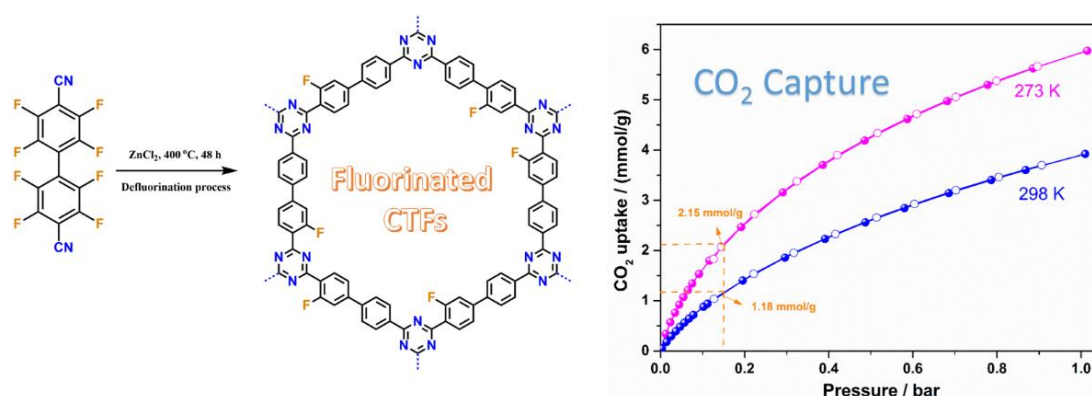
In this chapter, a set of fluorine functionalized covalent triazine frameworks have been designed and synthesized with 2,2',3,3',5,5',6,6'-octafluoro-4,4'-biphenyldicarbonitrile (F-DCBP) as the monomer under typical ionothermal conditions. Notably, the synergistic effects of polar C-F bonds and rich CO_2-philic N sites bestow upon the framework an excellent H_2 uptake (1.77 wt%, 77 K and 1 bar) as well as a significantly high CO_2 adsorption capacity (5.98 mmol/g, at 273 K and 1 bar), surpassing all related CTF materials measured under identical conditions that have been reported in literature to date and the material also exhibits a high CO_2/N_2 selectivity of 31. Additionally, the hydrophobicity of the CTF materials has been significantly enhanced owing to the incorporation of the hydrophobic fluorine groups, which was further confirmed by ambient water vapor sorption.

5.1. Introduction

In chapter 3, we have shown that the incorporation of CO_2-philic fluorine groups into the structure of CTFs can significantly improve their corresponding gas adsorption and separation performances. However, both the theoretical and experimental fluorine content in the studied structures was relatively low and compared with the benchmark CTF materials,[1-2] the gas adsorption (CO_2, H_2) uptakes of these materials were not that remarkable, and we believe that increasing the fluorine contents in the structure should be possible to achieve the improvement of the materials' gas adsorption and separation performance.

Thus, in this chapter, we prepared a perfluorinated building block, namely, 2,2',3,3',5,5',6,6'-octafluoro-4,4'-biphenyldicarbonitrile (F-DCBP), in which every hydrogen of 4,4'-biphenyldicarbonitrile (DCBP) was replaced by fluorine and the theoretical fluorine content (43 %) is much higher and we expect that the obtained CTFs can exhibit much higher CO_2 adsorption performance. As a proof of concept, we prepared a set of fluorine-containing covalent triazine frameworks, identified as F-DCBP-CTFs, by trimerization of F-DCBP via typical ionothermal synthesis conditions at 400 °C using different $ZnCl_2$/monomer ratios (Figure 5.1). The obtained F-DCBP-CTF materials were comprehensively characterized by solid state NMR, XPS, TEM and EDS mapping, SEM, PXRD, FT-IR, TGA, EA, gas adsorption and H_2O vapor adsorption measurements. Remarkably, the resulting fluorinated CTF materials exhibit relatively large surface areas and pore volumes, exceptionally high CO_2 and H_2 adsorption capacities as well as high CO_2/N_2 selectivity, outperforming most of the reported POPs to date. Furthermore, water vapor adsorption measurements confirmed significant enhancement of the hydrophobicity of the materials in comparison to the non-functionalized analogues.
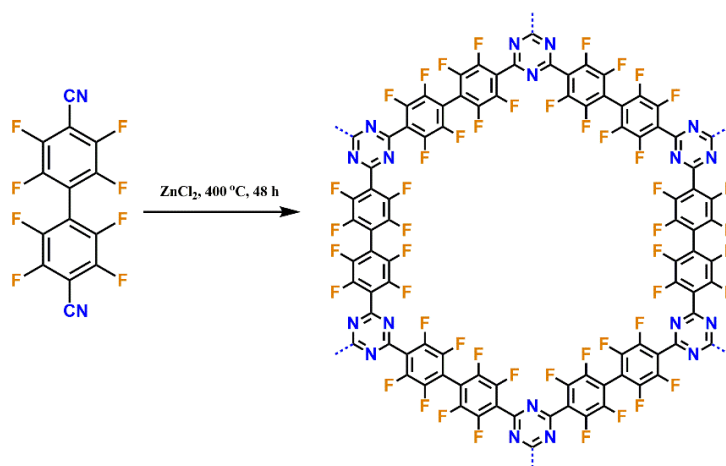
Figure 5.1. Reaction scheme and schematic ideal structure of F-DCBP-CTFs.

5.2. Results and Discussion

Synthesis and characterization of the CTF materials

The porous materials were prepared at 400 °C under typical ionothermal conditions using molten $ZnCl_2$ as Lewis acid catalyst.[3] The obtained F-DCBP-CTFs were identified as F-DCBP-CTF-1 and F-DCBP-CTF-2 when a $ZnCl_2$/monomer ratio of 5 and 10 was applied, respectively. For comparison, non-functionalized CTFs based on 4,4'-biphenyldicarbonitrile (DCBP) as the monomer were also prepared and will be referred to as DCBP-CTF-1 and DCBP-CTF-2 in the following. It should be noted that at a high temperature, the fluorine groups will be partially decomposed, confirmed by the gas release while opening the glass ampoules. Such gas release was also observed in the earlier reported FCTF-1 and the as-formed gases were identified as CF_4, C_2F_4 and F_2.[4] The crystallinity of the synthesized materials was examined by powder X-ray diffraction (Figure S5.1). As expected, all the CTFs are amorphous. The successful trimerization reaction was indicated by FT-IR measurements (Figure S5.2). The weak band at 2230 cm^{-1} for F-DCBP-CTFs points to the incomplete polymerization of the nitrile groups, while the characteristic weak bands at 1560 and 1380 cm^{-1} can be assigned to the triazine rings.[5-6] Elemental Analysis (EA) revealed that the nitrogen and carbon contents for the

synthesized DCBP-CTF materials are in accordance with the literature.[3] As outlined in Table 5.1, a $ZnCl_2$/monomer ratio of 5 resulted in the CTF materials with higher nitrogen content, surface area and porosity in comparison to the materials obtained using a $ZnCl_2$/monomer ratio of 10. More interestingly, the obtained F-DCBP-CTF materials have a much higher nitrogen content in comparison to the non-functionalized DCBP-CTF compounds, which are supposed to be one of the beneficial binding sites for enhanced CO_2 adsorption uptake in this framework. In all cases, the total amount of elements determined by EA is always lower than 100%, the residue mass can be assigned to trapped metal salts and water in the pores, which could not be removed completely.[3, 5]

Table 5.1. Elemental analysis and pore characteristics of all the synthesized CTF materials.

Sample	Elemental analysis (Calculated/Experimental)				$S_{BET}{}^a$ m²/g	$V_{0.1}{}^b$ cm³/g	$V_{tot.}{}^c$ cm³/g
	C	H	N	F			
DCBP-CTF-1	82.3/84.4	3.92/2.75	13.7/6.55	-	2437	1.41	1.48
DCBP-CTF-2	82.3/79.4	3.92/2.83	13.7/4.96	-	2036	1.51	2.26
F-DCBP-CTF-1	48.3/59.7	-/1.24	8.05/11.3	43/4.20^d	1574	0.51	1.50
F-DCBP-CTF-2	48.3/59.4	-/1.97	8.05/10.2	43/3.13^d	1126	0.34	1.56

a). BET surface area calculated over the pressure range 0.01-0.05 P/P_0 at 77 K; b). $V_{0.1}$, pore volume at $P/P_0 = 0.1$ at 77 K; c). V_{tot}, total pore volume calculated at $P/P_0 = 0.98$; d) determined by XPS.
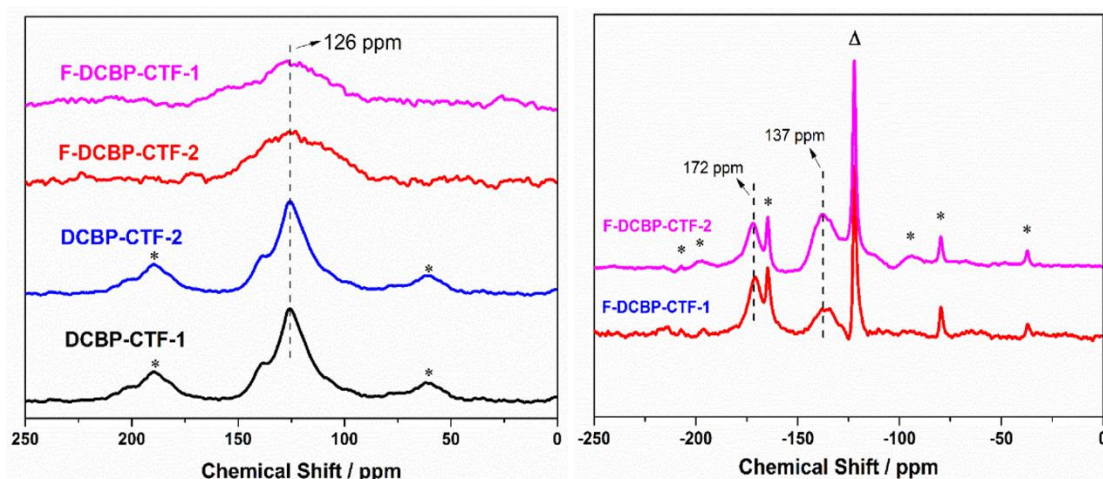

Figure 5.2. Solid state magic angle spinning ¹³C NMR and ¹⁹F NMR spectra of DCBP-CTFs and F-DCBP-CTFs. (Asterisks denote spinning sidebands and triangle symbol represents the background).

To obtain more detailed information about the structure of the materials, solid state cross-polarization magic angle spinning (CP/MAS) ^{13}C and ^{19}F NMR experiments were performed on all the CTF materials (Figure 5.2). As shown in Figure 5.2, the broad peak at 126 ppm corresponds to the aromatic carbons. It is however difficult to distinguish the positions of the various aromatic carbons owing to the partial graphitization, previously reported.[6-7] The presence of fluorine groups in the structure was confirmed by ^{19}F NMR measurements, since the signal for carbon-fluorine at approximately 137 ppm was clearly detected.[8-9] Additionally, X-ray photoelectron spectroscopy (XPS) measurements were also carried out to get more insights into the chemical states of the elements in the CTFs materials (Figure 5.3 and Figure S5.3-S5.5).
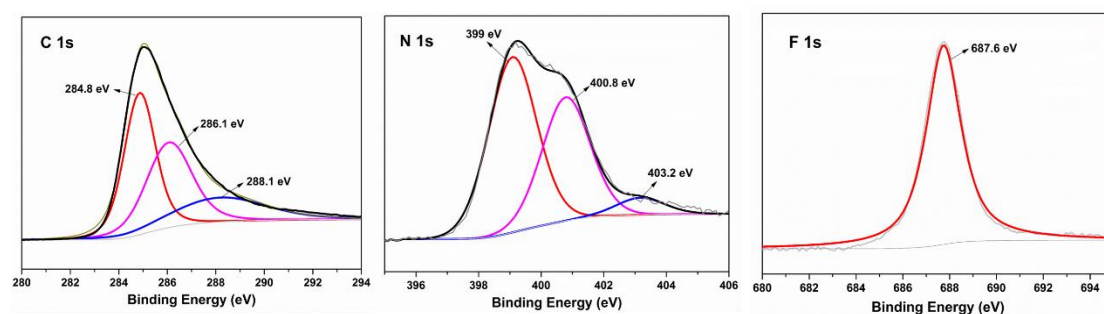
Figure 5.3. C1s, N1s and F 1s XPS spectra of F-DCBP-CTF-1.

For F-DCBP-CTF-1, the C 1s spectrum can be deconvoluted into three peaks. The dominant peak at 284.8 eV is related to the aromatic sp^2 carbon and the peak at 286.1 eV can be assigned to the triazine or nitrile carbon. The less pronounced peak at 288.1 eV is associated with carboxyl groups.[4, 10] The N1s spectrum is divided into three peaks as well. The first peak at 399 eV is related to the nitrile species, the peak at 400.5 eV is attributed to pyrrolic/pyridonic-N species and the peak at 403.2 eV is assigned to the oxidized N-O species.[4, 10-11] The single peak at 687.6 eV in the F 1s spectra of the F-DCBP CTFs corresponds to the aromatic C-F bond.[12] The fluorine content was also determined by XPS measurements. We note that the synthesized F-DCBP-CTFs only contain about 10 percentage of the theoretical fluorine atoms. Specifically, the fluorine content amounts 4.20 % for F-DCBP-CTF-1 and 3.13 %

for F-DCBP-CTF-2, which is much lower than the theoretical value (43%). The much lower F content is mainly because of the elimination of fluorine and the slight difference between F-DCBP-CTF-1 and F-DCBP-CTF-2 is due to the fact that $ZnCl_2$ is able to induce and accelerate the defluorination process, thereby generating different materials under different $ZnCl_2$ concentrations.[10, 13]

High angle annular dark field scanning-transmission electron microscopy (HAADF-STEM) and corresponding energy dispersive X-ray spectroscopy (EDX) mapping images of F-DCBP-CTF-1 (Figure 5.4) and F-DCBP-CTF-2 (Figure S5.6) show that C, N and F elements are well dispersed and homogeneously distributed throughout the materials.
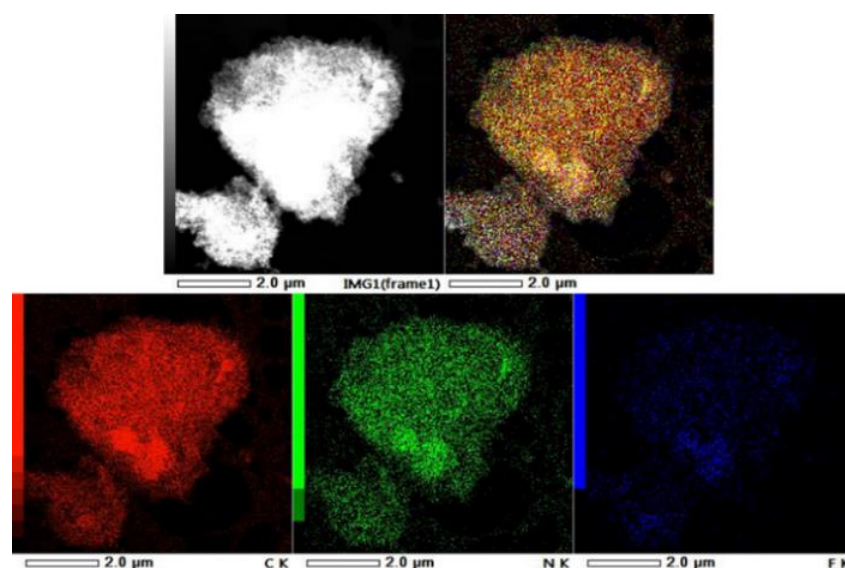
Figure 5.4. High angle annular dark field scanning-transmission electron microscopy (HAADF-STEM) and corresponding energy dispersive X-ray spectroscopy (EDX) mapping images of carbon (red), nitrogen (green) and fluorine (blue) on the sample of F-DCBP-CTF-1.

Scanning electron microscopy (SEM) images show that all the CTF materials are composed of tiny particles with irregular shapes and sizes (Figure S5.7 and Figure S5.8). The thermal stability of all the studied CTF materials was determined by thermogravimetric analysis (TGA) of which results indicate that the F-DCBP-CTF materials are stable up to 400 °C, thus slightly lower than the

DCBP-CTF materials (Figure S5.9). This can be attributed to the strong electron withdrawing effect of the fluorine atoms in the framework.[14]

Gas sorption properties

The porosity of all the obtained CTF materials was determined by nitrogen adsorption measurements collected at 77 K (Figure 5.5). At relative low pressure, all the isotherms exhibit a high N$_2$ uptake, indicating typical microporous character. Notably, for DCBP-CTF-2, a type IV isotherm with a H$_2$ hysteresis loop in the desorption branch is obtained, typical for mesoporous materials according to the IUPAC classification. In contrast to DCBP-CTF-2, the F-DCBP-CTF materials give rise to the type I isotherms with a steep rise of the isotherms at high relative pressure (P/P$_0$ > 0.9), indicating meso-/macropores presence to be attributed to interparticulate voids that exist between the highly aggregated particles.[15] As summarized in Table 5.1, the Brunauer-Emmett-Teller (BET) surface area and pore volume for DCBP-CTF-1 is calculated to be 2437 m^2/g and 1.48 cm^3/g, respectively. In contrast, the F-DCBP-CTF-1 exhibits a slightly lower surface area and pore volume of 1574 m^2/g and 1.5 cm^3/g, respectively.
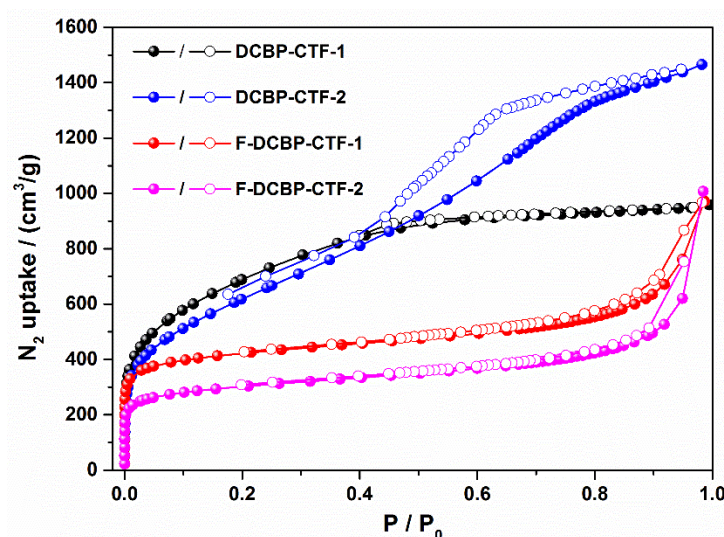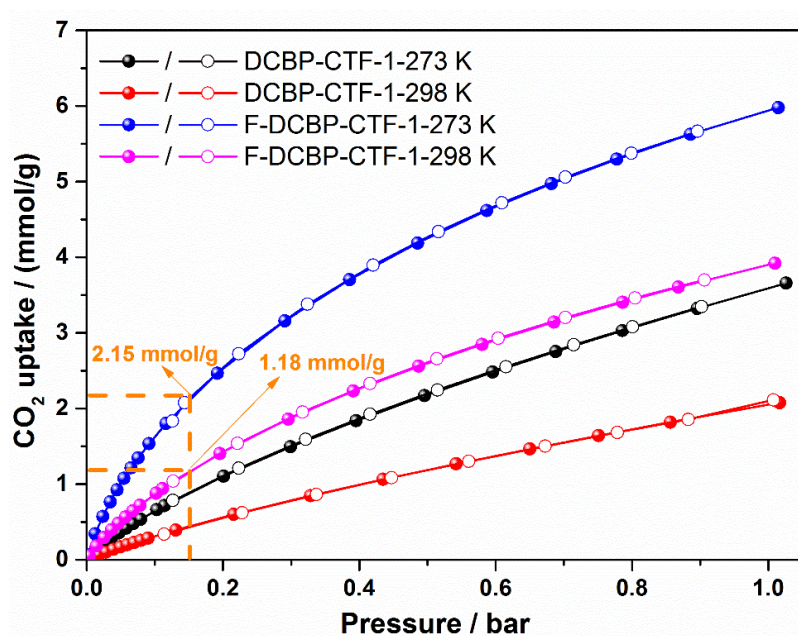

Figure 5.5. N$_2$ adsorption (solid symbols) and desorption (open symbols) isotherms of all the obtained CTF materials measured at 77 K.

Table 5.2. Summary and comparison of the gas sorption properties of the studied materials and the reported CTF materials.

Sample	CO_2 uptake (mmol/g)		H_2 uptake (wt%)	N_2 uptake (mmol/g)	Q_{st}^{max} (kJ/mol)	CO_2/N_2 Selectivity	Ref.
	273 K	298 K	77 K	298K			
F-DCBP-CTF-1	5.98	3.82	1.77	0.28	33.1	31	
F-DCBP-CTF-2	5.23	3.16	-	0.29	-	22	This work
DCBP-CTF-1	3.65	2.07	-	0.24	24.1	13	
DCBP-CTF-2	3.31	1.84	-	0.13	-	21	
FCTF-1	4.67	3.21	-	-	-	31[a]	4
lut-CTF400	4.55	2.72	1.36	0.20	37.5	63	5
F-CTF-1-600	5.53	3.41	-	-	-	19[a]	4
Bipy-CTF-600	5.58	2.95	2.1	0.28	34.4	37	5
CTF-py[HT]	5.97	4.22	2.63	0.25	27.1	29	2
HAT-CTFs	6.3	4.8	-	0.44	27.1	126	1

a). CO_2/N_2 selectivity was calculated by Ideal Adsorption Solution Theory (IAST).

Figure 5.6. CO_2 adsorption (solid symbols) and desorption (open symbols) isotherms of DCBP-CTF-1 and F-DCBP-CTF-1 at both 273 K and 298 K, respectively.

The porous nature and high nitrogen content along with the introduction of fluorine groups into the F-DCBP-CTF materials make them promising candidates for gas sorption and separation. Accordingly, the CO_2 adsorption isotherms for both DCBP-CTFs and F-DCBP-CTFs up to 1 bar at 273 K and 298 K were recorded (Figure 5.6 and Figure S5.10-5.11). In general, the materials synthesized with the $ZnCl_2$/monomer ratio of 5 show a better performance in CO_2 adsorption compared to those prepared with a

$ZnCl_2$/monomer ratio of 10, due to the higher microporosity, nitrogen content and fluorine groups of the materials (Table 5.2). Noteworthy, F-DCBP-CTF-1 exhibits a significantly high CO_2 adsorption capacity of 5.98 and 3.82 mmol/g at 273 K and 298 K and 1 bar, respectively (Table 5.2, entry 1). To the best of our knowledge, this value represents the highest CO_2 adsorption capacity for all the CTF materials synthesized at 400 °C reported thus far, as summarized in Table 5.2 and Table 1.3. It should be noted that direct comparison of the materials' CO_2 adsorption capacities remains difficult as they are synthesized under different conditions and will partially or completely carbonize at high temperatures, hence they are not CTFs anymore and normally called triazine-based porous carbon materials. More importantly, the realistic flue gas generally contains approximately 15 % CO_2 at a total pressure of 1 bar,[16] thus, the adsorption of CO_2 at ~0.15 bar is more relevant to the realistic CO_2 capture. Remarkably, at 0.15 bar and 273 K, F-DCBP-1 can adsorb 2.15 mmol/g CO_2, while at 298 K, this capacity only decreases moderately to 1.19 mmol/g, remaining significantly higher than most of the reported porous organic polymers.[16-17] The remarkable enhanced CO_2 adsorption capacity for F-DCBP-CTF-1 can be attributed to the strong electrostatic interactions between CO_2 molecules and the polar C–F bonds in the skeleton. Additionally, incorporation of nitrogen in POPs materials has already been proven to enhance the adsorption capacity of CO_2, an observation in line with our findings that F-DCBP-CTFs have a much higher nitrogen content and for this reason a higher CO_2 adsorption capacity compared to the DCBP-CTF materials. The outstanding CO_2 uptake at both low and moderate pressure together with the remarkable water tolerance and high thermal and chemical stability of the perfluorinated CTFs make them promising adsorbents for CO_2 capture from flue gas. To provide a better understanding of the CO_2 adsorption in the studied CTFs, we have also calculated the isosteric heat of CO_2 adsorption (Q_{st}) for both DCBP-CTF-1 and F-DCBP-CTF-1 materials using the Clausius-Clapeyron equation to fit CO_2 adsorption isotherms at 273 K and 298 K and

plotted it as a function of the capacity of adsorbed CO_2 (Figure S5.12). The Q_{st} value at low CO_2 adsorption uptake was calculated to be ~33.1 kJ/mol for F-DCBP-CTF-1, indicating the strong dipole-quadrupole interactions between CO_2 molecules and the framework of F-DCBP-CTF-1. Additionally, the lower Q_{st} value also means much lower regeneration cost of this material compared to conventional amine solutions.[18] The incorporation of fluorine groups into CTF materials not only resulted in enhanced CO_2 adsorption capacities but also afforded more preferential adsorption of CO_2 over N_2, i.e., higher CO_2/N_2 selectivity, another crucial factor for realistic CO_2 capture. We calculated the selectivity of all the CTF materials using the ratio of the initial slopes in the Henry region of the CO_2 and N_2 adsorption isotherms at 298 K. (Figure 5.7).

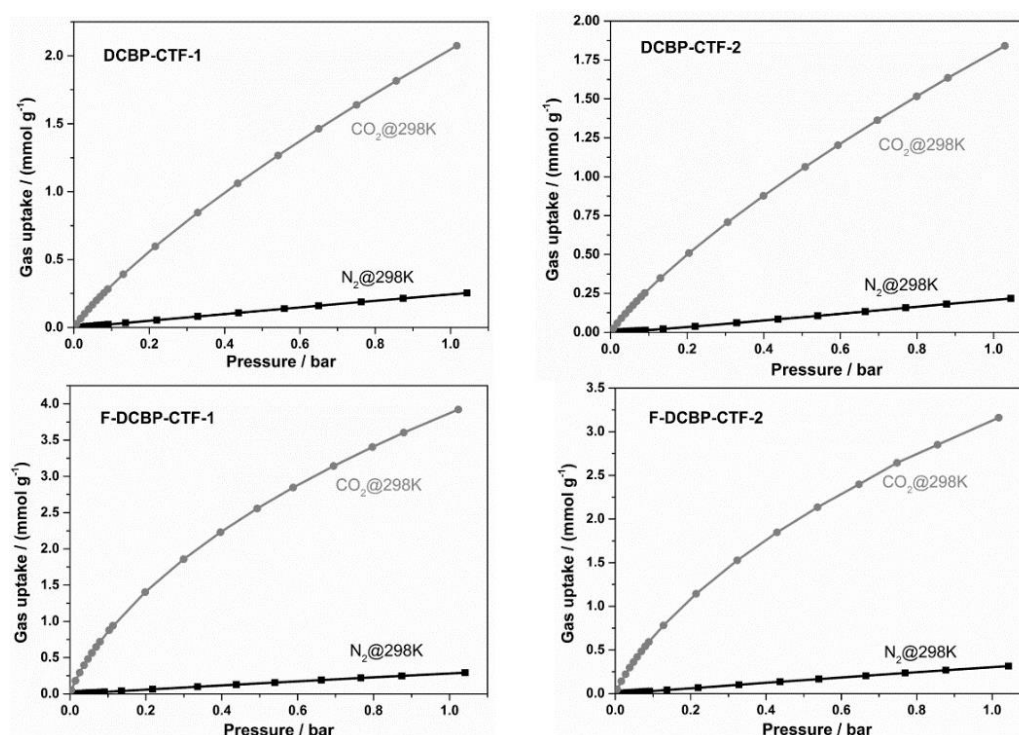**Figure 5.7.** N_2 and CO_2 uptakes measured on all presented CTF samples up to 1 bar at 298 K.

The calculated values are listed in Table 5.2 and a remarkable CO_2/N_2 selectivity of 31 was achieved by F-DCBP-CTF-1, much higher than that of DCBP-CTF-1 (13). The higher CO_2/N_2 selectivity further emphasizes the synergistic effects of microporosity and rich CO_2-philic sites (N and F) within

these polymeric networks. As such, given the exceptionally high CO_2 adsorption capacity and the intrinsic high thermal and chemical stability, these materials seem to be plausible adsorbents for practical application in a postcombustion CO_2 capture.

As a potential renewable and clean alternative to current fossil-fuel, hydrogen storage remains a major obstacle for its widespread implementation.[19] Recently, adsorptive hydrogen storage in porous materials (e.g. MOFs, COFs) has been explored as a possible approach for hydrogen storage.[20-21] For this reason, we further performed H_2 adsorption measurements at 77 K up to 1 bar with those materials that showed higher CO_2 uptake capacities (Figure 5.8 and Table 5.2). As shown in Figure 5.8, the H_2 adsorption capacity of DCBP-CTF-1 reaches 1.6 wt%, comparable to the previously reported result.[3] Notably, F-DCBP-CTF-1 exhibits a higher H_2 uptake of 1.77 wt%, surpassing most of the reported CTF materials and ranking only slight below fl-CTF-400 (1.95 wt%)[22] and PCTF-1 (1.86 wt%)[23] measured under identical conditions.
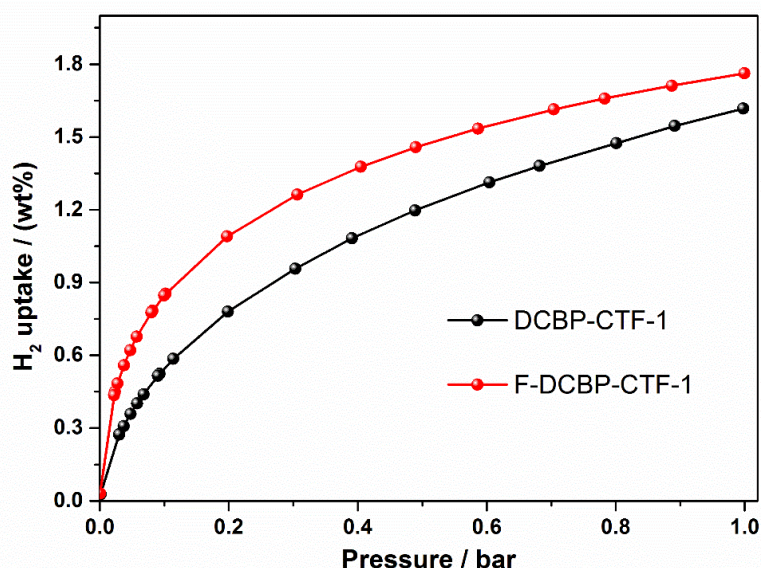

Figure 5.8. Low pressure H_2 adsorption isotherms for DCBP-CTF-1 (black) and F-DCBP-CTF-1 (red) measured at 77 K.

Water vapor sorption

To date, there are only few studies on the water sorption characteristics of
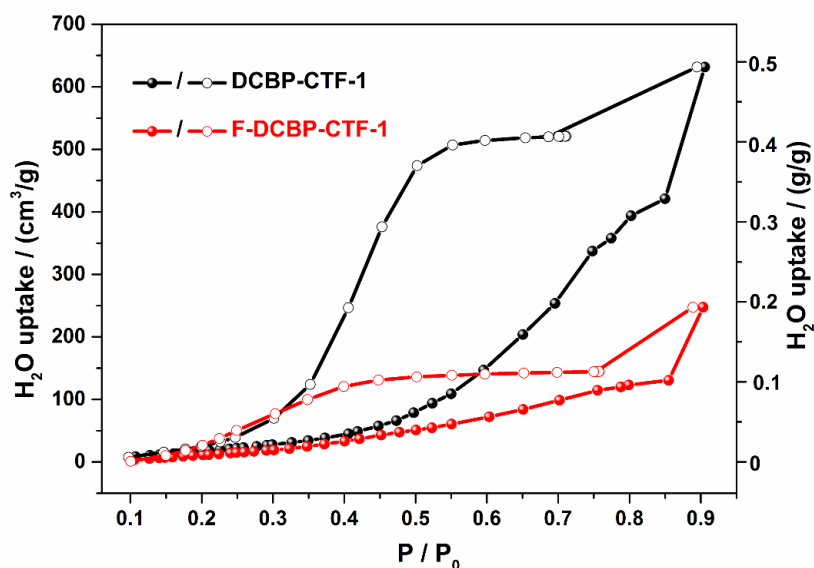
Figure 5.9. Water vapor adsorption (solid symbols) and desorption (open symbols) isotherms of F-DCBP-CTF-1 (red) and DCBP-CTF-1 (black) measured at 293 K.

CTFs.[5, 13] The hydrophobicity of the fluorine groups prompted us to explore the potential of the CTFs materials for water vapor sorption (Figure 5.9 and Figure S5.13). As shown in Figure 5.9, both CTF materials exhibit a type V isotherm, in which water molecules are only slightly adsorbed at low relative pressure, revealing the hydrophobic character of the pores, followed by a steep increase of water uptake at high relative pressures. A total water adsorption capacity of 630 cm^3/g (0.51 g/g) for DCBP-CTF-1 is obtained whereas the F-DCBP-CTF-1 only exhibits an adsorption capacity of 253 cm^3/g (0.21 g/g) at P/P_0 = 0.9 and 293 K.

5.3. Conclusions

In summary, a class of robust and hydrophobic fluorine-containing covalent triazine-based frameworks with large surface areas was synthesized under ionothermal conditions. Trimerization of the perfluorinated monomer and subsequent defluorination carbonization process of the network results in a significant loss of fluorine and carbon, yielding nitrogen-rich materials. The obtained porous materials display exceptionally high CO_2 and H_2 uptake capacities. The H_2 uptake for F-DCBP-CTF-1 can reach 1.77 wt% at 77 K and

1 bar, while the maximum CO_2 adsorption capacity for F-DCBP-CTF-1 is up to 5.98 mmol/g at 273 K and 1 bar (2.15 mmol/g at 273 K and 0.15 bar), exceeding most of the reported POPs materials in the literature to date. The perfluorinated CTFs also exhibit relatively high CO_2/N_2 selectivity compared to the non-functionalized CTFs. Moreover, in comparison to the DCBP-CTF materials, the hydrophobicity of the F-DCBP-CTF materials has been significantly enhanced due to the hydrophobic nature of the C–F bonds, confirmed by ambient water vapor sorption measurements. This highly fluorinated hydrophobic porous materials are not only of great interest for gas sorption and separation, but they also can be used for a wide range of applications including water/oil separation, capture of bio-renewable resources from water.

5.4. Experimental Section

General experimental methods

The ^{13}C and ^{19}F NMR spectra of the monomer were recorded on a Bruker Advance 400 MHz/500 MHz spectrometer using the peaks of TMS or residual solvent as standards. Trifluorotoluene (PhCF$_3$, δ = –63.72 ppm) was used as the internal standard in ^{19}F NMR spectra. Powder X-ray diffraction (PXRD) patterns were collected on a Thermo Scientific ARL X'Tra diffractometer, operated at 40 kV, 30 mA using Cu-K$_\alpha$ radiation (λ = 1.5406 Å). Fourier Transform Infrared Spectroscopy (FT-IR) in the region of 4000-800 cm^{-1} were performed with a Thermo Nicolet 6700 FT-IR spectrometer equipped with a nitrogen-cooled MCT detector and a KBr beam splitter. Elemental analyses (C, H, N) were carried out on a Thermo Scientific Flash 2000 CHNS-O analyzer equipped with a TCD detector. Thermogravimetric analysis (TGA) were performed on a Netzsch STA-449 F3 Jupiter-simultaneous TG-DSC analyzer in a temperature range of 20 - 800 °C under air atmosphere and a heating rate of 2 °C/min. Scanning electron microscopy (SEM) images of the CTFs

materials were measured on a JEOL JSM 7600F FEG/SEM. High angle annular dark field scanning-transmission electron microscopy (HAADF-STEM) and corresponding energy dispersive X-ray spectroscopy (EDX) mapping measurements was performed on a JEOL JEM-2200FS high resolution scanning transmission electron microscope equipped with an EDX spectrometer with a spatial resolution of 0.13 nm, image lens spherical aberration corrector, electron energy loss spectrometer (filter) and an emission field gun (FEG) operating at 200 KeV. All solid-state MAS NMR experiments were collected on an Agilent DD2-500 MHz spectrometer. ^{13}C MAS NMR spectra were acquired at 125.69 MHz using a 4 mm MAS NMR probe with a spinning rate of 8 kHz and a pulse width of 2.5 μs for a π/4 pulse, and 1800-2700 scans were accumulated with a 4 s recycle delay. ^{19}F MAS NMR spectra were acquired at 470.24 MHz using a 3.2 mm MAS NMR probe with a spinning rate of 20 kHz and a pulse width of 1.2 μs for a π/4 pulse, and 300 scans were accumulated with a 5 s recycle delay. X-ray photoelectron spectroscopy (XPS) measurements were performed using a Thermo Scientific K-Alpha+ X-ray Photoelectron Spectrometer. All samples were analyzed using a microfocused, monochromated Al K α X-ray source (1486.68 eV; 400 μm spot size). The K-Alpha+ charge compensation system was employed during analysis to prevent any localized charge buildup. The samples were mounted on conductive carbon tape and resulting spectra analyzed using the Avantage software from Thermo Scientific. N_2 adsorption isotherms were obtained using a Belsorp Mini apparatus measured at 77 K, whereas CO_2 and H_2 adsorption measurements were carried out on a Quantachrome iSorb-HP gas sorption analyzer. Water adsorption isotherms were measured on a Quantachrome Autosorb-iQ-TPX machine at 293 K. Prior to all the gas sorption measurements, the materials were activated by slowly heating up the samples with a heating rate of 5 °C/min up to 150 °C under vacuum for 3 h.

Synthesis procedures

All the chemicals were obtained from commercial sources and used as received without further purification.

General procedure for the preparation of the monomer F-DCBP. The monomer was synthesized according to the literature procedure with slight modification.[24] Typically, pentafluoro-benzonitrile (2.5 g, 13 mmol) as the starting material, 10 mL of anhydrous diethyl ether as the solvent was added to a 100 mL Schlenk flask, which was purged by Argon and equipped with a magnetic stir bar, the mixture was cooled with ice and maintained at 0 °C. To this, anhydrous ether solution (15 mL) of hexaethyl phosphorous triamide (1.6 g, 6.5 mmol) was added dropwise in 25 mins. Then the reaction mixture was allowed to stir at room temperature until the completion of the reaction (monitored by TLC). Afterwards, 10 mL of 1 M HCl aqueous solution was added to the mixture to quench the reaction. The mixture was filtrated and the filtrate was washed by CH_2Cl_2, the organic layers were collected, dried over anhydrous $MgSO_4$, evaporated and the title compound was obtained as a white crystalline solid by washing with cold diethyl ether. ^{13}C NMR (400 MHz, $CDCl_3$) δ 148.8 (m), 146.0 (m), δ 145.3 (m), 142.7 (m), 111.9 (m), 106.5 (s), 97.3 (m) ppm (Figure S5.14). ^{19}F NMR (470 MHz, $CDCl_3$) δ -129.6 to -129.8 (m, 4F), -133.4 to -133.5 (m, 4F) ppm (Figure S5.15). FT-IR (cm^{-1}, KBr pellet): υ 2250, 1656, 1488, 1289, 1260, 1007, 975 (Figure S5.16).

Synthesis of CTFs. The CTF materials using 4,4'-biphenyldicarbonitrile (DCBP) as the monomer was synthesized according to the previously reported procedure with slight modification.[3] Typically, the quartz ampoule was charged with DCBP (0.192 g, 1 mmol) and different ratios of anhydrous $ZnCl_2$ (0.68 g, 5 mmol for DCBP-CTF-1 and 1.36 g, 10 mmol for DCBP-CTF-2) in the glovebox under N_2 atmosphere. Afterwards, the ampoule was evacuated, flame-sealed and heated to 400 °C with a heating rate of 1 °C /min for 48 h. After cooling down to room temperature, the obtained crude product was grounded and washed thoroughly with water to remove the residual salt.

Afterwards, the crude material was stirred in diluted HCl overnight and then stirred in THF for another 24 h at room temperature. The resulting black powder was successively washed with water and acetone and then dried under vacuum at 150 °C overnight. F-DCBP-CTFs was synthesized by following the same procedure except F-DCBP was used as the monomer.

5.5. Supplementary Information

The supplementary information and figures of this chapter are listed in this section
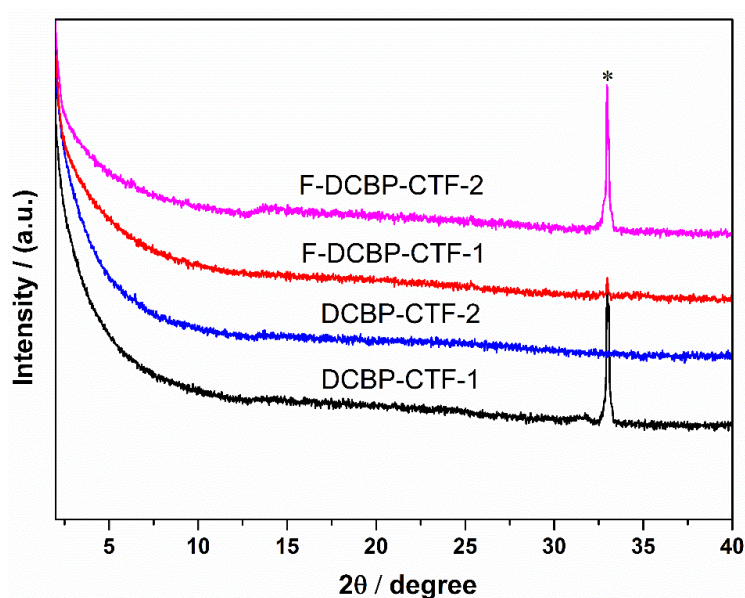

Figure S5.1. PXRD patterns of the DCBP-CTFs and F-DCBP-CTFs. Asterisks denote the background of the sample holder.
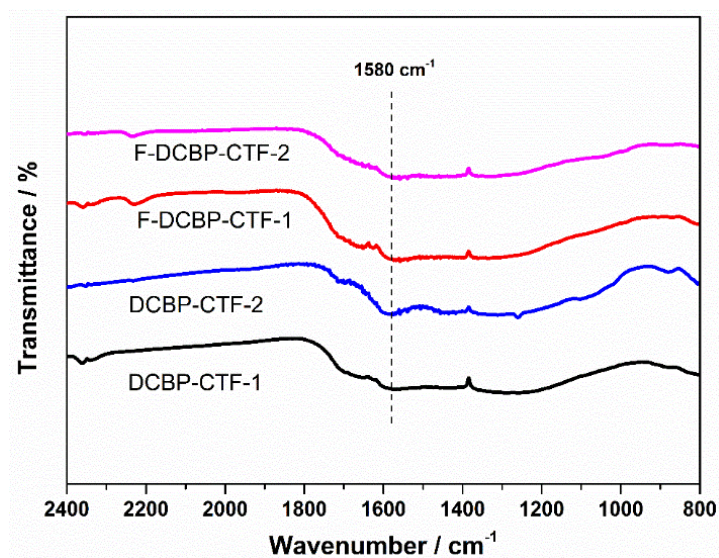
Figure S5.2. FT-IR spectra of the DCBP-CTFs and F-DCBP-CTFs.
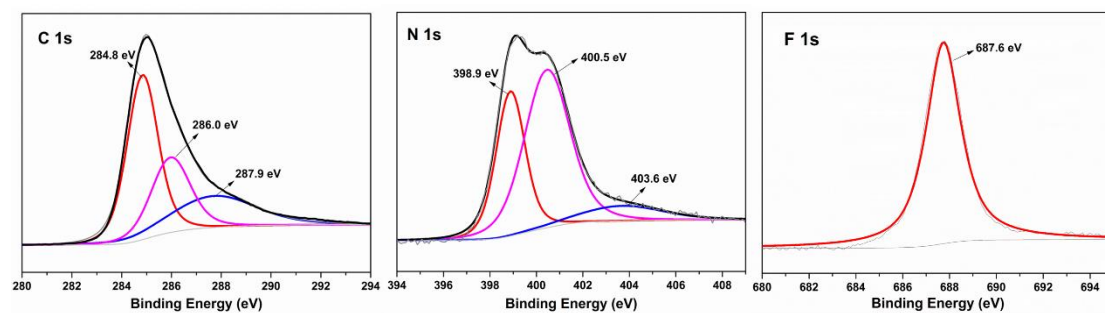
Figure S5.3. C1s, N1s and F 1s XPS spectra of F-DCBP-CTF-1
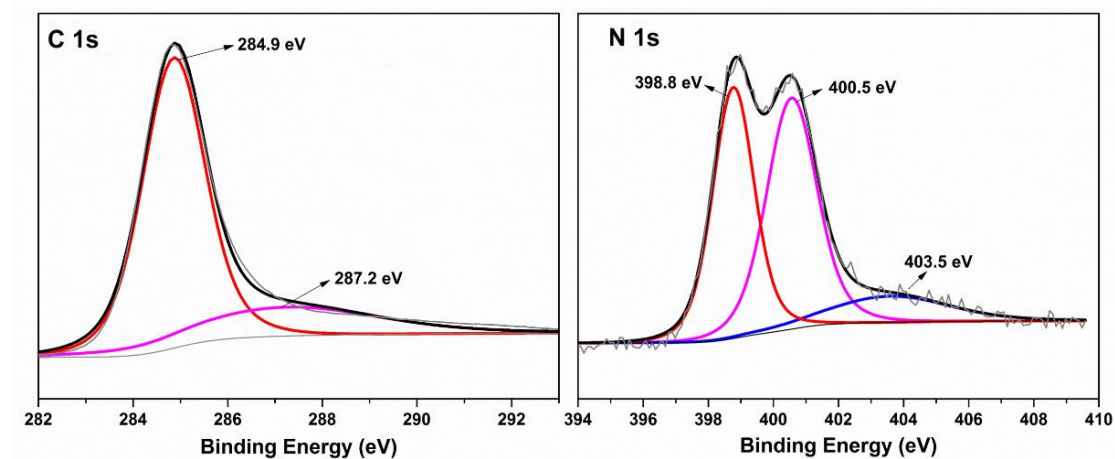
Figure S5.4. C1s and N1s XPS spectra of F-DCBP-CTF-1
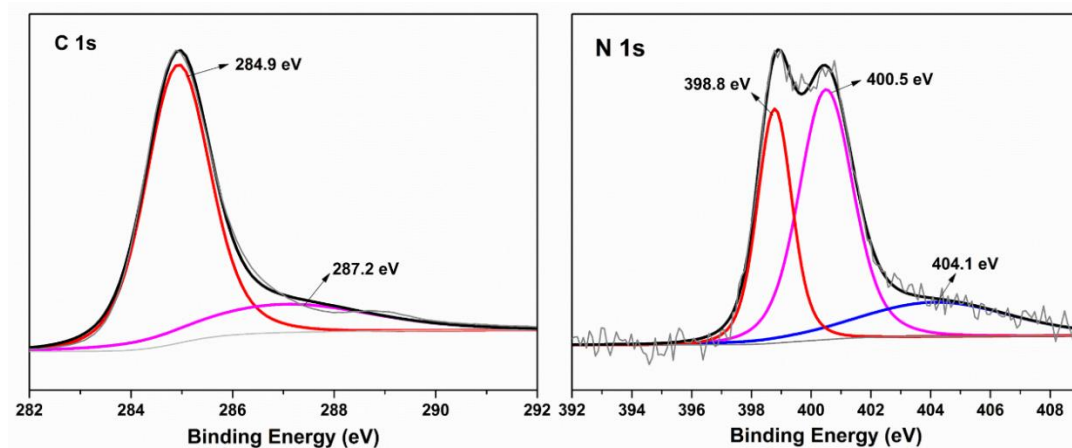
Figure S5.5. C1s and N1s XPS spectra of F-DCBP-CTF-2
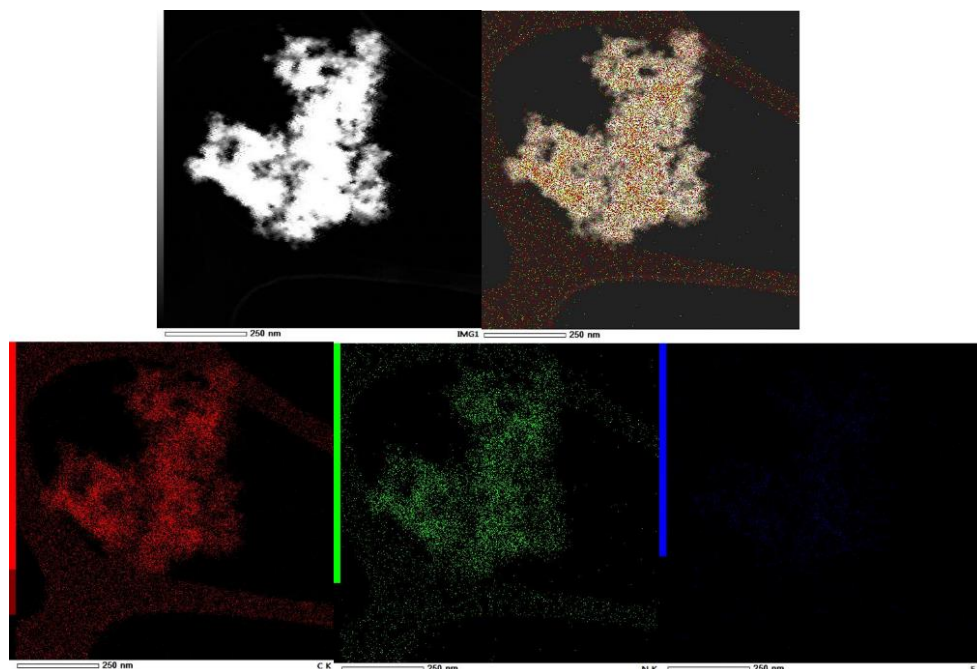
Figure S5.6. High angle annular dark field scanning-transmission electron microscopy (HAADF-STEM) and corresponding energy dispersive X-ray spectroscopy (EDX) mapping images of carbon (red), nitrogen (green) and fluorine (blue) on the sample of F-DCBP-CTF-2 .
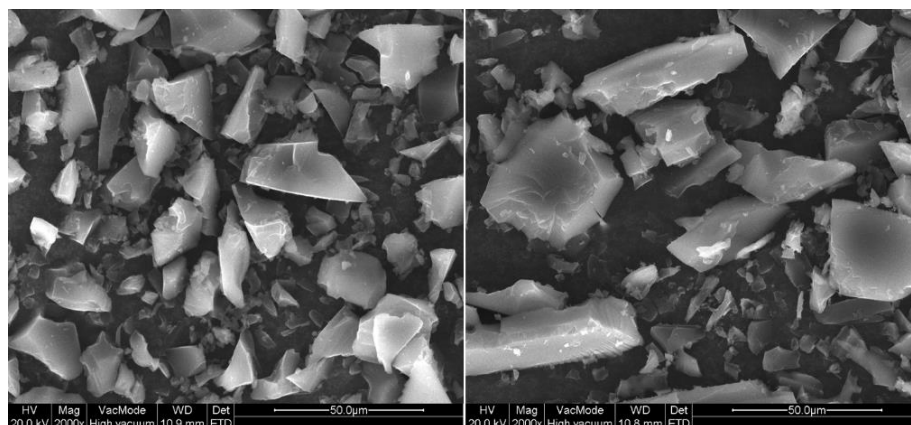
Figure S5.7. SEM images of the DCBP-CTF-1 (left) and DCBP-CTF-2 (right)
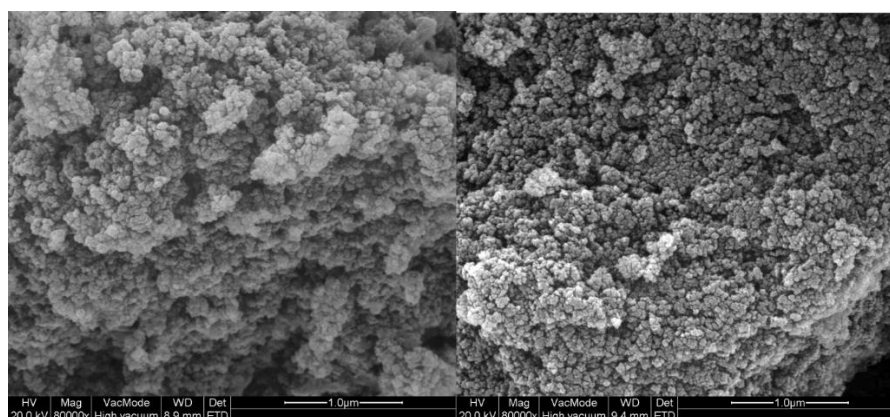
Figure S5.8. SEM images of the F-DCBP-CTF-1 (left) and F-DCBP-CTF-2 (right).
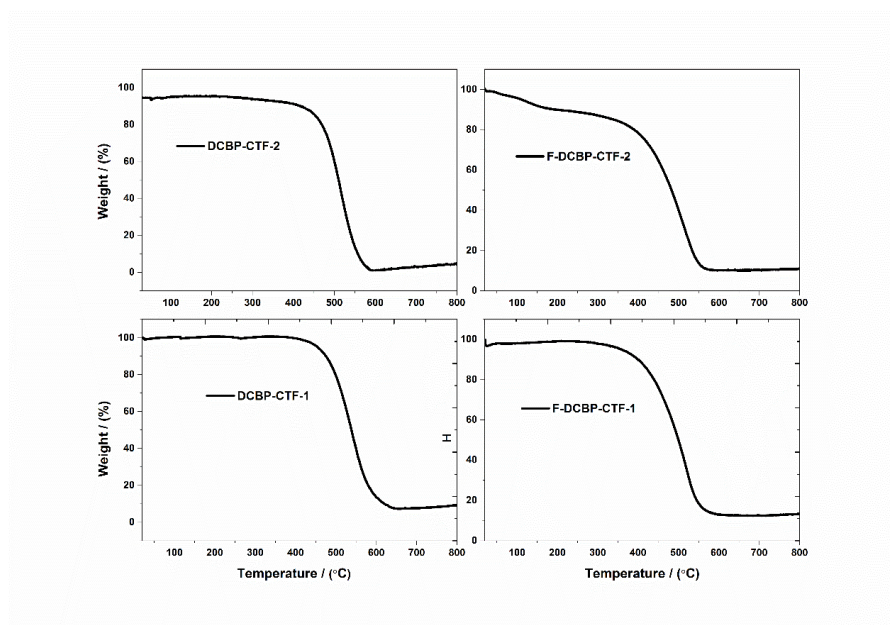
Figure S5.9. TGA curves of the obtained CTF materials measured at a heating rate of 2 °C/min under air flow.
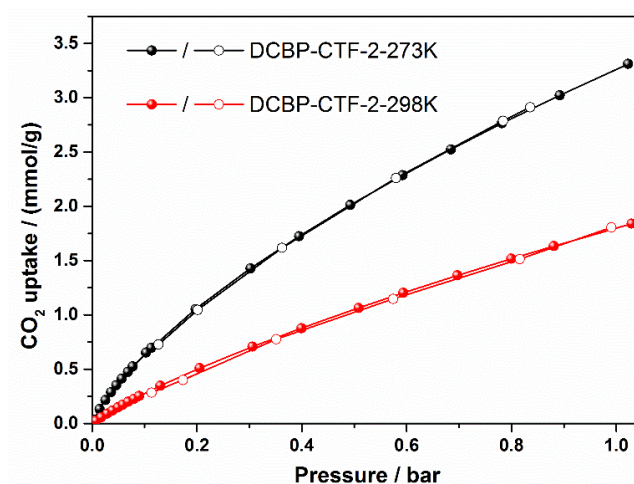
Figure S5.10. CO_2 adsorption (solid symbols) and desorption (open symbols) isotherms of DCBP-CTF-2 measured at 273 K and 298 K up to 1 bar.
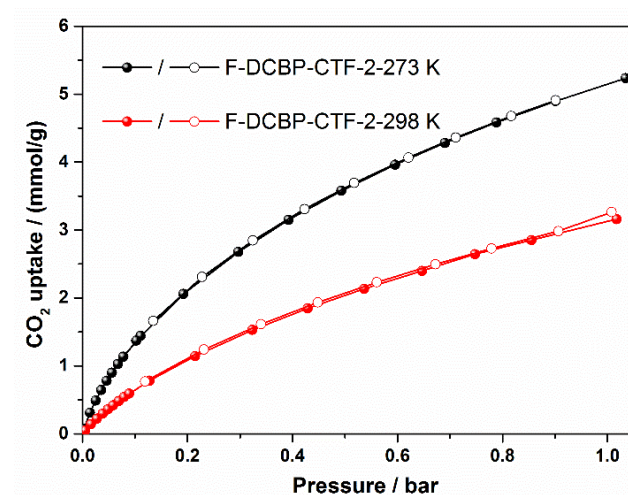
Figure S5.11. CO_2 adsorption (solid symbols) and desorption (open symbols) isotherms of F-DCBP-CTF-2 measured at 273 K and 298 K up to 1 bar.
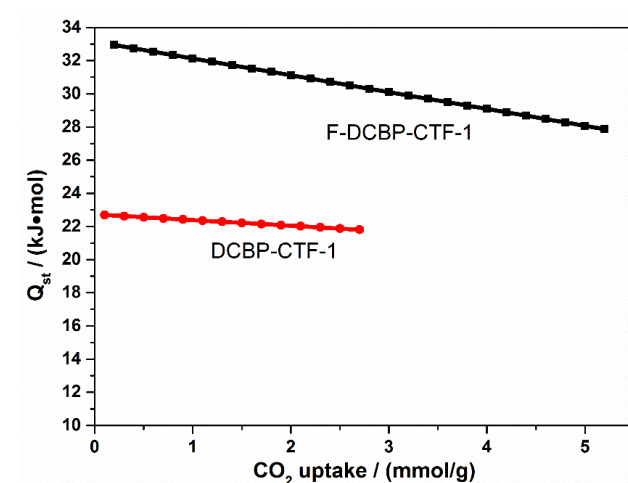
Figure S5.12. Isosteric heat of CO_2 adsorption (Q_{st}) for F-DCBP-1 (black symbols) and DCBP-1 (red symbols).
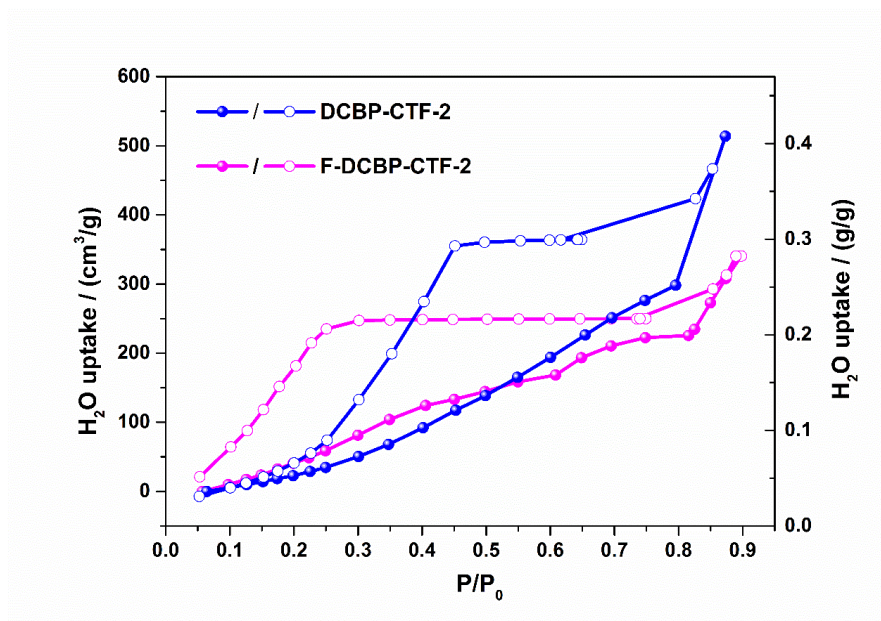
Figure S5.13. H_2O adsorption (solid symbols) and desorption (open symbols) isotherms for DCBP-CTF-2 (blue) and F-DCBP-CTF-2 (pink) measured at 20 °C.
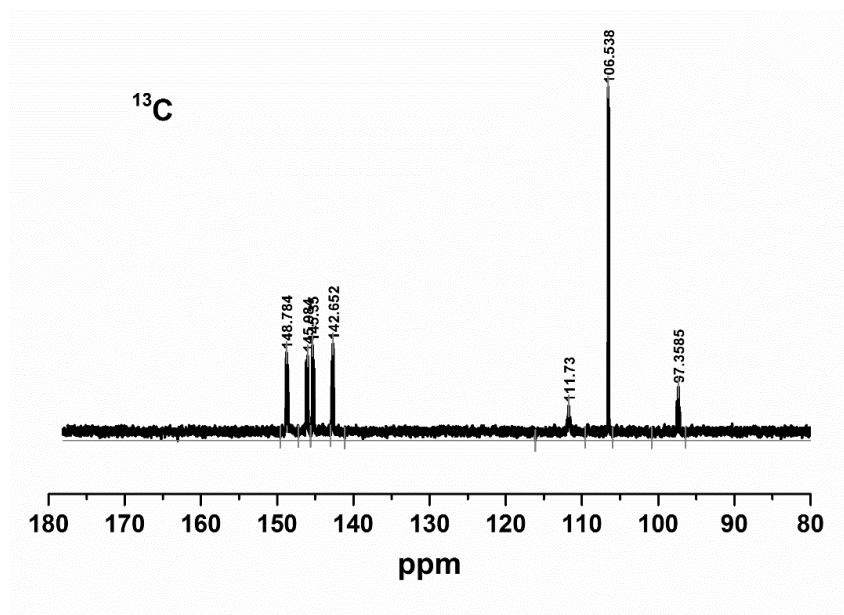
Figure S5.14. ^{13}C NMR spectrum of the monomer of F-DCBP.
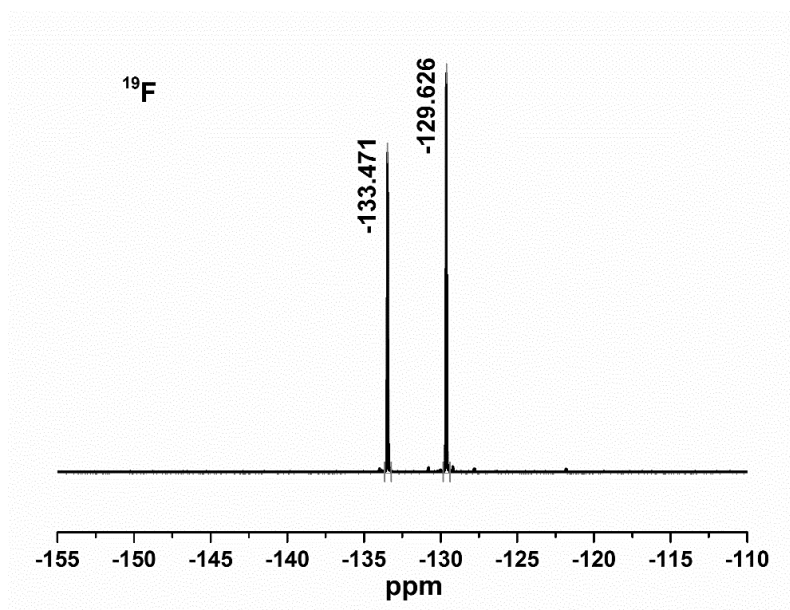
Figure S5.15. ^{19}F NMR spectrum of the monomer of F-DCBP
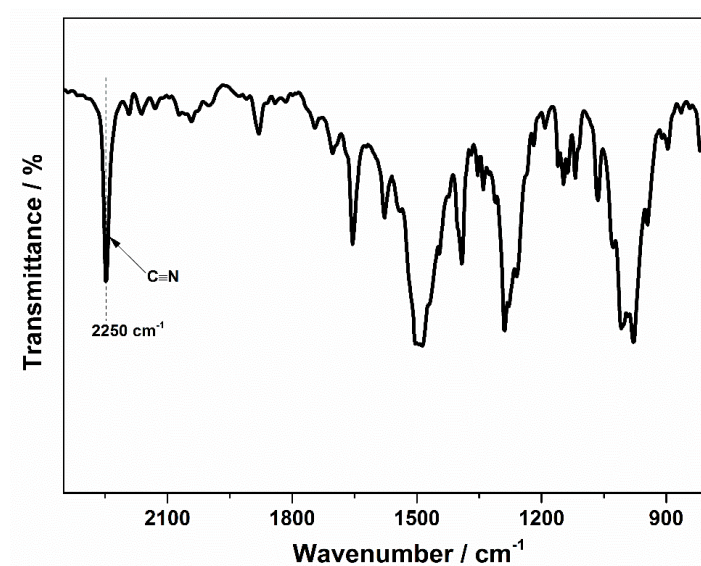
Figure S5.16. FT-IR spectrum of the monomer of F-DCBP

5.6. References

1.   Zhu, X.; Tian, C.; Veith, G. M.; Abney, C. W.; Dehaudt, J.; Dai, S., In Situ Doping Strategy for the Preparation of Conjugated Triazine Frameworks Displaying Efficient CO_2 Capture Performance. *J. Am. Chem. Soc.* **2016,** *138* (36), 11497-11500.

2.   Tuci, G.; Pilaski, M.; Ba, H.; Rossin, A.; Luconi, L.; Caporali, S.; Pham-Huu, C.; Palkovits, R.; Giambastiani, G., Unraveling Surface Basicity and Bulk Morphology Relationship on Covalent Triazine Frameworks with Unique Catalytic and Gas Adsorption Properties. *Adv. Funct. Mater.* **2017,** *27* (7), 1605672.

3.   Kuhn, P.; Antonietti, M.; Thomas, A., Porous, Covalent Triazine-Based Frameworks Prepared by Ionothermal Synthesis. *Angew. Chem. Int. Ed.* **2008,** *47* (18), 3450-3453.

4.   Zhao, Y.; Yao, K. X.; Teng, B.; Zhang, T.; Han, Y., A perfluorinated covalent triazine-based framework for highly selective and water-tolerant CO_2 capture. *Energy Environ. Sci.* **2013,** *6* (12), 3684-3692.

5.   Hug, S.; Stegbauer, L.; Oh, H.; Hirscher, M.; Lotsch, B. V., Nitrogen-Rich Covalent Triazine Frameworks as High-Performance Platforms for Selective Carbon Capture and Storage. *Chem. Mater.* **2015,** *27* (23), 8001-8010.

6.   Wang, K.; Huang, H.; Liu, D.; Wang, C.; Li, J.; Zhong, C., Covalent Triazine-Based Frameworks with Ultramicropores and High Nitrogen Contents for Highly Selective CO_2 Capture. *Environ. Sci. Technol.* **2016,** *50* (9), 4869-4876.

7.   Gu, C.; Liu, D.; Huang, W.; Liu, J.; Yang, R., Synthesis of covalent triazine-based frameworks with high CO_2 adsorption and selectivity. *Polym. Chem.* **2015,** *6* (42), 7410-7417.

8.   Chen, Q.; Schmidt-Rohr, K., ^{19}F and ^{13}C NMR Signal Assignment and Analysis in a Perfluorinated Ionomer (Nafion) by Two-Dimensional Solid-State NMR. *Macromolecules* **2004,** *37* (16), 5995-6003.

9.   Giraudet, J.; Dubois, M.; Guérin, K.; Delabarre, C.; Hamwi, A.; Masin, F., Solid-State NMR Study of the Post-Fluorination of $(C_{2.5}F)_n$ Fluorine–GIC. *J. Phys. Chem. B* **2007,** *111* (51), 14143-14151.

10. Hu, X.-M.; Chen, Q.; Zhao, Y.-C.; Laursen, B. W.; Han, B.-H., Straightforward synthesis of a triazine-based porous carbon with high gas-uptake capacities. *J. Mater. Chem. A* **2014,** *2* (34), 14201-14208.

11. Osadchii, D. Y.; Olivos-Suarez, A. I.; Bavykina, A. V.; Gascon, J., Revisiting Nitrogen Species in Covalent Triazine Frameworks. *Langmuir* **2017,** *33* (50), 14278-14285.

12. Byun, J.; Patel, H. A.; Thirion, D.; Yavuz, C. T., Charge-specific size-dependent separation of water-soluble organic molecules by fluorinated nanoporous networks. *Nat. Commun.* **2016,** *7*, 13377.

13. Dey, S.; Bhunia, A.; Breitzke, H.; Groszewicz, P. B.; Buntkowsky, G.; Janiak, C., Two linkers are better than one: enhancing CO_2 capture and separation with porous covalent triazine-based frameworks from mixed nitrile linkers. *J. Mater. Chem. A* **2017,** *5* (7), 3609-3620.

14. Pachfule, P.; Banerjee, R., Metal-Organic Frameworks: Fluorinated Frameworks. In *Encyclopedia of Inorganic and Bioinorganic Chemistry*, John Wiley & Sons, Ltd: 2011.

15. Li, B.; Huang, X.; Liang, L.; Tan, B., Synthesis of uniform microporous polymer nanoparticles and their applications for hydrogen storage. *J. Mater. Chem.* **2010,** *20* (35), 7444-7450.

16. Zou, L.; Sun, Y.; Che, S.; Yang, X.; Wang, X.; Bosch, M.; Wang, Q.; Li, H.; Smith, M.; Yuan, S.; Perry, Z.; Zhou, H. C., Porous Organic Polymers for Post-Combustion Carbon Capture. *Adv Mater* **2017,** *29* (37), 1700229-n/a.

17. Trickett, C. A.; Helal, A.; Al-Maythalony, B. A.; Yamani, Z. H.; Cordova, K. E.; Yaghi, O. M., The chemistry of metal–organic frameworks for CO_2 capture, regeneration and conversion. *Nat. Rev. Mater.* **2017,** *2,* 17045.

18. Lu, W.; Yuan, D.; Sculley, J.; Zhao, D.; Krishna, R.; Zhou, H.-C., Sulfonate-Grafted Porous Polymer Networks for Preferential CO_2 Adsorption at Low Pressure. *J. Am. Chem. Soc.* **2011,** *133* (45), 18126-18129.

19. García-Holley, P.; Schweitzer, B.; Islamoglu, T.; Liu, Y.; Lin, L.; Rodriguez, S.; Weston, M. H.; Hupp, J. T.; Gómez-Gualdrón, D. A.; Yildirim, T.; Farha, O. K., Benchmark Study of Hydrogen Storage in Metal–Organic Frameworks under Temperature and Pressure Swing Conditions. *ACS Energy Letters* **2018,** *3* (3), 748-754.

20. Suh, M. P.; Park, H. J.; Prasad, T. K.; Lim, D.-W., Hydrogen Storage in Metal-Organic Frameworks. *Chem. Rev.* **2012,** *112* (2), 782-835.

21. Zhao, D.; Yuan, D.; Zhou, H.-C., The current status of hydrogen storage in metal-organic frameworks. *Energy Environ. Sci.* **2008,** *1* (2), 222-235.

22. Hug, S.; Mesch, M. B.; Oh, H.; Popp, N.; Hirscher, M.; Senker, J.; Lotsch, B. V., A fluorene based covalent triazine framework with high CO_2 and H_2 capture and storage capacities. *J. Mater. Chem. A* **2014,** *2* (16), 5928-5936.

23. Bhunia, A.; Vasylyeva, V.; Janiak, C., From a supramolecular tetranitrile to a porous covalent triazine-based framework with high gas uptake capacities. *Chem. Commun.* **2013,** *49* (38), 3961-3963.

24. Taylor, R. G. D.; Bezzu, C. G.; Carta, M.; Msayib, K. J.; Walker, J.; Short, R.; Kariuki, B. M.; McKeown, N. B., The Synthesis of Organic Molecules of Intrinsic Microporosity Designed to Frustrate Efficient Molecular Packing. *Chem. Eur. J.*   **2016,** *22* (7), 2466-2472.

CHAPTER 6

Conclusion and Outlook

The Past

The Future

The Present
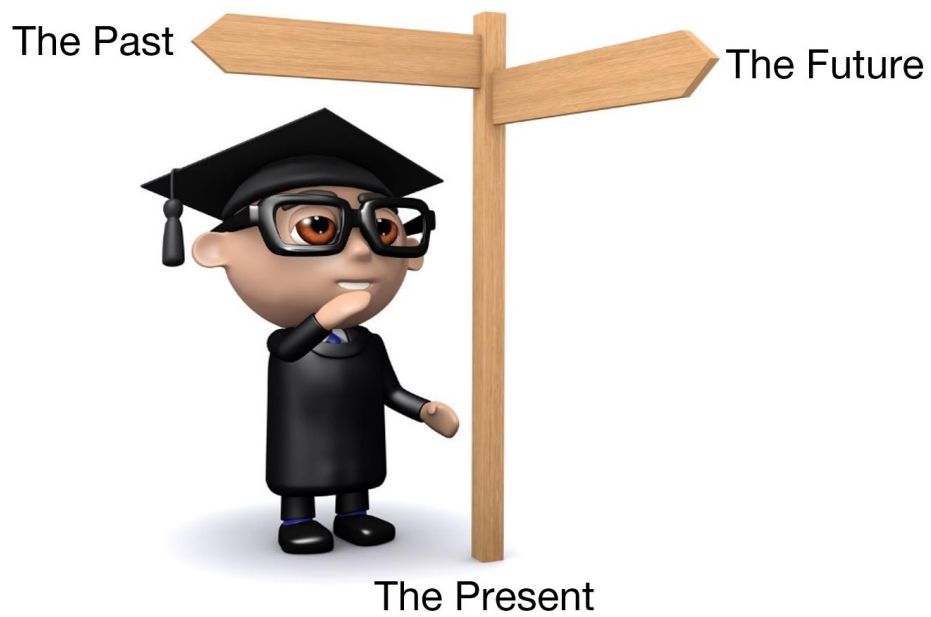
6.1. General Discussion

Since the discovery of the first CTF material in 2008, this new type of advanced porous materials have been extensively investigated in a variety of applications such as gas adsorption and separation, catalysis, membranes and electronic devices due to their high surface area, low skeleton density, extremely high physicochemical stability as well as diverse structural tunability and functionalities. Among all the possible applications, gas adsorption and separation is still one of the major research fields for CTF materials with the focus on the adsorption and separation of CO_2, CH_4, H_2 and hydrocarbon compounds. The diverse structural tunability and functionality is an important feature of CTFs, which can be controlled by the selection of the building blocks, the zinc chloride concentration and the synthesis temperatures. Another key element of this type of materials is their nitrogen functionalities, both from the triazine rings formed in situ and from the N-heterocycles used as the building units. These are able to bind carbon dioxide molecules through quadrupole-dipole and quadrupole-induced dipole interactions, which is beneficial for carbon capture and storage. In search of a particular functionality for some task-specific applications, fluorine groups are promising candidates because of the fact that (1) the high electronegativity of F can further promote CO_2 adsorption through electrostatic interaction; (2) F groups can effectively reduce the micropore size to < 0.5 nm, thus facilitating CO_2 uptake and CO_2/N_2 separation by kinetic selectivity and (3) the hydrophobic C-F bonds can strongly improve the hydrophlic stability. This knowledge is crucial for the tailored design of CTF materials for efficient carbon capture and separation. To date, the benchmark CTFs for CO_2 capture is found to be HAT-CTF-450/600 (prepared at 600 °C), exhibiting the CO_2 adsorption capacity of 6.3 mmol/g at 273 K and 1 bar, while CTF-py performs the best among all the CTFs synthesized at 400 °C (5.08 mmol/g at 273 K and 1 bar). Along the same line, CTF-py^{HT} (prepared at 750 °C) exhibits the highest H_2 adsorption capacity of

2.63 wt% at 77 K and 1 bar, while fl-CTF-400 represents the highest value (1.95 wt%) for all the reported CTFs synthesized at 400 °C.

In this thesis, four new CTF materials based on a set of nitrogen- and fluorine-functionalized building blocks were designed and systematically evaluated as the high-performance platforms for the application of gas adsorption and separation. Significantly, the studied CTF materials in this thesis exhibit exceptionally high gas adsorption and separation performances (Figure 6.1), they are expected to be promising as the high-performance platforms for further possible realistic applications.
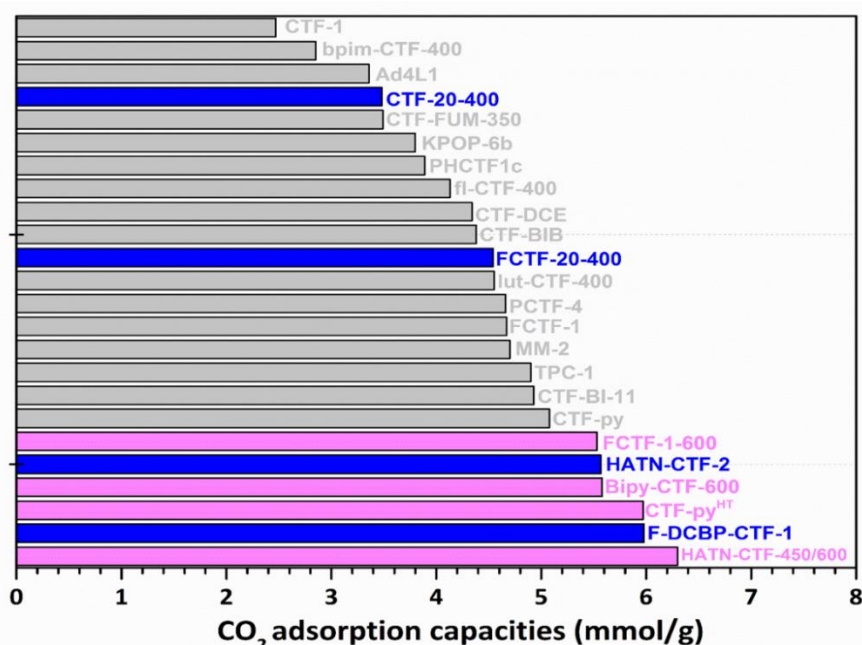
Figure 6.1. A summary of the reported CTF materials for CO_2 adsorption at 273 K and 1 bar. (The CTFs prepared at 400 °C in this thesis (blue); the CTFs prepared at 600 °C in literature (pink); the reported CTFs prepared at 400°C in literature (grey).

6.2. Detailed Conclusions

In this thesis, we focus on the rational design and synthesis of novel CTF materials by employing a series of building blocks with abundant CO_2-philic functionalities and explore their potential for the application of gas adsorption and separation.

In Chapter 2, we described the design and synthesis of a novel N-

heteroaromatic tetranitrile, 4,4′,4″,4‴-(1,4-phenylenebis(pyridine-4,2,6-triyl)) tetrabenzonitrile, which was further used as the building block for the preparation of a set of nitrogen-rich CTF materials. In this chapter, the influence of several parameters, such as the $ZnCl_2$/monomer ratio and reaction temperatures, on the structure and porosity of the resulting frameworks was systematically examined. We found that the higher $ZnCl_2$/monomer ratio and higher synthesis temperature can lead to the materials with higher porosity and surface area, while the gas adsorption capacities are more related to the accessible micropores as well as the nitrogen content of the CTF materials. More specifically, for the CTFs synthesized at 400 °C, increasing the $ZnCl_2$/monomer ratio can significantly improve their corresponding gas uptakes, while at 500 °C, the $ZnCl_2$/monomer ratio almost has no effect on their gas adsorption performances. These observations provided us crucial information for the following research.

In Chapter 3, we incorporated the CO_2-philic fluorine groups into the aforementioned tetranitrile to expect to improve the materials' gas adsorption and separation performances. As confirmed by TEM and EDX element mapping and F1s XPS measurements, the remaining fluorine groups are homogeneously distributed in the CTF materials. Remarkably, compared with the non-fluorinated CTF materials (chapter 2), the fluorinated CTFs exhibit much higher CO_2 adsorption capacity (4.54 mmol/g at 273 K and 1 bar) and show exceptionally high H_2 adsorption capacity (1.88 wt% at 77 K and 1 bar), which is only slightly lower than the benchmark CTF materials (1.95 wt% under identical conditions). Furthermore, the studied materials also exhibit higher CO_2/N_2 and CO_2/CH_4 selectivities than those of corresponding non-fluorinated ones. Our findings confirmed that incorporation of CO_2-philic fluorine functionalities into the frameworks of CTFs is an efficient and straightforward approach to achieve better gas adsorption and separation performances.

Hexaazatrinaphthalene (HATN) derivatives are ideal building blocks for the

construction of supramolecular architectures and functional materials due to their excellent electron-deficient property, high π-π stacking tendency and abundant nitrogen content. As a proof of concept, **in Chapter 4**, we for the first time prepared a set of nitrogen-rich hexaazatrinaphthalene-based CTFs and evaluated their carbon capture and separation properties. We found that nitrogen content of the obtained CTF materials was significantly high (up to 21.8% out of the theoretical value of 27.8%), which is almost the highest value for all the reported CTF materials. More importantly, the materials exhibit extremely high CO_2 adsorption capacity (5.57 mmol/g at 273 K and 1 bar), surpassing the benchmark CTF materials synthesized at 400 °C (5.08 mmol/g at 273 K and 1 bar). Furthermore, the materials also show superior H_2 adsorption capacity of 1.74 wt% and significantly high CO_2/N_2 (up to 53) and CO_2/CH_4 (up to 9.8) selectivities. We believe that these impressive results render the studied CTF materials as promising candidates for efficient CO_2 capture and separation.

We are interested in fluorine groups not only because of the fact that the strong electronegativity of F can promote CO_2 adsorption through electrostatic interactions but also the hydrophobic nature of F, which can improve both the materials' stability and performances under moisture conditions. **In Chapter 5**, we presented the design and synthesis of a perfluorinated nitrile by replacing every hydrogen atom of 4,4'-biphenyldicarbonitrile by fluorine atoms, which was then used as the building block for the preparation of hydrophobic fluorinated CTFs. Interestingly, as confirmed by XPS measurements, most of the fluorine groups were decomposed and only 10% of theoretical fluorine groups was reserved in the structure, which is in accordance with the findings of chapter 2. However, this fluorine-containing CTF material exhibit exceptionally high CO_2 adsorption capacity (5.98 mmol/g at 273 K and 1 bar), which is higher than all the reported CTFs synthesized at 400 °C and only slightly lower than that of HAT-CTF-450/600 (6.3 mmol/g under the same

conditions, synthesized at 450 °C and 600 °C). Its outstanding CO_2 adsorption capacity, high tolerance to water and good reusability makes them promising candidates for selective CO_2 capture from flue gas and other relevant applications.

From this dissertation work, we can conclude that incorporation of both nitrogen sites and fluorine sites into the structure of CTFs can have a beneficial effect on their gas adsorption and separation properties. Although it is not easy or proper to directly compare and determine which functional groups are better and more efficient, concerning the environmental issues, nitrogen sites seems more friendly than fluorine sites, as some fluorine species will be formed and released after the synthesis.

In summary, this thesis is an original and inspiring research in the exploration of efficient porous adsorbents for the application of gas adsorption and separation. CTFs, being in general more stable than the majority of MOFs and more tunable than zeolites and activated carbons, are quite stable and attractive platforms for various applications. This field is currently growing and it is easy to foresee a rapid further development in the coming years.

6.3. Future Perspectives

CTFs represent a very well tunable and expandable platform for various applications. The materials' physical and chemical properties can be tailor-made and fine-tuned towards the desired applications, while the numerous N-moieties and functionalities can provide the possibility to bind more gas molecules or coordinate more catalytically active sites. Their superior tunability, chemical and thermal stability, porosity and specific surface areas compared to the traditional solid adsorbents render them highly promising for possible practical applications. However, it does not mean this type of materials is perfect and there is still room for improvements from the view of both science and industry. In my opinion, maybe one can expect to improve and expand the

potential applications of this type of materials in the following aspects.

Until now, most researchers focus on CTFs synthesized via the ionothermal approach to induce high porosity and specific surface areas in sealed ampoules. However, almost all the CTF materials are amorphous dark materials with strong absorbance in the spectral range of many common spectroscopic techniques. These features make the characterization of these materials difficult and hamper a better understanding of their structural and chemical properties. The actual or real structural properties are therefore still literally hidden within a "black box" and substantial research efforts to unravel the true nature and structure of CTF materials are urgently needed in this newly developed and emerging field.

Although CTFs are remarkable materials, it has to be mentioned that their synthesis is somewhat tedious. Due to the high temperatures applied, the reaction has to be conducted in evacuated and sealed glass or quartz ampoules. In this respect care has to be taken that the organic monomers are not decomposing or that the (hygroscopic) $ZnCl_2$ is applied in a dry state, as any evolving gases increase the pressure in the ampoule and will explode. It is therefore recommended to fill the ampoules with salt and monomer in a glove box and to have a very diligent glass blower available for sealing them, which limited the large-scale CTF synthesis and possible realistic applications. Furthermore, the batch to batch reproducibility for the synthesis of CTFs is somewhat doubtful. As the synthesis and side reactions under high temperatures are uncontrollable, it is not that easy to obtain the completely same batches of materials. Thus, exploring other mild, cost-effective and scalable synthesis approaches for the preparation of (crystalline) CTFs and combination of modelling and theoretical calculations should be promising for future possible industrial implementation.

Up to date, all the applications of CTFs are confined to the laboratory under "ideal" conditions and it is too early to say or predict the possibility of industrial

implementation. To evaluate the potential of CTFs for realistic applications, it will be of great importance and necessary for scientists to carry out the experiments under simulated or real industrial conditions and the researchers are ought to pay more attention to the following aspects, including but not limited to sustainability, mechanical stability, scalability, economic potential and lifetime of the CTF materials.

Furthermore, at this moment researchers mainly focus on CO_2 adsorption and the investigation of their separation selectivities by calculations according to the single gas adsorption isotherms. However, breakthrough measurements are necessary to evaluate the possible realistic separation properties of the materials. To the best of my knowledge, there are almost no reports on CTF materials for other kinds of gas adsorption and separation (e.g. SO_2, NO_x, C_3H_6/C_3H_8), thus it will be really interesting for researchers to pioneer and investigate these applications.

Nonetheless, these examples only represent some of the challenges, any newly developed and emerging field has to go through and which most likely be tackled within the development of this field. Overall, we can foresee a rapid and promising development of this field in the coming years.

Curriculum Vitae

GUANGBO WANG

Personal

Address: Department of Chemistry, Faculty of Science, Ghent University, Krijgslaan 281 (S3), 9000 Ghent, Belgium.

Tel: (0032)486918166

E-mail: guangbo.wang@ugent.be; wanggb001@gmail.com

Educational Background

Ghent University   2014/10-2018/10

Ph.D, Department of Chemistry.

Dalian University of Technology   2011/09-2014/06

Master, Department of Catalysis Chemistry

Shandong University of Science and Technology   2007/09-2011/06

Bachelor, School of Chemical Engineering

Publications

1. <u>G.-B. Wang</u>, K. Leus, S. Couck, P. Tack, H. Depauw, Y.-Y. Liu, L. Vincze, J. F. M. Denayer and P. Van Der Voort, Enhanced gas sorption and breathing properties of the new sulfone functionalized COMOC-2 metal organic framework, *Dalton Trans.*, 2016, 45, 9485-9491.

2. <u>G.-B. Wang</u>, K. Leus, K. Hendrickx, J. Wieme, H. Depauw, Y-Y Liu, V. Van Speybroeck and P. Van der Voort, A series of sulfonic acid functionalized mixed-linker DUT-4 analogues: synthesis, gas sorption properties and catalytic performance, *Dalton Trans.*, 2017, 46, 14356-14364.

3. <u>G.-B. Wang</u>, K. Leus, H. S. Jena, C. Krishnaraj, S.-N. Zhao, H. Depauw, N. Tahir, Y.-Y. Liu and P. Van Der Voort, A fluorine-containing covalent triazine

framework with excellent selective CO_2 capture performance, *J. Mater. Chem. A.* 2018, 6, 6370-6375.

4. <u>G.-B. Wang</u>, K. Leus, S.-N. Zhao and P. Van Der Voort, Newly designed covalent triazine framework based on novel N-heteroaromatic building blocks for efficient CO_2 and H_2 capture and storage. *ACS Appl. Mater. Interfaces*, 2018, 10, 1244–1249.

5. <u>G.-B. Wang</u>, N. Tahir, I. Onyshchenko, N. De Geyter, R. Morent, K. Leus and P. Van Der Voort, Novel hexaazatrinaphthalene-based covalent triazine frameworks as high-performance platforms for efficient carbon capture and storage (In preparation).

6. <u>G.-B. Wang</u>, I. Onyshchenko, N. De Geyter, R. Morent, K. Leus and P. Van Der Voort, Highly enhanced gas adsorption performance in a fluorinated microporous covalent triazine framework. (In preparation)

7. <u>G.-B. Wang</u>, K. Leus and P. Van Der Voort, Reticular structure of Al-soc-MOF-1: a high-performance platform for exceptional methane storage. (In preparation)

8. H. Depauw, I. Nevjestic, J. De Winne, <u>G.-B. Wang</u>, K. Haustraete, K. Leus, A. Verberckmoes, C. Detavernier, F. Callens, E. De Canck, H. Vrielinck and P. Van Der Voort, Microwave induced "egg yolk" structure in Cr/V-MIL-53, *Chem. Commun.*, 2017, 53, 8478-8481.

9. H. Depauw, I. Nevjestic, <u>G.-B. Wang</u>, K. Leus, F. Callens, E. De Canck, K. De Buysser, H. Vrielinck and P. Van Der Voort, Discovery of a novel, large pore phase in a bimetallic Al/V metal-organic framework, *J. Mater. Chem. A.* 2017, 5, 24580-24584. (Front Cover)

10. S.-N. Zhao, <u>G.-B. Wang</u>, D. Poelman and P. Van Der Voort, Luminescent lanthanide MOFs: a unique platform for chemical sensing, *Materials,* 2018, 11, 572. (Invited review and Front Cover)

11. H. S. Jena, C. Krisnaraj, G.-B. Wang, K. Leus and P. Van Der Voort, A vanadyl complex anchored on acetyl acetone functionalized covalent triazine framework: a hybrid green catalyst with excellent reactivity, *Chem. Mater.* 2018, *30, 4102-4111.*

12. X. Feng, H. S. Jena, K. Leus, G.-B. Wang, J. Ouwehand and P. Van Der Voort, L-proline modulated zirconium metal organic frameworks: simple chiral catalyst for aldol addition reaction, *J. Catal.* 2018, 365, 36-42.

13. S-N. Zhao, G.-B. Wang, D. Poelman and P. Van Der Voort, Metal organic frameworks based materials for heterogeneous photocatalysis, *Molecules.* 2018, in preparation (Invited review).

Conference Presentations

1. 17th Netherlands' Catalysis and Chemistry conference (NCCC-XVII), Noordwijkerhout, The Netherlands, March 7-9th, 2016 (Poster)

2. MOF-2016: 5th International Conference on Metal-Organic Frameworks & Open Framework Compounds, Long Beach, CA, USA, September 11-15th, 2016 (Poster).

3. EuroMOF2017: The 2nd European Conference on Metal-Organic Frameworks and Porous Polymers, Delft, The Netherland, October 29th – November 1st, 2017 (Poster).

4. ChemCYS 2018, Chemistry Conference for Young Scientists, Blankenberge, Belgium. February 21-23th, 2018 (Poster).